Optimization of WAG in Smart Wells: An Experimental Design Approach

Proefschrift

ter verkrijging van de graad van doctor
aan de Technische Universiteit Delft,
op gezag van de Rector Magnificus prof. dr. ir. J.T. Fokkema,
voorzitter van het College voor Promoties,
in het openbaar te verdedigen op maandag 25 juni 2007 om 17:30 uur
door

Talal Ebraheem Hamzah ESMAIEL

Master of Science in Petroleum Engineering
Stanford University
Bachelor of Science in Petroleum Engineering
University of Wyoming
Bachelor of Science in Chemical Engineering
University of Wyoming

geboren te Sharq, Kuwait

Dit proefschrift is goedgekeurd door de promotor:
Prof. ir. C.P.J.W. van Kruijsdijk

Samenstelling promotiecommissie:

Rector Magnificus,	voorzitter
Prof. ir. C.P.J.W. van Kruijsdijk,	Technische Universiteit Delft, promotor
Prof. dr. ir. J.D. Jansen,	Technische Universiteit Delft
Prof. dr. J. Bruining,	Technische Universiteit Delft
Prof. Adel El-Sharkawy,	Kuwait University
Dr. M. Salman,	Kuwait Institute for Scientific Research
Prof. dr. P. Zitha,	Technische Universiteit Delft
Dr. Carlos Glandt,	Shell International Exploration and Production

The research for this thesis was financially supported by Kuwait Institute for Scientific Research

Table of Contents

Chapter 1 Introduction to the World of Oil

The hydrocarbon world is an important part of our everyday lives beyond the fuels we are all familiar with to millions of products including heat and electricity for our homes to vital components in plastics, clothing, medications, roads, and cosmetics. Most people directly associate oil derived fuels with the transportation industry where in the USA 97% of these fuels come from oil[1]. The US Energy Information Administration[1] estimated a total world wide energy consumption of 15TW with 86% being supplied by fossil fuels. In 2003 the Netherlands had 82% of its energy supplied by fossil fuels and the EU had 80% supplied by fossil fuels.

The oil and gas companies play a major role in the USA and global economy as highlighted by the several indices[2] tracking various aspects of the industry. These include but are not limited to the Dow Jones U.S. Oil & Gas Index, Dow Jones Utilities Index, and the NYSE Energy Sector Index. As of March 2007 six of the 43 companies with a market capitalization of over $100 billion traded in the USA are major integrated oil and gas companies headlined by Exxon Mobil Corporation, the largest company by earnings as well as market capitalization.

1.1 The World Outlook

The world of politics, war, religion and oil all seem to be intertwined in various ways. **Figure 1** shows some of the major events in the oil industry since the early 1970's. These include wars, an embargo, and even a revolution that all had major affects on the oil industry.

1.1.1 World Wide Reserves

L E J Brouwer, Senior Managing Director, Royal Dutch/Shell once said:

"*Oil is seldom found where it is most needed, and seldom most needed where it is found.".*

This leads to the inevitable question of where the oil is and how much oil is there. To answer this question first a brief definition of resources is provided. Discovered reserves (aka known reserves) are divided into proved, prospective and unproved reserves. Proved reserves are quantities of oil and gas that can be expected to be recoverable with the current technology and economic conditions. Prospective reserves are those that may be recoverable in the future with advanced technology and changes in economic conditions. Unproved reserves will not be discussed here.

The US reserves of about 22 billion barrels are a fraction of the 2004 estimates of approximately 1.3 trillion barrels of oil worldwide[1]. The countries with the largest reserves are Saudi Arabia, Canada, Iran, Iraq, Kuwait, UAE, Venezuela and Russia. These reserves can be seen in **Figure 2**. The vast majority is located in the Middle East and historically was controlled by OPEC. This control by OPEC and the Middle East is lessening with major discoveries and improved technology in recovering heavy oil primarily in Canada and Venezuela.

1.1.2 Supply and Demand

The world supplies and consumes over 70 million barrels of oil per day currently with little spare capacity. The US, the world's largest user, consumes nearly 18 million barrels of crude per day. The US only produces about 5 million barrels per day, which leaves a net import of 13 million barrels per day.40 % of these imports are from OPEC countries. This is in sharp contrast to 30 years ago when OPEC accounted for 60% of US imported but the US produced a larger percentage of its oil domestically.

The market is becoming increasingly global, and the largest energy consumers such as the US, China, Japan, and the EU rely heavily on imports. As events depicted in **Figure 1** show, geopolitical factors greatly affect the oil industry. Due to these inherent risks, countries are forever searching for more oil and better ways of producing the reserves that they have.

1.1.3 Recovery of Oil

The recovery process of oil is divided into 3 phases of its lifespan. These are primary recovery, secondary recovery, and tertiary recovery.

Primary recovery occurs during the life of the reservoir when there is enough natural pressure to flow the fluids to the surface. As early as 1880 when wells began to loose formation pressure operators added gas vacuum pumps to wells. This increased the pressure differential between the reservoir and the surface and increased production for some time. This phase can last several years and typically yields 5-15% recovery. These recoveries are very sensitive to the reservoir properties.

Secondary recovery involves the injection of water into the reservoir. The injection of water aims to re-pressurize the reservoir and displace the oil towards the producers. The earliest floods were called circle floods because of the growth pattern of the water zones. As water broke through in the surrounding wells, they were in turn turned into injectors. The first 5-spot pattern was attempted in 1924 and these pattern floods are now very popular.

The first documented water flood began in 1905 in Pennsylvania although illegal at the time. After the legalization in 1921 most reservoirs did not undergo water flooding after production rates during primary recovery became uneconomical. This was primarily due to economic conditions at the time. By the 1940's it was common practice and typically resulted in recoveries of an additional 5-20% beyond primary production.

Tertiary recovery primarily involves the injection of gas into the reservoir. Typically this serves the same purpose as water injection, the re-pressurizing of the reservoir and viscous displacement of the oil. The first documented case was forced air injection in 1911 and by the 1930's it became increasingly popular. This historically marked the end of the lifespan of the reservoir and typical recoveries of 20-40%.

Other tertiary recovery techniques include thermal recovery and chemical floods. These are more advanced techniques that often use fluids not native to the reservoir. These techniques have the aim of overcoming forces such as surface tension and viscosity that may inhibit the oil flow.

In addition to the lifecycle of the reservoir described above, technology serves a significant role in the recovery of oil and gas. Many people envision the oil industry as the images of old movies such as *Boom Town* starring Clark Gable, Spencer Tracy, Claudette Colbert, Hedy Lamarr, and Frank Morgan. Wooden drilling rigs, no environmental concerns, and absolute gun slinging mayhem. Things have changed.

Computational power allows for reservoir simulation studies to be an integral part of the reservoir management. Advancement in seismic and logging allow better visualization of the reservoir and access to increasing amounts of data on which to develop models and make decisions. The ability to work in over a mile of water, and practices being safe enough to work in environmentally sensitive regions such as the Arctic have given oil companies access to parts of the earth's surface previously untapped. Additionally, high temperate / high pressure (HT/HP) space age titanium alloys allow us to go further into the earth than ever thought possible, outside the realms of science fiction, 20 years ago.

Smart wells are a technological development just now gaining popularity that has the potential to help further the recovery of oil and gas reservoir. This technology in conjunction with advanced tertiary recovery techniques such as WAG and a robust production plan show the future potential of the industry in a good light.

1.1.4 Oil Prices

Oil price forecasting is far from an exact science. Companies and countries take different approaches to integrating oil prices into their decision making process. Traditionally, most tend to use a single price, usually on the conservative side due to the natural risk adverse nature of corporations and governments, and not a range of possibilities or a stochastic price model. As oil price volatility greatly influences economic analysts are steering away from single price models.

The oil price has a significant effect on the Net Present Value (NPV) of the project. The NPV allows for the assignment of positive and negative revenue and to give a time value to the cash flow. This cash flow is all discounted to time zero using the discount rate for comparison. The capital cost is subtracted from this to get the project NPV as discussed later.

In December 2003 a survey of 27 oil analysts by Bloomberg[3] showed an average estimate of a 13% decline in oil prices for 2004. In actuality oil prices were about 45% higher in 2004 than in 2003 and oil companies had a very profitable year due to the high oil prices. The analysts were not "wrong" inasmuch as world wide economic factors did not react as anticipated.

Historical price data shows that this is true on several different scales due to different reasons. **Figure 3** shows inflation adjusted average annual oil prices from 1865 to 1998. Several things occurred during that time but a few can be highlighted to see how unforeseen events affect the oil prices. 1945 is primarily due to post war reconstruction, 1974 the OPEC oil embargo, 1979/80 the Iranian revolution, 1990 the Gulf War and the 1998 Asian economic crisis.
The past century has shown times of relative stability like the 50's and 60's to extremely volatile times like the 80's. Developing a 5 or 10 year production plan based on a single estimated oil price could cause some potential problems.

> *"I don't think it's going to go to 100 us$ but if it does the crash is going to be even more spectacular…It will make the hi-tech bubble look like a picnic … this thing is not going to last."* Steve Forbes

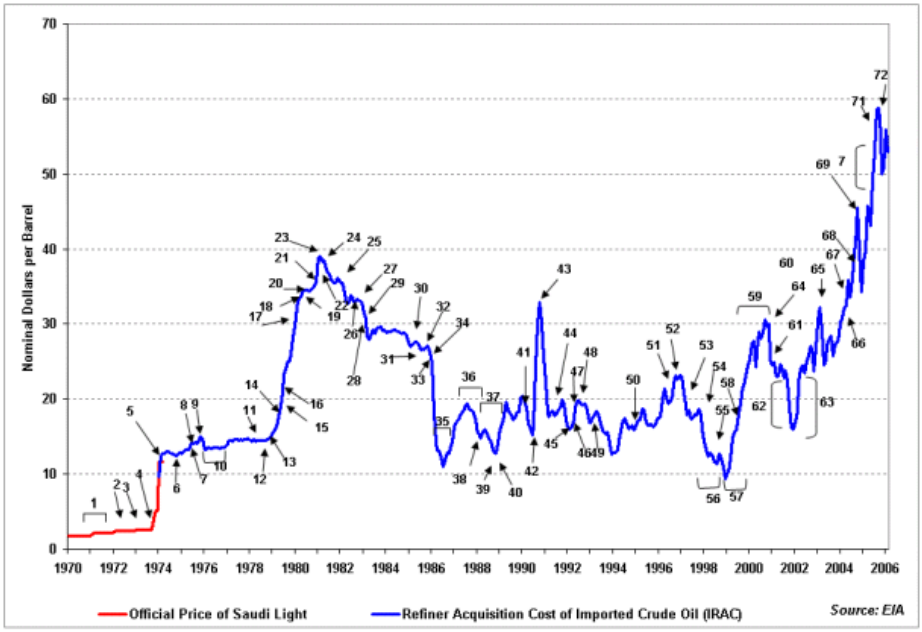

1. OPEC begins to assert power; raises tax rate & posted prices
2. OPEC begins nationalization process; raises prices in response to falling US dollar.
3. Negotiations for gradual transfer of ownership of western assets in OPEC countries
4. Oil embargo begins (October 19-20, 1973)
5. OPEC freezes posted prices; US begins mandatory oil allocation
6. Oil embargo ends (March 18, 1974)
7. Saudis increase tax rates and royalties
8. US crude oil entitlements program begins
9. OPEC announces 15% revenue increase effective October 1, 1975
10. Official Saudi Light price held constant for 1976
11. Iranian oil production hits a 27-year low
12. OPEC decides on 14.5% price increase for 1979
13. Iranian revolution; Shah deposed
14. OPEC raises prices 14.5% on April 1, 1979
15. US phased price decontrol begins
16. OPEC raises prices 15%
17. Iran takes hostages; President Carter halts imports from Iran; Iran cancels US contracts; Non-OPEC output hits 17.0 million b/d
18. Saudis raise marker crude price from 19$/bbl to 26$/bbl
19. Windfall Profits Tax enacted
20. Kuwait, Iran, and Libya production cuts drop OPEC oil production to 27 million b/d
21. Saudi Light raised to $28/bbl
22. Saudi Light raised to $34/bbl
23. First major fighting in Iran-Iraq War
24. President Reagan abolishes remaining price and allocation controls
25. Spot prices dominate official OPEC prices
26. US boycotts Libyan crude; OPEC plans 18 million b/d output
27. Syria cuts off Iraqi pipeline
28. Libya initiates discounts; Non-OPEC output reaches 20 million b/d; OPEC output drops to 15 million b/d
29. OPEC cuts prices by $5/bbl and agrees to 17.5 million b/d output
30. Norway, United Kingdom, and Nigeria cut prices
31. OPEC accord cuts Saudi Light price to $28/bbl
32. OPEC output falls to 13.7 million b/d
33. Saudis link to spot price and begin to raise output
34. OPEC output reaches 18 million b/d
35. Wide use of netback pricing
36. Wide use of fixed prices
37. Wide use of formula pricing
38. OPEC/Non-OPEC meeting failure
39. OPEC production accord; Fulmar/Brent production outages in the North Sea
40. Exxon's Valdez tanker spills 11 million gallons of crude oil
41. OPEC raises production ceiling to 19.5 million b/d
42. Iraq invades Kuwait
43. Operation Desert Storm begins; 17.3 million barrels of SPR crude oil sales is awarded

44. Persian Gulf war ends
45. Dissolution of Soviet Union; Last Kuwaiti oil fire is extinguished on November 6, 1991
46. UN sanctions threatened against Libya
47. Saudi Arabia agrees to support OPEC price increase
48. OPEC production reaches 25.3 million b/d, the highest in over a decade
49. Kuwait boosts production by 560,000 b/d in defiance of OPEC quota
50. Nigerian oil workers' strike
51. Extremely cold weather in the US and Europe
52. U.S. launches cruise missile attacks into southern Iraq following an Iraqi-supported invasion of Kurdish safe haven areas in northern Iraq.
53. Iraq begins exporting oil under United Nations Security Council Resolution 986.
54. Prices rise as Iraq's refusal to allow United Nations weapons inspectors into "sensitive" sites raises tensions in the oil-rich Middle East.
55. OPEC raises its production ceiling by 2.5 million barrels per day to 27.5 million barrels per day. This is the first increase in 4 years.
56. World oil supply increases by 2.25 million barrels per day in 1997, the largest annual increase since 1988.
57. Oil prices continue to plummet as increased production from Iraq coincides with no growth in Asian oil demand due to the Asian economic crisis and increases in world oil inventories following two unusually warm winters.
58. OPEC pledges additional production cuts for the third time since March 1998. Total pledged cuts amount to about 4.3 million barrels per day.
59. Oil prices triple between January 1999 and September 2000 due to strong world oil demand, OPEC oil production cutbacks, and other factors, including weather and low oil stock levels.
60. President Clinton authorizes the release of 30 million barrels of oil from the Strategic Petroleum Reserve (SPR) over 30 days to bolster oil supplies, particularly heating oil in the Northeast.
61. Oil prices fall due to weak world demand (largely as a result of economic recession in the United States) and OPEC overproduction.
62. Oil prices decline sharply following the September 11, 2001 terrorist attacks on the United States, largely on increased fears of a sharper worldwide economic downturn (and therefore sharply lower oil demand). Prices then increase on oil production cuts by OPEC and non-OPEC at the beginning of 2002, plus unrest in the Middle East and the possibility of renewed conflict with Iraq.
63. OPEC oil production cuts, unrest in Venezuela, and rising tension in the Middle East contribute to a significant increase in oil prices between January and June.
64. A general strike in Venezuela, concern over a possible military conflict in Iraq, and cold winter weather all contribute to a sharp decline in U.S. oil inventories and cause oil prices to escalate further at the end of the year.
65. Continued unrest in Venezuela and oil traders' anticipation of imminent military action in Iraq causes prices to rise in January and February, 2003.
66. Military action commences in Iraq on March 19, 2003. Iraqi oil fields are not destroyed as had been feared. Prices fall.
67. OPEC delegates agree to lower the cartel’s output ceiling by 1 million barrels per day, to 23.5 million barrels per day, effective April 2004.
68. OPEC agrees to raise its crude oil production target by 500,000 barrels (2% of current OPEC production) by August 1—in an effort to moderate high crude oil prices.
69. Hurricane Ivan causes lasting damage to the energy infrastructure in the Gulf of Mexico and interrupts oil and natural gas supplies to the United States. U.S. Secretary of Energy Spencer Abraham agrees to release 1.7 million barrels of oil in the form of a loan from the Strategic Petroleum Reserve.
70. Continuing oil supply disruptions in Iraq and Nigeria, as well as strong energy demand, raise prices during the first and second quarters of 2005.
71. Tropical Storm Cindy and Hurricanes Dennis, Katrina, and Rita disrupt oil supply in the Gulf of Mexico.
72. President Bush authorizes SPR release.

Figure 1: World Oil Market and Oil Price Chronologies: 1970 – 2006. This chronology was originally published by the Department of Energy's Office of the Strategic Petroleum Reserve, Analysis Division. Updates for 1995-2006 are from the Energy Information Administration1.

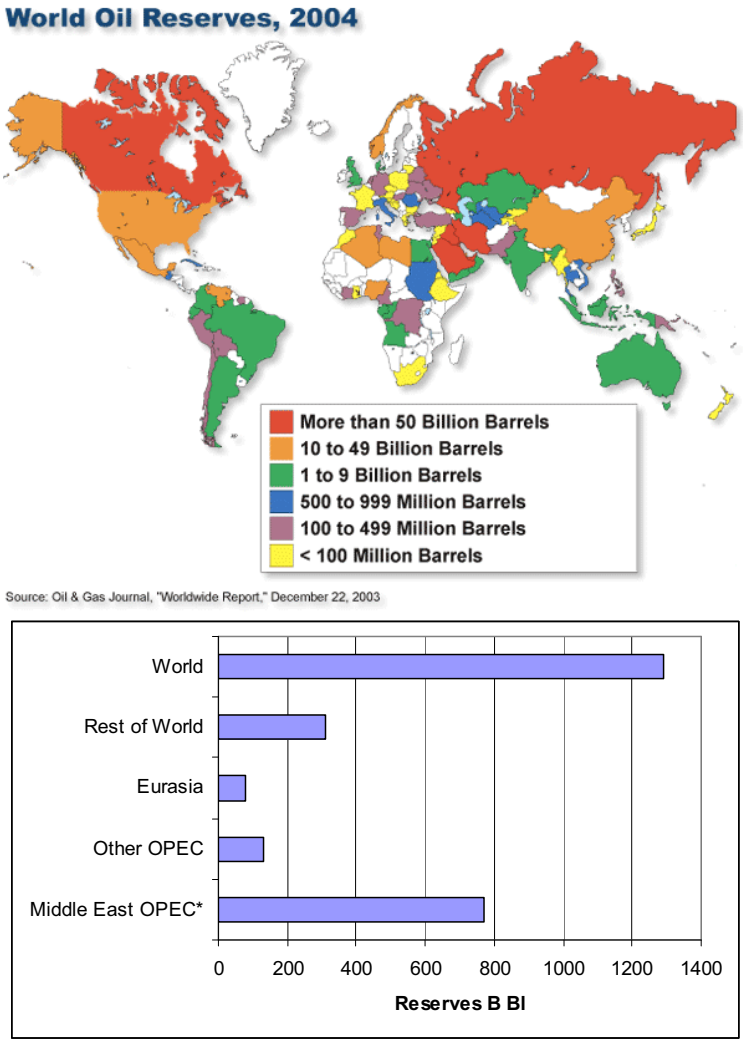

Figure 2: World Oil Reserves shown on (top) a map of the world and (bottom) divided by regions4.

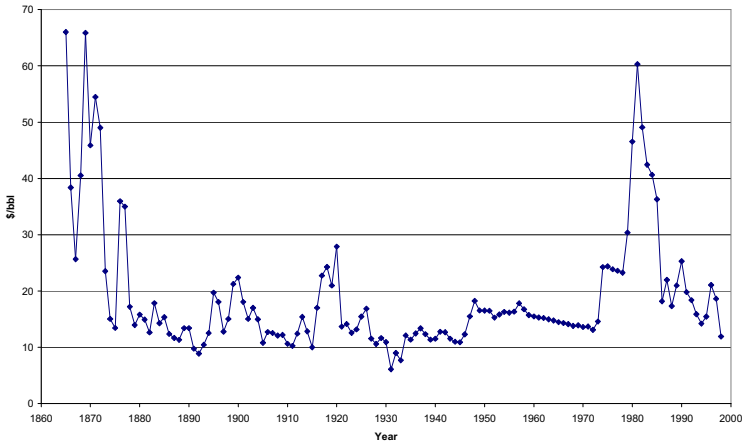

Figure 3: Inflation Adjusted Historic Oil Prices.

1.2 WAG and Smart Wells

1.2.1 WAG

Water-alternating-gas (WAG) injection is a tertiary oil recovery process that has been growing in popularity since it was first introduced in the 1950's. Initially the method was aimed simply to improve sweep efficiency during gas injection. Early in the use of WAG the improved recovery was fully attributed to contact with unswept zones. Later it was believed that the improvement was due to a combination of better mobility control and improved microscopic sweep efficiency.

The first WAG process reported in literature was in Canada 1957. As the process is approaching half a century old, much of the fundamentals require more understanding through research. The majority of published literature discussing field cases do not provide details of the simulation model used or the decision analysis by management. Therefore the process of WAG is not well understood yet. In addition, there always exists uncertainty in the reservoir model even though technology has advanced significantly. The uncertainty in the reservoir model is attributed to the ambiguity in the reservoir and geological parameters.

WAG fields applications have been reported to be generally successful. WAG has been applied onshore and offshore including injections with hydrocarbon and non-hydrocarbon gases. WAG projects have been both miscible and immiscible, and applied to several rock types. Further details will be provided in Chapter 3.

1.2.2 Smart Wells

Earlier in section 1.1.3 some examples in advanced well drilling technology were given. These include the ability to drill horizontal wells, multilateral wells, as well as deeper and better-targeted wells. The problem with these is that the only way to target the flow in the past was to decide where to perforate the wells and how to set the surface choke. To change where the well was in communication with the reservoir a work over would then need to be performed on the well.

Smart wells incorporate downhole valves that can separate different zones of the well. Initially they were used to shut off watered out zones more easily than cementing and perhaps again perforating a well. These early applications were primarily aimed at the producing wells and as a reactive measure to early breakthrough.

Intuitively there is considerable scope in applying the technology to both the injector and producer wells and to act in a proactive manner. During the lifespan of the reservoir the optimal locations for injection and production will change. Additionally the flexibility of the smart well system can offer other benefits in an uncertain realm of reservoir management.

1.3 Research Goals

The first known field application of WAG in literature was a pilot study in Canada in 1957 and until mid 2001 only 59 WAG field applications have been found in literature. Nearly 4 of 5 projects were miscible injection and over half the projects were sandstone and over half located in the USA. Very few have been unsuccessful even though predicted increased recovery was almost always higher than actual[5].

Characterization of the WAG process will provide insight into the fundamentals of the process. The benefits and drawbacks relative to water and gas flooding must be understood prior to evaluating the value of WAG. Following the characterization of the WAG process opportunities with WAG can be explored.

The primary operational problem cited in literature is early breakthrough in production wells. The second problem most cited is injectivity abnormalities caused by factors such as wettability, entrapment and heterogeneity. This makes it potentially a prime candidate for smart wells based on initial success with smart wells in mitigating early breakthrough. Smart well technology ("down-hole measurement and control") has progressed significantly over the last few years. Previous research has concentrated on the application of the technology to secondary recovery. Intuitively smart wells should work well in conjunction with the WAG process so these links will be investigated.

Reservoir models always have a degree of uncertainty associated with them. This provides the motivation for studies of the process at different scales to identify the uncertainty associated with the process. The sensitivity of recovery or economics to various reservoir, fluid and production parameters will provide further understanding into the WAG process.

Previous work on optimization concentrated primarily on controlling slug sizes to control the gas/water profile. The final objective of this study is to incorporate an experimental design approach to study the WAG process focusing on optimization of the process. The uses of this approach allow for a reservoir screening of when and how well WAG works. This methodology also provides a novel approach to quantifying the various value streams associated with smart wells and WAG. This includes an increase in the NPV or expected monetary value (EMV) and a measure of risk reduction.

The Integrated System Approach Petroleum Production (ISAPP) program is a joint research venture in upstream oil and gas production technology. TNO, Shell and Delft University of Technology (TU Delft) work together with the goal that future hydrocarbon production systems will be more intelligent. This research though not directly funded by the program is part of the vision set out by ISAPP. **Figure 4** illustrates where this work fits into the closed-loop reservoir management vision within ISAPP.

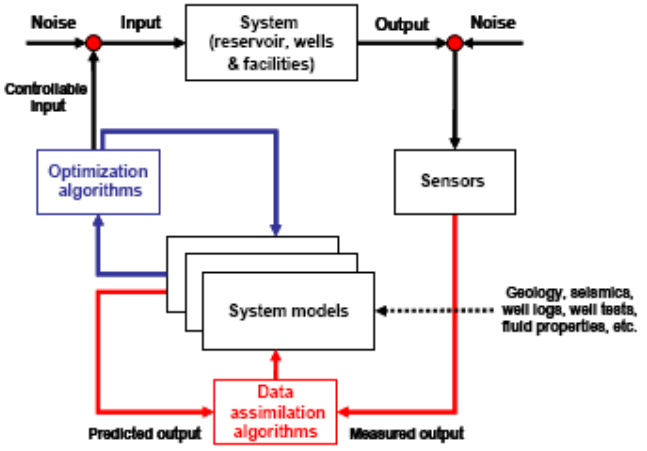

Figure 4: Reservoir management depicted as a closed-loop model-base controlled process[6].The primary concentration in this study is the blue loop looking at optimization algorithms.

1.4 Outline of Thesis

Chapter 1 has provided a motivation and brief introduction to the research work to be presented in this thesis work. Chapter 2 discusses some of the conceptual benefits and drawbacks of the WAG process. The discussion of 2 reservoir models where WAG is implemented is presented in this chapter. In Chapter 3 the application of smart wells in water flood and a WAG flood reservoir are presented. Here it is shown how the combination of the WAG process and smart well technology can work together to improve recovery.

Modeling is a game of uncertainty and ignoring this uncertainty can lead to bad decisions. Chapter 4 introduces a Design of Experiment (DOE) framework to model uncertainty and derives the sensitivities of reservoir, fluid, and production parameters to the recovery. Decision analysis is a key concept in optimization. In designing these studies multiple objective functions are possible including physical measures such as recovery or economic measures such as net present value (NPV). Making these decisions under uncertainty requires further considerations. These concepts are discussed as they relate to this study in Chapter 5. Chapter 5 builds on the design framework presented earlier to provide insight in how the information derived can be used to optimize the recovery.

The general observations and a discussion of the results of the research are presented in Chapter 6. Conclusions and recommendations are also presented in Chapter 6.

References:

1. US Department of Energy Statistical Database, Annual Oil Market Chronology, EIA, 2006 http://www.doe.gov/
2. The New York Stock Exchange: Another Century, by James E. Buck (Editor), Greenwich Pub.; Revised edition (December 1999)
3. Bloomberg News Broadcast, Tuesday, December 23 - 2003 at 08:45
4. Christensen, J.R., Stenby, E.H., Skauge, A., "A Review of WAG Field Experience", paper SPE 71203, SPE Reservoir Evaluation & Engineering April 2001
5. Oil & Gas Journal, "Worldwide Report", December 22, 2003
6. Jansen, J.D., "Model-based Control of Subsurface Flow", 8th International Symposium on Dynamics and Control of Process Systems (DYCOPS), Cancun, 6-8 June 2007

Chapter 2 Water Alternating Gas - WAG

Following the discovery and assessment of a new oil field engineers begin the task of planning for the maximization of the ultimate recovery. Depending on the properties of the reservoir including rock type, compartmentalization, and oil density not all reservoirs act alike.

When Ozark mountaineer Jed Clampett accidentally strikes oil on his property while "shootin' fer some food." in the pilot of Beverly Hillbillies the oil wells seemingly blow oil into the air under their own power. This is where most reservoirs start in reality. Oil reservoirs are pressurized and the high pressure provides the energy to allow the oil to flow to the surface.

Recovery methods can in general be broken down into four segments. The first ingredient that tends to drive the early years of production is the natural energy of the reservoir. This pressure gradient caused by the reservoir in contact with wellbore connected to the surface provides a natural flow. The second ingredient to the recovery process is the supplementing of energy to the reservoir. This is done by injecting a fluid to cause the drive, or push, of the oil toward the producer or by gravity drainage caused by buoyancy forces. The next ingredient is the enhancement of the oil properties through the reduction in viscosity or interfacial tension. The final ingredient involves enhancement of the reservoir by geochemical or geomechanical enhancement.

The sweep efficiency is a measure of the effectiveness of the injected fluid to contact the reservoir. The volumetric sweep efficiency is the fraction of the reservoir volume contacted by the injected fluid. The volumetric sweep efficiency depends on many parameters including the well pattern and flow rates, permeability, heterogeneities, density difference and mobility ratios. Large-scale features tend to affect the sweep efficiency and small-scale heterogeneities the displacement efficiency. These are illustrated in **Figure 1**.

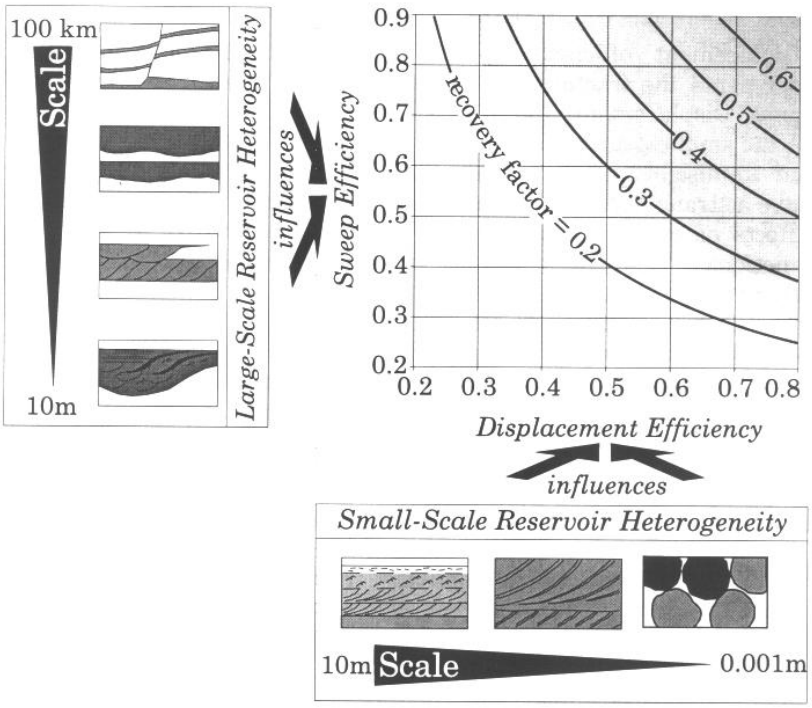

Figure 1: Effects of large and small scale heterogeneities on recovery[1].

The displacement efficiency is a measure of the fraction of oil recovered from a volume of reservoir in contact with the injectant. The displacement efficiency is affected by wettability, pore network morphology, wettability and small-scale heterogeneities such as lamination causing capillary entrapment. The combination of the sweep and displacement efficiency affects the total recovery efficiency, or fraction of total oil produced.

The oil recovery factor (**Eq.1**) can be divided in two factors, the macroscopic sweep efficiency and the microscopic sweep efficiency. Further more the macroscopic sweep efficiency is defined by the horizontal and the vertical sweep efficiencies. This can be formulated as:

$$R_f = E_v.E_h.E_m \qquad (1)$$

The horizontal sweep efficiency is related to the end-point mobility ratio (**Eq.2**) and the vertical sweep efficiency

depends on viscous to gravity forces ratio (**Eq.3**):

$$M = \frac{k_{rg}/\mu_g}{k_{ro}/\mu_o} \qquad (2)$$

$$R_{v/g} = \left(\frac{v\mu_o}{kg\Delta\rho}\right)\left(\frac{L}{h}\right) \qquad (3)$$

where M is mobility, k_r is relative permeability of the oil or gas, v is the velocity, μ is the viscosity, k is the absolute permeability, L is length, h is height, g is gravity and $\Delta\rho$ is the difference in density of the 2 phases.

The natural flow to the surface may last several years but as the pressure declines so will the flow. Generally downhole pumps are added but this only prolongs the inevitable lack of flow due to lack of reservoir pressure. At this point in the reservoir's life cycle a flood is generally applied to the reservoir. Production wells can be converted into injectors or new wells may be drilled and fluid is then forcibly pumped into the reservoir.

Water is a popular choice of injectant due to its abundant availability. The primary purpose of injecting water is maintenance of pressure by replacing produced fluids to drive or "push" the oil towards the producer wells.

Waterflooding has a few key issues. Water is heavier than most oils and by gravity tends to naturally under ride the oil in the reservoir. Depending on the density of the oil as well as flow rates, and variables such as vertical permeability, reservoir thickness, well spacing, and heterogeneities, this under ride can be minimal or severe. The roles these play can be seen in the viscous to gravity forces ratio (**Eq.3**) as defined above. Large density differences and high vertical connectivity cause greater gravity problems. Areal heterogeneities also result in non-ideal flow fronts as these cause channeling that may lead to early breakthrough and bypassing of sections of the reservoir. This results in an inefficient sweep of the oil and results in water reaching the producer faster than desired.

The other popular choice is a gas flood. Depending on the depth and pressure of the reservoir the flood may be miscible or immiscible. Miscibility means that the 2 phases, oil and gas, can mix and form a single-phase mixture. These gas floods have their own issues. Maintaining miscibility in gas floods is often quite difficult. Ideally gas mobility increases result in increased injectivity and the wells may become rate-limited. If there is a decline in injectivity this can result reservoir pressure declines during production. Moreover gas with a lower density than oil will then tend to override the oil leaving large volumes of the reservoir unswept and causing early breakthrough. During an immiscible flood heterogeneities cause worse fingering and bypassing of oil than water. This problem gets worse as the mobility ratio becomes larger. However, gas is more efficient than water on a microscopic sweep basis as the miscible flood causes a reduction in the oil / water interfacial tension.

One process that incorporates the use of water and gas is named Water Alternating Gas or WAG
The Eclipse[2] manual defines the WAG process as:

> *"An enhanced oil recovery process whereby water injection and gas injection are alternately injected for periods of time to provide better sweep efficiency and reduce gas channeling from injector to producer. This process is used mostly in CO_2 floods to improve hydrocarbon contact time and sweep efficiency of the CO_2."*

Water alternating gas is an EOR process that combines the benefits of water and gas injection. Typically an extended water flood and / or gas flood is performed until the field is no longer economic and is subsequently abandoned. In the WAG process alternating slugs of gas and water are injected into the reservoir. The injection periods of each phase tend to last from 1 to 6 months. The WAG process is illustrated in **Figure 2**.

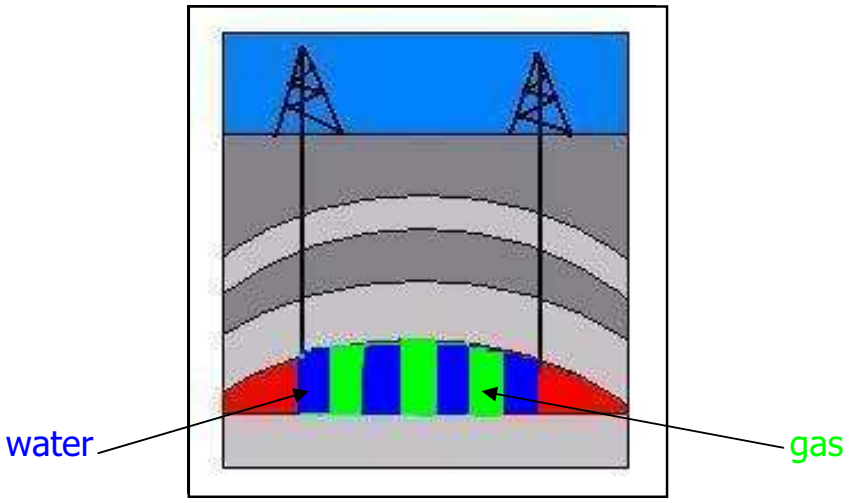

(a)

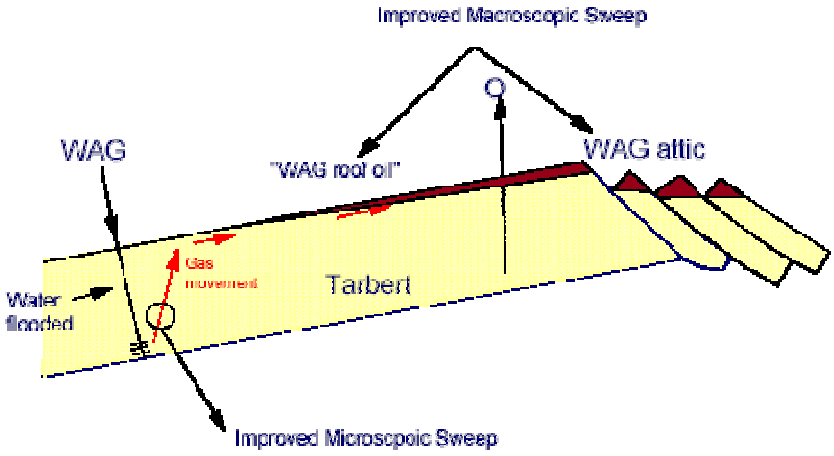

(b)

Figure 2: The WAG process. Figure 2a represents an ideal piston like displacement of the fluid while figure 2b shows how WAG can access difficult to reach oil.

2.1 Concept of WAG

The tertiary recovery process known as WAG is a combination of the two secondary recovery processes of water flooding and gas injection. The WAG process was proposed originally to aim for the ideal system of oil recovery: improvements in macroscopic and microscopic sweep efficiency at the same time. The water is used to control the mobility of the gas as can be seen in **equations 4 and 5**. The fractional flow of water is a function of the water saturation, and similar for gas, thereby limiting the fractional flow of one phase by switching to another injectant. The effects of the changes in mobility are illustrated in **Figure 3** where the fractional flow is shown to be sensitive to the fluid mobilities.

The cyclic nature of the WAG process causes an increase in water saturation during the water injection half cycle and a decrease of water saturation during the gas injection half cycle. This process of inducing cycles of imbibition and drainage causes the residual oil saturation to WAG to be typically lower than that of water flooding and similar to those of gas flooding. The 3 phase system results in a wettability where oil is the intermediate wetting phase further improving the microscopic displacement efficiency.

$$f_w = \frac{k_w/\mu_w}{k_w/\mu_w + k_o/\mu_o + k_g/\mu_g} \qquad (4)$$

$$f_g = \frac{k_g/\mu_g}{k_w/\mu_w + k_o/\mu_o + k_g/\mu_g} \qquad (5)$$

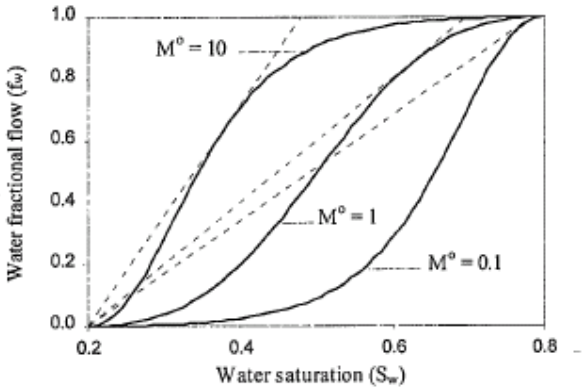

Figure 3: Water fractional flow for 3 oil / water end-point mobilities

The WAG process also works to improve the sweep efficiency in conjunction with enhancement of the microscopic displacement. The causes of low sweep efficiency for water or gas floods are described above. In the worst case scenario gas can sweep the attic and water the cellar resulting in the sweep improvement being additive. The WAG flood improves upon this by utilizing the water bank to reduce the gas fingering and vice versa to improve the sweep efficiency. The banks can also provide gravity stabilization further improving the sweep efficiency.

The two most common distinctions in the classification of the WAG process are miscible WAG injection and immiscible WAG injection. Miscible WAG injection occurs when the reservoir is above the minimum miscibility pressure (MMP) and is immiscible when below the MMP. A miscible flood injects a miscible gas into the reservoir and maintains the pressure above the MMP eliminating the interfacial tension between the oil and water. This is because the gas and oil mix to create one homogeneous fluid mixture above the MMP. In this study the initial reservoir pressure is just above the MMP and therefore often moves in and out of miscibility in part or all of the reservoir.

The research presented here concentrates on the macroscopic issues but a few key points should be made regarding the microscopic and intermediate level. Due to the cyclic nature of the flood, the increasing and decreasing phase saturation would need valid hysteresis based relative permeability curves to simulate the production. Additional core flood experiments, often not performed would be helpful by determining proper residual saturations and relative permeability curves[3,4].

2.2 WAG History

Water-alternating-gas (WAG) injection is an enhanced oil recovery process that has been growing in popularity since it was first introduced in the 1950's. The first WAG process reported in literature was in Canada 1957. As the process is approaching half a century old, much of the fundamentals require more understanding through research. The majority of published literature discussing field cases do not provide details of the simulation model used or an analysis of the management decisions.

Christensen, Stenby and Skauge[5] provided a review of 60 fields where WAG has been applied. The study identifies the use of WAG in several formation types with differing injectant gases and drive mechanisms.

Two major operational issues come up in the WAG projects that have been reported in literature[6]. These issues are early breakthrough usually of gas and / or reduced injectivity primarily during the water injection phase. There are two major operational parameters that affect the economics of a WAG project. These operational aspects are the half-cycle slug sizes and the WAG ratio.

The WAG process has been applied in several types of reservoirs under several conditions. Just over half the reported WAG projects have occurred in sandstones with 1 in 5 in dolomite formations, 1 in 10 in carbonate and 1 in 10 in limestone. Over 80 percents of the WAG floods have been performed onshore, but offshore floods are increasing. The type of injectant gas is evenly split between CO_2 and hydrocarbon gas with a few using nitrogen. Also, about 80 percent of the floods are miscible.

To understand the effects of CO_2 and Hydrocarbon gas during the WAG process a few concepts must be introduced:

- Swelling: When the oil is saturated with a gas it increases in volume.
- Saturation Pressure: The pressure at a given temperature at which phase changes occur. A liquid at its saturation pressure and temperature will flash into a vapor phase when the pressure is lowered.
- Viscosity (saturated oil): When oil is saturated by a gas the viscosity of the saturated oil is lowered by the introduction of the gas.

CO_2 is a popular choice of injectant. Some of the key issues in choosing the injectant gas are:

- CO_2 is marginally more effective than methane or dry gas in swelling of oil on a mole% basis.
- CO_2 is more than twice as effective as methane or dry gas for lowering of the saturation pressure.
- Saturated oil viscosity is lower by CO_2 than methane on a mole% basis.

There are considerations with the choice of CO_2 as the injectant. These include:

- CO_2 quality affects corrosion.
- There may not be an available source of CO_2.

Hydrocarbon gas is also a popular choice due to:

- Hydrocarbon gas is naturally occurring.
- Hydrocarbon gas is usually readily available as produced gas.
- Clean / dry hydrocarbon gas is not corrosive.

Hydrocarbon gas considerations include:

- As the market price for the gas increases there is increased pressure to sell the gas.
- Impurities such as sulphur can cause corrosion.
- Sulphur gas impurities are a serious health and safety issue.

2.3 WAG Model Studies

Christensen, Stenby and Skauge[1] provided an overview of WAG used in several types of reservoirs discussed above. Two different reservoirs are studied in more detail in this chapter. The first set of models is based on a pattern flood

pilot study for a large oil field with detailed fluid description available. The injectant is chosen to yield a (marginally) miscible WAG.

The second type of model we introduce represents a naturally fractured reservoir with its own characteristic behavior. This model is introduced in section 2.3.2.

2.3.1 Miscible WAG Model - WAG Pilot Study

A comparison of gas flooding, water flooding and a WAG flood are explored in this study. The purpose of this is to demonstrate the benefits of the WAG process and the control available during the process. The model represents a pilot study area of a giant carbonate field.

2.3.1.1 Reservoir Model

The model represents a giant carbonate reservoir with 4 distinct layers apparent in the model. The layers are 10 to 13 meters thick. The reservoir model was extracted from the statistics of a giant reservoir model with the size of 20x30 km aerially and roughly 40 m vertically. The average grid block size for the base reservoir was too large (300x300 m) to allow a detailed pattern flood analysis. Additionally the run time for the full field model was in the order of a week. Therefore, based on geo-statistical information derived from the full field model, an area in the flank of the reservoir was considered and a sector model was constructed. Derived from the full field model the correlation lengths were in the order of 2000 ft areally and strongly correlated vertically within each of the 4 layers. The top 40 ft and bottom 30 ft had average permeabilities of 10's of mD and in the order of 100 mD for the middle 80 ft of the reservoir.

The mean and standard deviation of these permeabilities along with their correlation are used to build the pattern flood model. A sequential Gaussian simulation creates one realization of the permeability field and this is used. Major uncertainties in the model result from these derived correlations.

This reservoir is an ideal candidate for a miscible WAG flood. The reservoir sitting at about 8,000 ft. deep is of sufficient pressure for a miscible flood. Taber et al.[7] screening criteria are met requiring a high oil saturation (>30% PV), relatively light oil (>23 API), low viscosity (<3 cp), and deeper than 4,000 ft.

The reservoir model is 2,641 by 2,641 by 144 feet, modelled 19 by 19 grid blocks aerially and 26 in the vertical. A standard 5-spot pattern with a central injector and 4 producers is used with all sides bounded by no flow boundaries. The reservoir model is implemented in a commercial reservoir simulator to model the WAG process. A detailed fluid description with the 7 components describes the oil and gas.

The choice of injection gas is also critical in the decision making process. Hydrocarbon gas is used in some studies and CO_2 in other studies. All of the models using CO_2 are run in compositional mode. Lorentz-Bray-Clark viscosity correlation is used to give viscosity values to the pseudo component mixtures. A Soave-Redlich-Kwong equation of state is used for the 7 component mixture.

The 7 components in the compositional mixture are:

'CO2+H2S'
'C1+N2'
'C2+C3'
'C4-C5'
'C6-C9'
'C10-C14'
'C15-C20+'

Allowing for CO_2 to be modeled separately as there is negligible sulfur in the field.

An initial WAG ratio of 1:1 is used with 3 months per injection phase. For testing the influence of the WAG process two additional choices were implemented in the model. A ratio of 1:3 with 1 months and 3 months, and 3:1 with 3 months water and 1 month gas are implemented along with the original WAG setting.

As described in the WAG introduction, two primary problems faced in WAG processes are early breakthrough and loss of injectivity. The economic constraints placed on the wells are a maximum water cut of 0.5 stb/stb and a maximum GOR of 5 Mscf/stb at which point the well is shut-in. The wells are also tested every 100 days and connections can be reopened if the test shows the well can operate below the GOR and water cut constraints. This initial model with a 7% hydrocarbon pore volume (HCPV) slug size and conventional wells experienced major breakthrough problems forcing the wells to be shut in, resulting in lost production.

2.3.1.2 METHODOLOGY

The problem being addressed is the optimal recovery of oil under the production / economic constraints imposed on the wells. The base geological model is used to study the feasibility of WAG injection.

Three cases are run to compare the WAG process to gas injection and water injection. The fourth case modifies the WAG ratio and the slug size to improve recovery. The first step in the optimization is determining the optimum WAG parameters at the start of the project. Perturbing the 2 parameters, in an experimental design approach explained in chapter 5, that include the WAG ratio and slug size does this.

The optimal case resulted in a large slug size of 9% HCPVI/yr with a WAG ratio of 3:1. In this case the optimal results were derived for a single realization of the reservoir. Initially 9 simulations covering the low, median

and high values of the WAG ratio and slug size as seen are **Table 1** are run. A performance indicator, in this case recovery is measured and the slug size and WAG ratio are optimized.

All production wells are placed on a reactive control mode at this time. A reactive control is an action taken upon water / gas breakthrough or when a certain level of water / gas cut is reached in a well. This control involves closing a downhole valve when this limit is reached in a well or a portion of a well. The optimum WAG parameters determined at this stage are assumed constant throughout the simulation. The ranges for the WAG ratio and slug size can be seen in **Table 1**.

	Minimum	Median	Maximum
WAG Ratio	0.33	1	3
Slug Size %	4	7	10

Table 1: Factor setting for the WAG Ratio, water and gas slug sizes.

2.3.1.3 Scope for Improvement

Without seeing an increase in the expected value of the project due to the WAG process there would be little reason to pursue this study. **Figure 4** shows the improvement of the project oil recovery and the gas production total versus several case scenarios. The optimized case showed a small increase in gas production along with a significant increase in oil production. These scenarios provided for comparison are all using the same well configuration and constraints and intend to show the value of the different aspects of the process. Case 1 is a water flood performed on the field. Case 2 is a gas flood performed on the field. Case 3 is a WAG process with the original WAG parameters used. Case 4 is the optimized case with smart wells operated under the reactive controls determined in this study. All conventional wells can close reactively when economic or production constraints are violated as can sections of the smart well.

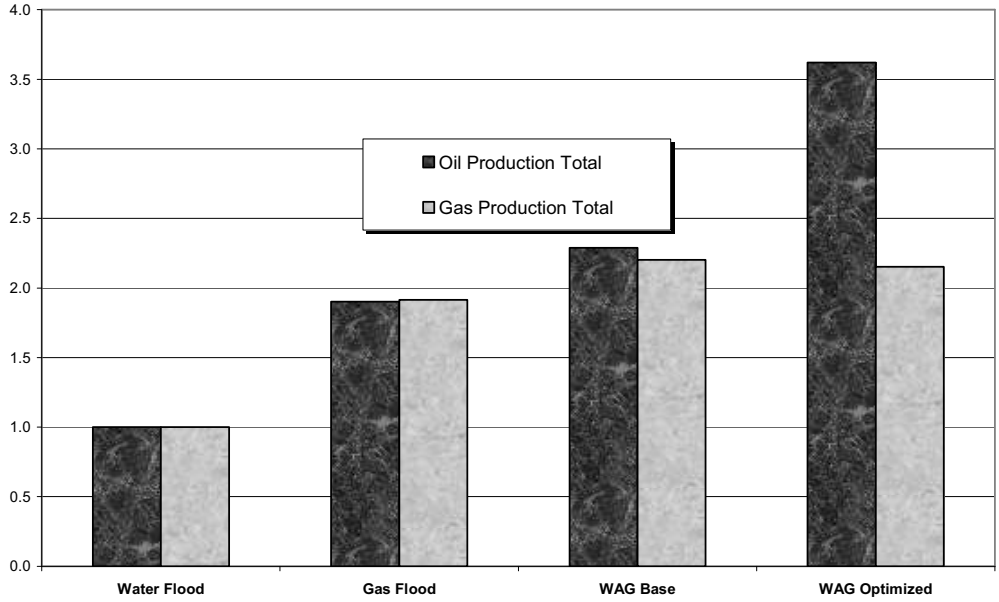

Figure 4: Field oil and gas production normalized totals for the 4 comparison cases.

Figure 5 shows the oil recovery curves for the four cases. Note that the optimized case extends the peak production time by over 2 years compared to the base WAG project. Control of the injection and production wells has increased oil production by over 58% with respect to the base WAG process while still operating under all the production and economic constraints. The optimal case resulted in a large slug size of 9% HCPVI/yr with a WAG ratio of 3:1.

The full scope of improvement in the NPV was also analyzed. The NPV is a function of the oil produced as well as the gas and the water both injected and produced. This means the improvement is a result of mitigating gas and water production in conjunction with the improved sweep efficiency although it must be noted that water production was minimal at all stages. All the positives are seen in this optimization except that a few hundred extra barrels of water were produced over the entire time span of the project. This includes delayed gas breakthrough, and extended peak oil production as well as larger cumulative oil production and lower cumulative gas production.

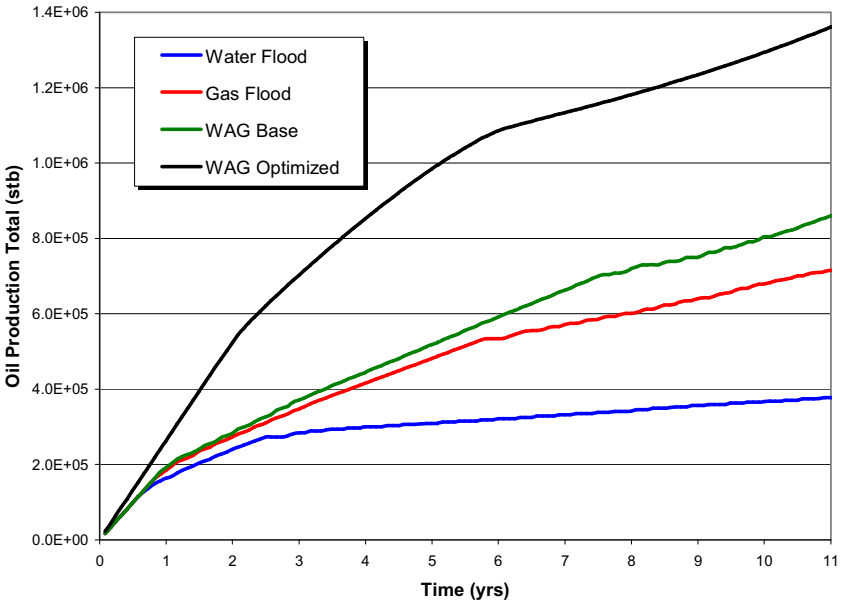

Figure 5: Oil production curves for the 4 comparison cases.

2.3.2 Fractured Reservoir

The second model discussed in this chapter is looking at a WAG flood in a fractured reservoir. Literature has provided little detailed evidence of WAG operations working in a fractured reservoir. The objective of this phase of the study is to screen the feasibility of WAG working in a fractured reservoir and to get a feel for the forces involved.

The fluid flow differs in fractured media due to the existence of the fractures. The rock matrix contains the bulk of the reservoir fluid in place and the high permeable fractures provide the main transport in the reservoir. The matrix blocks are connected through the fracture system and therefore the length scale attributed to the viscous component is limited to a single block.

This section will discuss how a fractured reservoir is modeled, the recovery mechanisms associated with the flow, the model used and the results. In section 2.3.5 two dimensionless numbers representing the flow in the fractured system are used to characterize the displacement process. This allows a screening of the WAG flood across a range of reservoir properties.

2.3.2.1 Modeling a fractured reservoir

Modeling typical massively fractured reservoirs with conventional fine grid, single porosity models is neither feasible nor is this level of detail necessary for practical applications. Thus the traditional yet efficient and effective approach to model naturally fractured reservoirs has been through a dual porosity model, where the fracture and matrix systems are separated into different continua, each with its own set of properties. The foundation of this model was laid down by Barenblatt[8] and Warren and Root[9] more than forty years ago. In **Figure 6** the idea of dual porosity of Warren and Root[9] is shown. The matrix-fracture interaction governing mass transfer between matrix and fracture is modeled through a transfer function[8]. This transfer function is the heart of the dual porosity model as it controls the matrix-fracture interaction and production performance of a naturally fractured reservoir as seen in **Figure 7**. The various existing formulations of the dual porosity model mainly differ in the manner how the transfer function is defined.

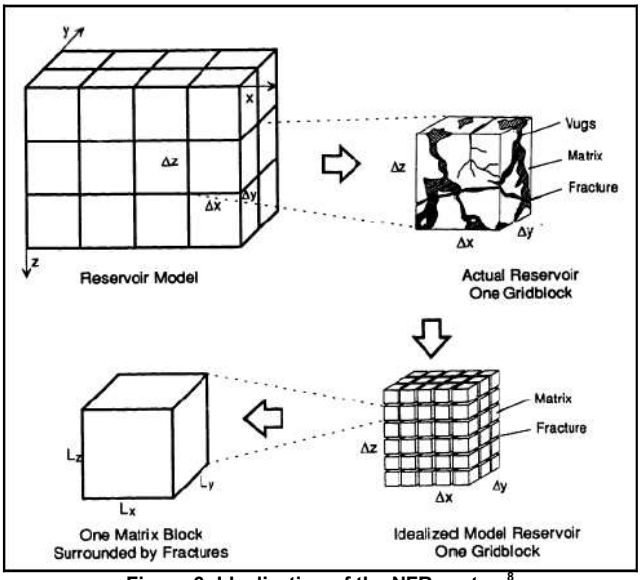

Figure 6: Idealization of the NFR system[8]

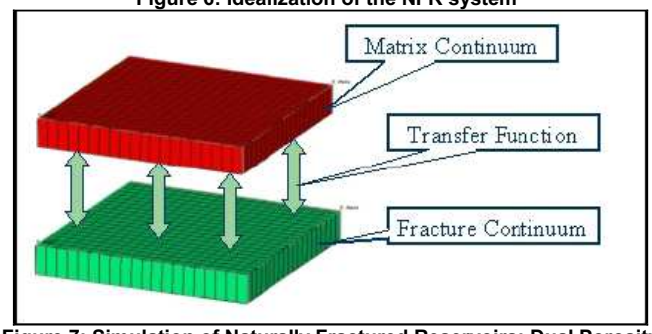

Figure 7: Simulation of Naturally Fractured Reservoirs; Dual Porosity

The first proposed transfer function[8] is:

$$q_{mf} = V\rho\frac{k_m}{\mu}\sigma\left(\overline{p} - p_f\right) \qquad (6)$$

where V is de matrix volume, ρ is the density of the fluid, μ is the viscosity, k_m is the absolute matrix permeability, $\overline{p}$ is the average pressure, p_f is the fracture pressure and σ is the shape factor which has the dimensions of $\left[\frac{1}{L^2}\right]$. A direct generalization of the equation above is[10]:

$$\tau_{mf} = k_m V\sigma\lambda_p\rho_p\left[\left(p_p - \gamma_p D\right)_f - \left(p_p - \gamma_p D\right)_m\right] \qquad (7)$$

where D_m and D_f are the matrix and fracture depths, λ_p is the mobility of phase p, ρ_p is the density of phase p and γ_p is a gravity constant of phase p. There is a lot of discussion about the physical meaning and the functional form of the shape factor. It has been considered that the shape factor is just a function of the fracture geometry[9] but some authors believe that the shape factor should be treated as a time dependent parameter[11]. It has been recognized that the shape factor is process-dependent: gravity drainage process requires a different shape factor than other production mechanisms like pressure depletion and capillary imbibition. The underlying reason is that depletion and (counter-current) capillary imbibition act in all directions whereas gravity forces act only in a vertical direction[12]. The shape factors that are used in the commercial simulator that is used in this study are:

$$\sigma = 4\left[\frac{1}{l_{mx}^2} + \frac{1}{l_{my}^2} + \frac{1}{l_{mz}^2}\right] \qquad (8)$$

for capillary imbibition, in which l_{mx}, l_{my} and l_{mz} are the matrix block dimensions and:

$$\sigma = \frac{2}{\left(\Delta z\right)^2} \qquad (9)$$

for gravity drainage, in which Δz is half the gridblock thickness.

2.3.2.2 Recovery mechanisms

During WAG injection, water slugs will be alternated with gas slugs. Consequently different physical mechanisms will play a role in naturally fractured reservoirs. Contrary to conventional single-porosity reservoirs, viscous forces usually play only a minor role in the oil recovery of densely fractured reservoirs. Instead, fluid flow between the matrix blocks and the fracture system is dominated by gravity- and capillary forces.

Capillary imbibition

Many of the non-carbonate fractured reservoirs found today are classified as mainly water wet. In this study we look at a strongly water wet reservoir. The matrix rock in such a reservoir will have a positive water-oil capillary pressure. When water is injected into the fractures, the water will flow under capillary forces into the matrix system, displacing the oil. Inside the fractures we assume that the capillary pressure is zero. This process is called spontaneous imbibition and is independent of matrix block height (i.e. only sensitive to surface to volume ratio) and capillary continuity.

Gravity drainage

When gas is injected, it has a preference to flow into the highly permeable fracture system. The matrix blocks, initially saturated with oil, become totally surrounded by the gas in the fracture system. The phase density difference and gravity force create a potential for gas to displace the oil. The pressure difference due to gravity is:

$$\Delta P = DZ_m \left(X_G - X_g \right) \left(\rho_o - \rho_g \right) g \qquad (10)$$

In which X_G is the fractional height of the gas in the fracture, X_g is the fractional height of the gas in the matrix and DZ_m is the matrix block height.

2.3.2.3 Reservoir Model

To study the WAG process in fractured reservoirs we will now focus on a particular reservoir model. The reservoir model is 1,320 by 1,320 by 500 feet, modeled using 10 by 10 grid blocks aerially and 5+5 (matrix + fracture) in the vertical. One injector and one producer are placed in opposite corners and all sides are bounded by no flow boundaries. The wells are connected to all 5 fracture grid blocks. The reservoir model is implemented in a commercial reservoir simulator to model the WAG process.

The matrix permeability ranges from an average of 10 mD to 90 mD and the fracture permeability from 1 to 3 Darcy. These represent mildly fractured systems that range in fracture to matrix permeability in the order of 10-300. Much more highly fractured systems tended to be computationally unstable during WAG floods.

The base case for every run was water-injection, gas-injection and WAG injection. An initial WAG ratio of 1:1 is used with 3 months per injection phase. For testing the influence of the WAG process two additional choices were implemented in the model. A ratio of 1:3 with 1 months and 3 months, and 3:1 with 3 months water and 1 month gas are implemented along with the original WAG setting. The reservoir simulation model was run for 4 years with the recovery at 4 years used as a performance indicator.

2.3.2.4 Scale-up pseudoization

We performed two-dimensional fine-grid simulations of the WAG injection in a system consisting of one matrix block with a discretely modeled fracture. The result of this fine-grid simulation is assumed to be the solution of the fluid displacement in the matrix block. The recovery of the coarse-grid dual porosity simulation should match the fine grid result. By modifying the capillary pressure curves and the relative permeabilities this can be achieved. These so called pseudo curves are used to simulate displacements on a pattern scale in a naturally fractured reservoir in a more accurate way.[13]

2.3.2.5 Methodology

The first step taken in investigating the performance of WAG in naturally fractured reservoirs is looking at sensitivity issues of the WAG process. Several parameters were varied, such as fluid parameters: the density and viscosity of the oil, physical reservoir parameters: matrix and fracture permeability and the shape factor and injection parameters: injection rate and WAG ratio. The ranges that are used in this study are provided in **Table 2**. To get a grip on how all these parameters are influencing the recovery, two dimensionless numbers are derived and calculated for certain reservoir operating conditions. The two numbers represent different physical forces in the reservoir. If we can identify flow regions based on these numbers, we can forecast reservoir performance and hence optimize operations. The relative magnitudes of these forces are defined by the following two dimensionless numbers based on literature about the scaling of multiphase flow[14]:

Relative Range	Units	Low	Medium	High
Coded Value	[-]	-1	0	1
Oil density	[lb/ft^3]	50	55	60
Oil viscosity	[cP]	20	70	120
Sigma	[1/ft^2]	0.1	1	1.9
Matrix permeability	[mD]	10	50	90
Fracture permeability	[mD]	1000	2000	3000
Injection rate	[bbl/day] [Mcf/day]	5000	6000	7000
WAG ratio	[-]	1:3	3:3	3:1

Table 2: Coded parameters with values used in the water, WAG and gas pattern flood simulations

$$N_{cv,m} = \frac{Lp_c^* k_m}{H^2 q_m \mu_o} \frac{M}{1+M} \qquad (11)$$

for the capillary over viscous forces ratio, in which L is the reservoir length, p_c^* is the characteristic transverse capillary pressure, k_m is the average matrix permeability, H is the reservoir thickness, q_m is the total Darcy flow velocity in the matrix, μ_o is the oil-viscosity, M is the mobility ratio and:

$$N_{gv,f} = \frac{\Delta\rho g L k_f}{H q_f \mu_o} \frac{M}{1+M} \qquad (12)$$

for the gravity over viscous forces ratio, in which $\Delta\rho$ is the density difference of the injectant and the oil, g is the gravity constant, k_f is the average fracture permeability and q_f is the total Darcy flow velocity in the fracture.

The total Darcy flow velocity is approximated by the oil inter-block flow in a gridblock in the middle of the reservoir in the matrix or fractures and is averaged over time. This approximation is good in homogenous reservoirs. However in more heterogeneous reservoirs an average over a vertical line of gridblocks is needed to have a proper approximation of the Darcy velocity. The density difference during WAG injection is taken as an average, related to the WAG ratio, of the water, gas and oil density.

2.3.2.6 Results and Discussion

Several simulations have been run to validate the proxy model that can be seen in **Figure 8 and Figure 9**. A top view of a combination of response surfaces is shown in **Figure 8** where the maximum recovery is used to select the response surface at each point. For detailed explanations of these design concepts see chapter 4. The recovery after four years of gas injection, WAG 1:3, WAG 3:3, WAG 3:1 and water injection as function of the capillary to viscous and gravity to viscous forces can be determined relatively easily. In **Figure 9** the three-dimensional plot of the five response surfaces can be seen. It is clear that in the gravity-dominated area the injection of gas is the most efficient. Towards the more capillary-dominated area the injection of more water becomes very important. However it is very clear that the injection of only water is in every case less favorable. Two runs have been investigated in more detail to get more insight in why the WAG injection is, under a certain balance of forces, working better than gas injection and why worse. These runs have been modeled using 40 by 40 grid blocks aerially and 40 (dual) in the vertical and were run for 10 years. The position of the two runs, **a** and **b**, in the forces-chart can be seen in **Figure 8**.

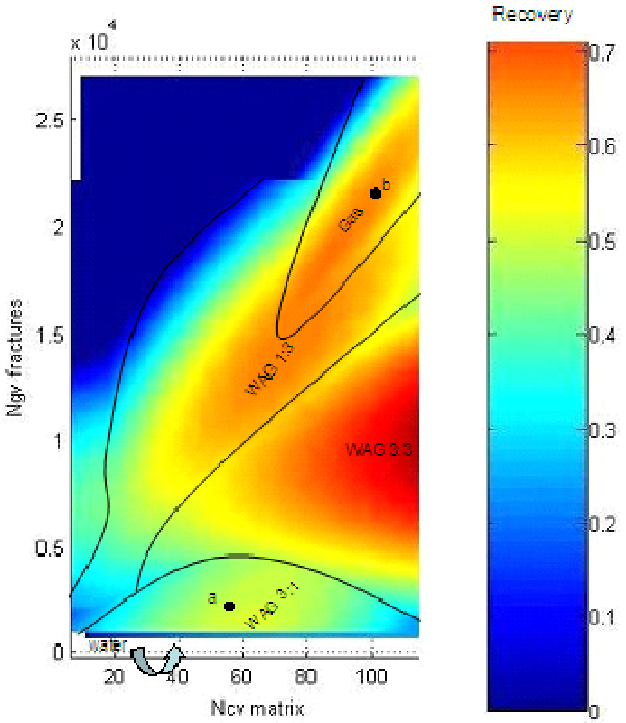

Figure 8: The top view of the overlaying different response surface models of the five injection methods. Recovery is displayed as function of the main physical forces

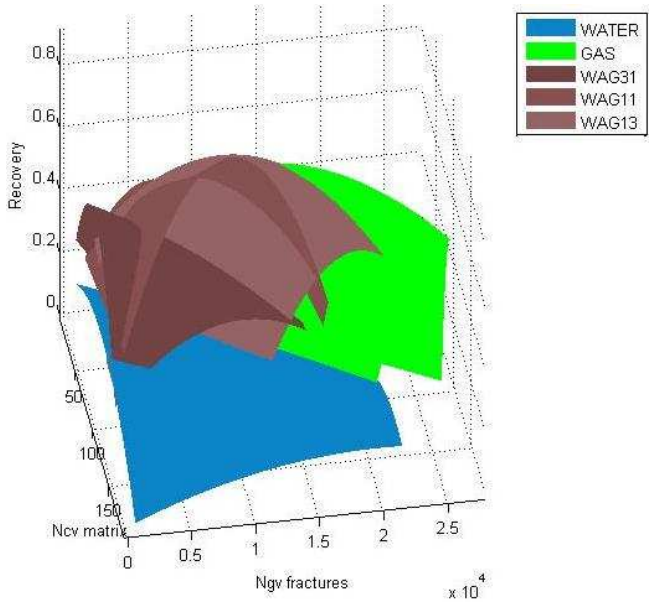

Figure 9: The 3D view of the response surface models

One of the key results here is that the response, in terms of recovery, of a fractured reservoir can be described by the two force ratios. These are the capillary over viscous forces ratio in **Equation 11** and the gravity over viscous forces ratio in **Equation 12**. It can be seen in **Figures 8 and 9**, which were fit and validated with several runs, that these forces work for water floods, gas floods and WAG floods. This is the first time that an experimental design approach has been shown to work in estimating the performance of water floods, gas floods and WAG floods in fractured reservoirs.[15]

Successful WAG injection

There are two processes that can be identified as the cause of the success of the WAG injection. The first is the delay of the breakthrough time of the injected gas and the second is the better macroscopic sweep of the combination of gas and water injection.

If we take a closer look at the two runs, run **a** and run **b** in **Figure 8**, it becomes very clear that the time until the breakthrough of gas and water is crucial in the performance of the WAG injection. Point **a** is a run where viscous- and capillary-forces are dominant over gravity-forces. In **Figure 10** we can see that due to the injection of water cycles the

gas breakthrough is delayed for almost a 1000 days. The water is imbibed into the matrix much better because of the high capillary forces. A lot of extra production is created early in the life of the field, which is, regarding the time-value of money, economically very positive. If we are looking at a run where we are injecting the same amount of gas in the same period of time as during the WAG injection, the time till breakthrough is much shorter. So the water is actually preventing the gas from fast breakthrough.
If we look at point **b** where the gravity-forces are dominant over capillary- and viscous-forces, we see that the water is rushing through the fractures much faster than the gas and a fast water breakthrough is occurring. The injection of only gas is, in this case, favorable over the WAG injection. In **Figure 11** the loss of production due to the fast water breakthrough can be seen.
The better macroscopic sweep is due to the difference in density; gas is lighter than oil and has a preference of flowing to the top of the reservoir and water is heavier than oil and has a preference to flow to the bottom of the reservoir. The combination of the two increases the overall sweep efficiency.
In a visualization program both processes can be seen if we depict the matrix oil saturation of run **a** in our reservoir. The water bank that blocks the gas from flowing fast to the producer and the overall better efficiency can be seen in the upper part of **Figure 12.** In the lower part of **Figure 12** the large unswept zone at the bottom of the reservoir can be seen if we inject only gas.

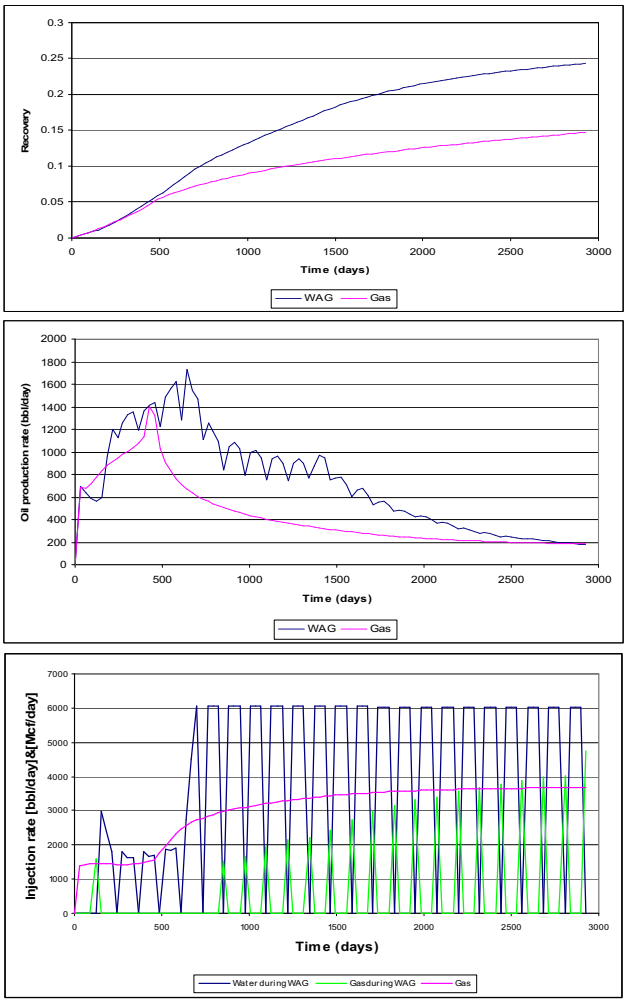

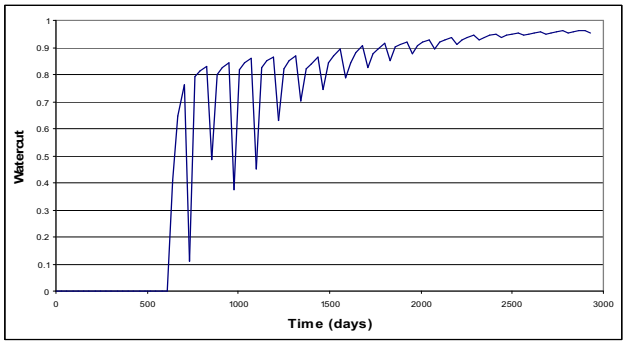

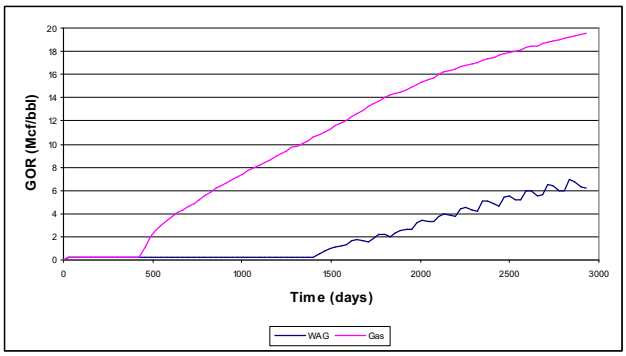

Figure 10: The charts of the good performing WAG injection

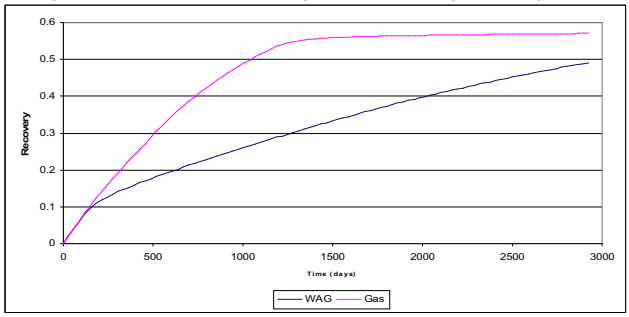

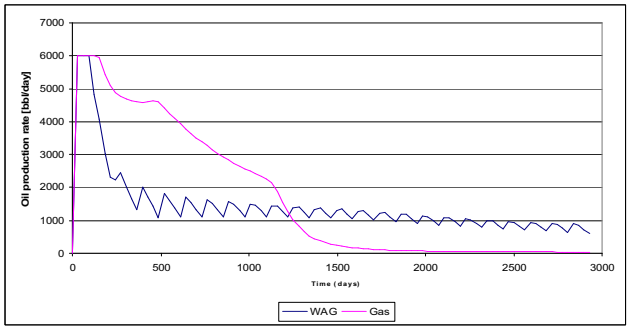

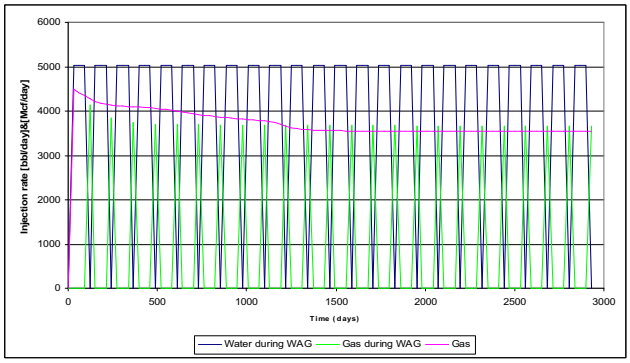

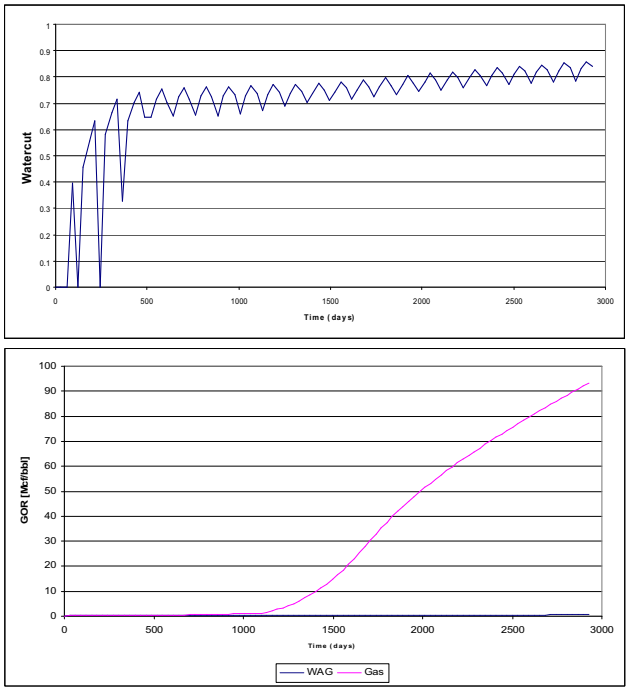

Figure 11: The charts of the bad performing WAG injection

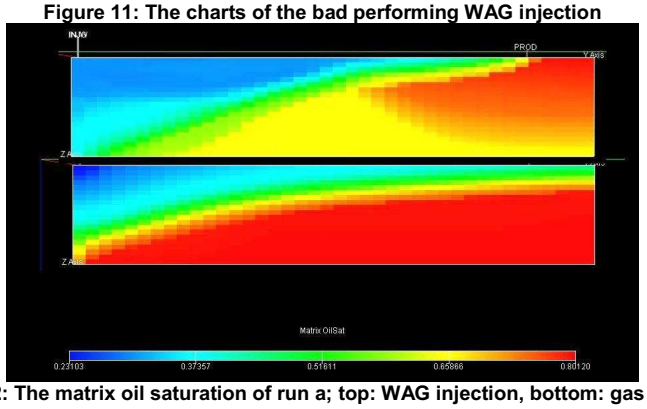

Figure 12: The matrix oil saturation of run a; top: WAG injection, bottom: gas injection

2.4 Conclusions

The WAG process has been shown to be beneficial over gas or water injection in 2 different reservoir types. In the conventional reservoir a single reservoir model is shown where a base and optimized WAG flood are compared to water injection and gas injection base cases. WAG results in large increases in recovery but also results in a small increase in gas production. Although much of this can be attributed to extending the peak production period, gas production may be an issue. Reduction of water injectivity was a problem with some of the WAG ratios but not a problem in the optimized case.

As discussed earlier the 2 major issues in WAG are early breakthrough and loss of injectivity. Early breakthrough of gas in the fractured reservoir was mitigated by the water cycles and helped increase the recovery. Injectivity was much less of an issue in fractured reservoirs.

Smart wells were used in the sense that the well could be shut, tested and reopened, but not used in a proactive control mode. As the geologic features creates a natural path for early gas breakthrough even with an optimized WAG flood the use of smart wells should be investigated in conjunction with WAG. Chapter 3 will introduce the use of smart wells and provide examples of their benefits.

References:

1. van Lingen, P.P., Barzanji, O.H.M., van Kruijsdijk, C. P.J.W., “WAG Injection to Reduce Capillary Entrapment in Small-Scale Heterogeneities”, paper SPE 36662, SPE Annual Technical Conference Denver, Colorado, U.S.A, 6-9 October 1996
2. Eclipse Reference Manual 2005a, Schlumberger Information Solutions, 2005
3. Green, J.W., Willhite, G.P., “Enhanced Oil recovery”, SPE Textbook Vol. 8, 1998
4. Stalkup, F.I.: Miscible Displacement, Monograph Series, SPE, Richardson, Texas (1980)
5. Christensen, J.R., Stenby, E.H., Skauge, A., “A Review of WAG Field Experience”, SPE 71203, SPE Reservoir Evaluation & Engineering April 2001
6. Rogers, J.D., Grigg, R.B., “A Literature Analysis of the WAG Injectivity Abnormalities in the CO_2 Process”, paper SPE 73830.
7. J.J. Taber, F.D. Martin, R.S. Seright, “EOR Screening Criteria Revisited - Part 1: Introduction to Screening Criteria and Enhanced Recovery Field Projects”, SPE Reservoir Engineering Volume 12, Number 4 August 1997 Pages 189-198
8. Barenblatt, G.E., Zheltov , I.P. and Kochina, I.N., 1960, “Basic Concepts in the Theory of Homogeneous Liquids in Fissured Rocks”, Journal of Applied Mathematical Mechanics(USSR)
9. Warren, J.E. and Root, P.J., “The Behavior of Naturally Fractured Reservoirs”, SPE Journal, Sept. 1963
10. Kazemi, H., Merrill, L., Portefied, K. and Zeman, P., “Numerical Simulation of Water-Oil Flow in Naturally Fractured Reservoirs”, SPE Journal, Dec. 1976
11. Sarma,P., June 2003, "New Tranfer Functions for Simulation of Naturally Fractured Reservoirs with Dual Porosity Models", MS Thesis Stanford University
12. Boerrigter, P.M., van de Leemput, B.L.E.C., Pieters, Johan, Wit, Krijn, Ypma, J.G.J., Koninklijke/Shell E&P laboratorium,”Fractured Reservoir Simulation: Case Studies”, SPE 25615 Middle East Oil Show Bahrain, 3-6 April 1993
13. Gurpiner, O, Kossack C.A., “Realistic Numerical Models for Fractured Reservoirs”, SPE 59041 SPE International Petroleum Conference and Exhibition, Villahermosa, Mexico, 1-3 February 2000
14. Dengen Zhou, Fayers, F.J., and Orr, J.R., “Scaling of Multiphase Flow in Simple Heterogenous Porous Media”, SPE 27833 SPE Ninth Symposium on Improved Oil Recovery, Tulsa, Oklahoma, USA, 17-20 April 1994
15. Heeremans, J.C., Esmaiel, T., and van Kruijsdijk, C.P.J.W.: Feasibility Study of WAG Injection in Naturally Fractured Reservoirs, SPE 100034 SPE/DOE Symposium on Improved Oil Recovery, Tulsa, Oklahoma, USA, 22-26 April 2006

Chapter 3 Well types

Wells have existed throughout most of the history of mankind. According to Greek historian Polybius the first documented horizontal wells were constructed in Iran more than 2000 years ago. Modern historians believe similar wells were used in Egypt's Western Desert 2500 years ago. These wells were known as ghanats in Farsi, and foggara or phalaj in Arabic. These wells targeted shallow aquifers, but the history of horizontal well applications in the oil industry date more recently.

Modern equipment allowing for high temperature and pressure wells up to 400F and 16000 psi allow acess to deeper reservoirs. Also, improved drilling techniques including offshore technology have allowed wells to reach areas previously unreachable. Russian scientists drilled a study well to a depth of 12.262 km, or about 7 miles, to take core samples and study the Earth's crust. Oil wells do not reach this depth but routinely are over 10000 feet deep.[1] For reference, it is about 4,000 miles to the center of the Earth so the world's longest hole reached 0.175% of the way. Wells are routinely drilled in over 5000 feet of water. In late 2003 the first well was drilled in over 10000 feet of water by ChevronTexaco in the Gulf of Mexico.

The first patents for horizontal or "extended reach" wells appeared in the 1930's and were commonly used after the 1950's. These have gained popularity in the past 20 years as drilling technology has advanced dramatically. **Figure 1** shows the dramatic increase horizontal well reach achieved in the early 1990's. By the beginning of this decade milestones such as 35000 feet of vertical displacement at over 5000 feet depth was reached at the Wytch Farm[2] field in the UK. The water flooding example discussed earlier and in this chapter incorporates a horizontal injection and production well in a simplified 2-d oil / water areal reservoir.

A conventional well is a vertical well. Many pilot studies still use conventional vertical wells. Early water floods were known as circle floods as the water bank tended to grow in a circular pattern extending from the injection well. As water entered a production well, it was switched to an injector. Two decades later the first 5-spot pattern flood was performed in Pennsylvania in 1924. The WAG floods in this study use an inverted 5-spot pattern with a central injector and 4 producer wells.

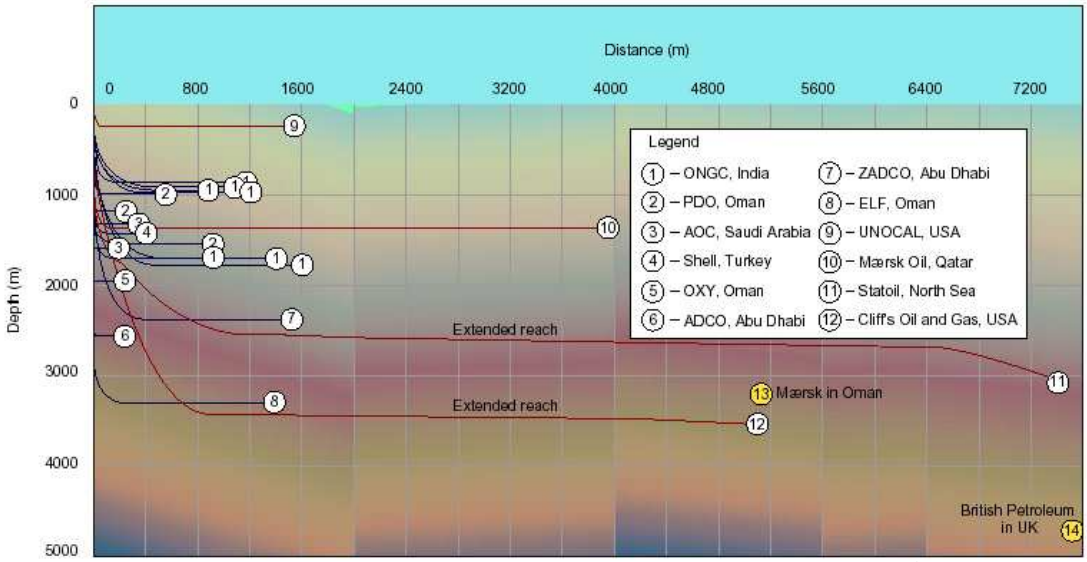

Figure 1: Comparison of selected wells drilled in 1990 (blue) and 1994 (red).[2]

3.1 Conceptual Benefits of Smart Wells

Smart or intelligent wells involve downhole measurement and control technologies added to a conventional or nonconventional well. The measurement devices ideally can read flowrate (total and phase), pressure and temperature. The control is achieved by a number of interval control valves (ICV) that can be open / shut or variable. **Figure 2** is a schematic of a simple smart well that can independently control the inflow from 2 separate production zones.

Early applications of smart wells concentrated on the commingled production from isolated zones as seen in **Figure 2**. Later applications apply the benefits of smart wells in a continuous production zone. The models used in the chapter fall into the latter category.

Smart wells have 2 key elements to their operation. These are measurement and control. Here flow rates and pressures are measured for each production interval in the well, and the valves can be closed to control the flow in each well segment. The simplest control scheme used here in the early stages of the studies involves a reactive control scheme. Here the constraints on a well determine when an action takes place. When the GOR or water cut constraint is reached, the worst offending production zone is closed.

The main objective of this phase of the study is to investigate the value of smart wells.

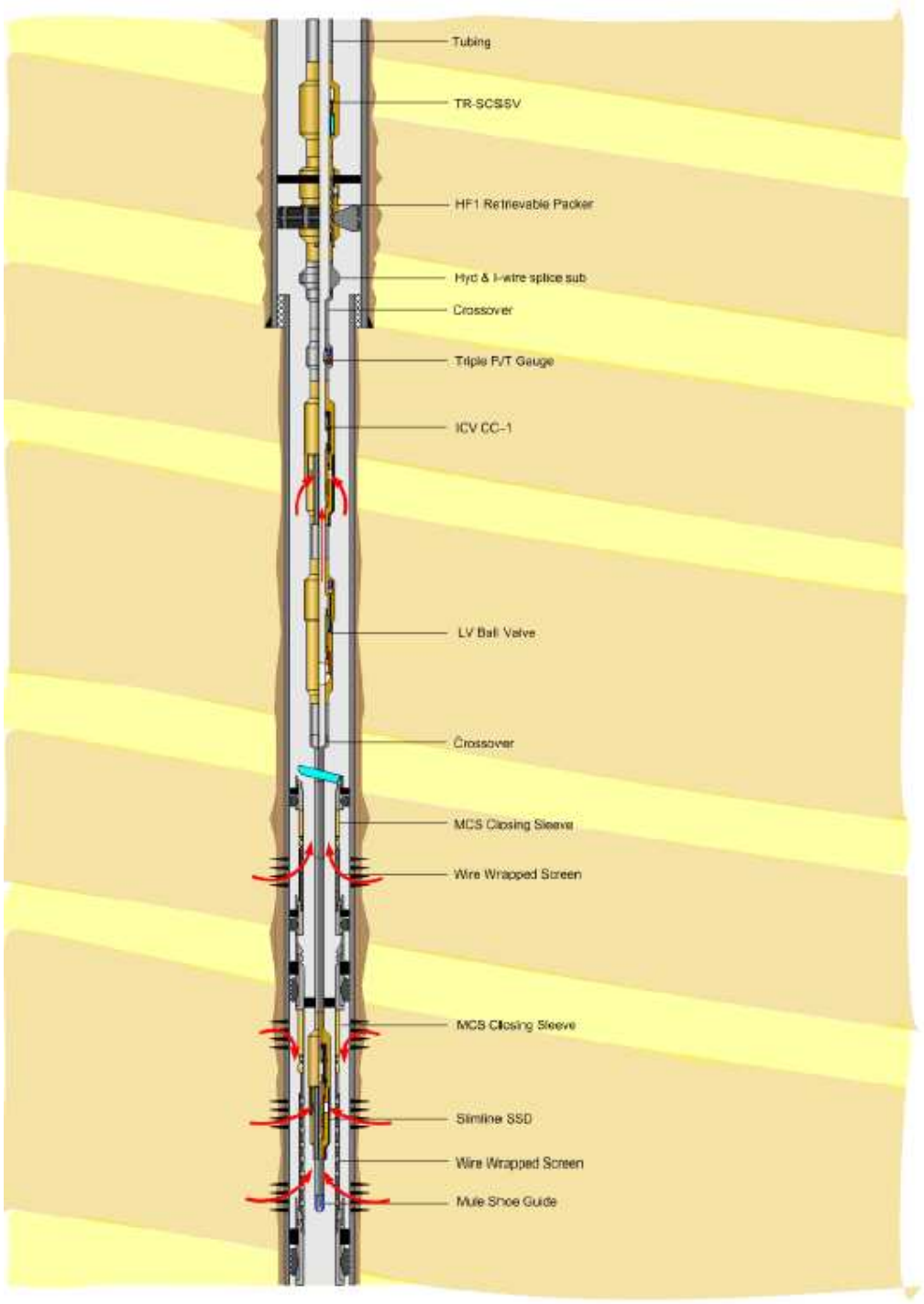

Figure 2: – Schematic of a smart well.

3.2 WAG Pilot Study

The model described in Chapter 2 is used here to demonstrate the viability of using smart wells in the WAG flood of a carbonate reservoir. The simplest of smart wells is used in this demonstration where reactive control of the ICV's is used to keep the wells within their constraints. Each production well is divided in 2 sections each being controlled. Additionally the valves are open / shut and not continuously variable valves meaning that if the well violates a production constraint, the worst offending connection is closed.

3.2.1 Scope for Improvement

The first thing management will usually ask is the improvement in the ultimate recovery of the field. **Figure 3** shows the improvement of the project oil recovery that shows a significant 39% increase by adding the simplest of smart wells in a reactive control mode. The smart well case shows an increase in gas production during the early years of the project as seen in **Figure 4**. This may raise some concerns until an analysis of the field GOR is seen in **Figure 4a**. The increase in gas production is primarily due to the drastic increase in oil production early in the lifespan of the reservoir.

One of the wells cannot stay open for an entire month without smart well controls and the 4 wells operate inefficiently. The GOR constraint causes frequent shutdowns in the base case as seen in **Figure 4b**. Peak production is maintained for over 2 years with the smart wells.

Water production was minimal in both cases although in percentage terms the smart well produced 4 times the water. In a full economic analysis the water production is insignificant in these 2 production scenarios.

Net Present Value (NPV) is a standard tool in capital budgeting for evaluating long-term projects. In its basic principles, a project with a positive NPV should be undertaken, and higher NPV's are preferred. The full scope of improvement in the NPV was also analyzed. The NPV is defined as:

$$\text{NPV} = \sum_{t=0}^{n} (f_o r_o - f_w r_w - f_g r_g) \frac{1}{(1+b)^t} \qquad (1a)$$

$$\text{NPV} = \int_{t=0}^{n} (f_o r_o - f_w r_w - f_g r_g) \frac{1}{(1+b)^t} dt \qquad (1b)$$

Where q is a flow rate, or total flow over a discreet time, r is a revenue or cost associated with the production of each fluid, and b is the discount rate. The discount rate is used to discount future cash flows to their present value. For a continuous model such as flow estimated from a decline curve, the integral model may be used, and when a reservoir simulation is used, the discreet discounted cash flow model for NPV in formula 1b is used.

NPV is a function of the oil produced as well as the gas and the water produced. This means the improvement is a result of mitigating gas and water production in conjunction with the improved sweep efficiency although it must be noted that water production was minimal at all stages. All the positives are seen in this optimization except that a few hundred extra barrels of water were produced over the entire time span of the project.

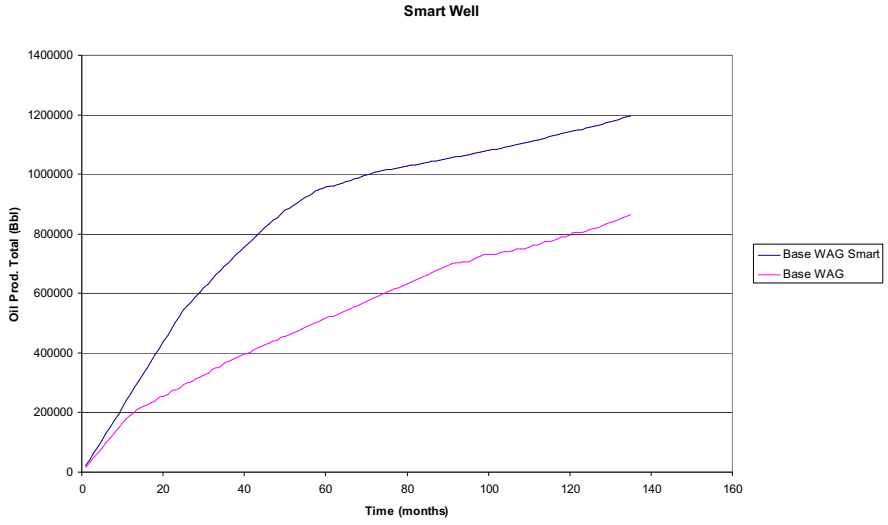

Figure 3 – Field oil production for a conventional well and smart well under WAG.

The re-active smart well results in a large increase in ultimate recovery. With the constraints for GOR and water-cut in place and not violated it is interesting to see how the flows for each of these phases has changed.

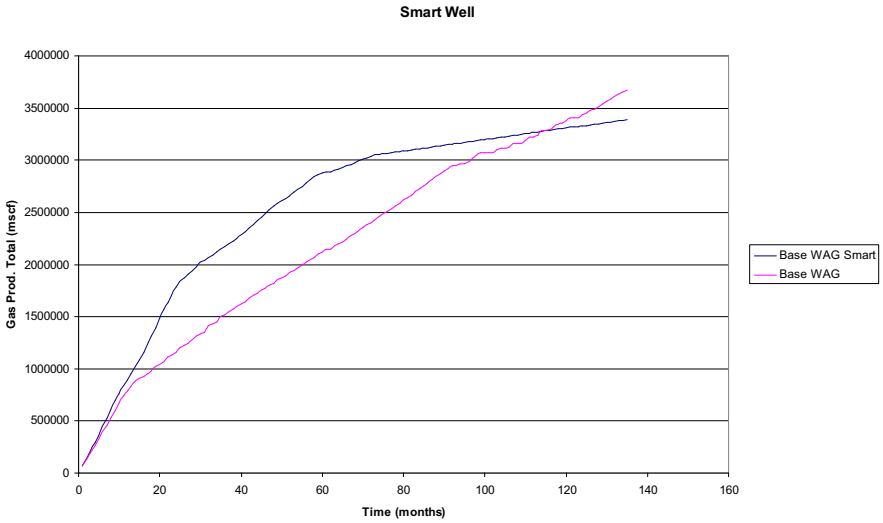

Figure 4 – Field gas production for a conventional well and smart well under WAG.

Total gas production remains almost the same but much more gas is produced earlier in the life of the reservoir. To further investigate the gas production, a look at the GOR is important.

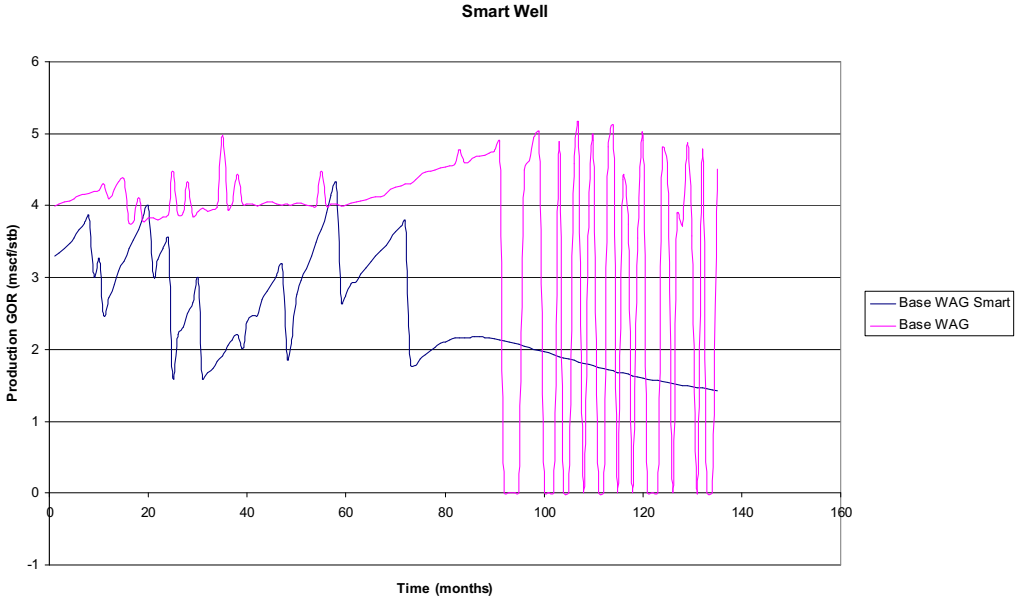

(a)

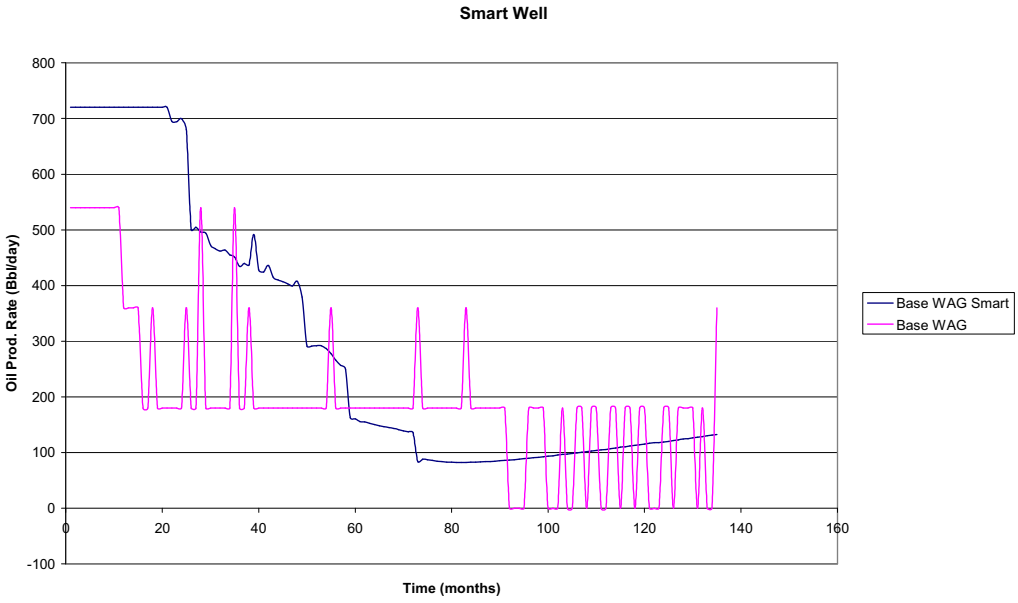

(b)

Figure 5 – (a) Field GOR for a conventional well and smart well under WAG. (b) Field daily oil production for a conventional well and smart well under WAG.

Figure 5 provides a handful of interesting insights into these 2 simulations. In pink is the conventional well showing very erratic behavior. The spikes in the GOR correspond the the opening and closing of the wells visible in the oil production rates. One of the producing wells cannot operate under the GOR constraints for more than a few days.

The re-active smart well in blue maintains peak production for 2 years and followed by a period of declining production. As segments of wells are shut, the well still is able to produce some oil yielding a smoother decline in production.

This stage of the analysis shows the major benefit of measurement and control. The control scheme in place is re-active and therefore only requires production rates at the well segments to control the wells. Here a significant increase in recovery and economics results from a control scheme that does not require perfect knowledge of the reservoir.

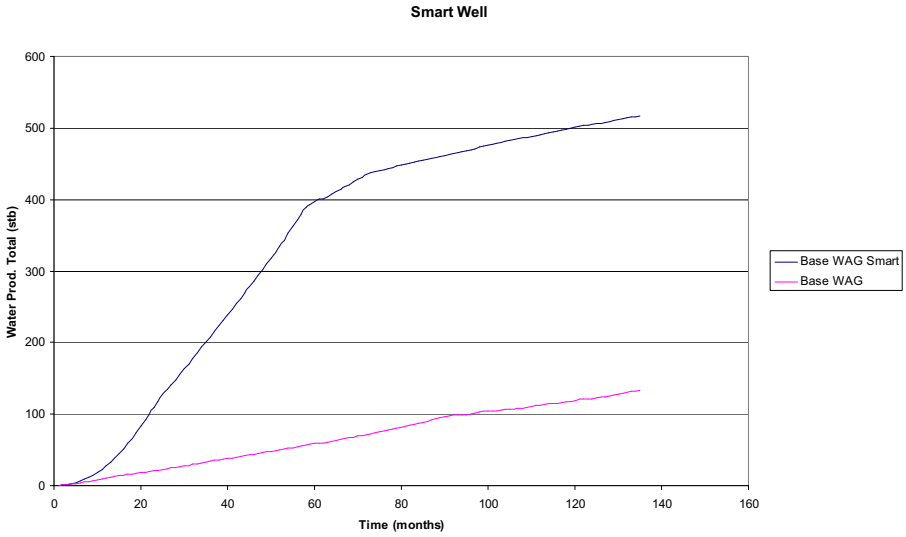

Figure 6 –Field water production for a conventional well and smart well under WAG.

Water production is minimal for both well configuration and plays no role in the well controls. The water production also has little influence on the economics of this project.

To gain broader insight into the robustness of the control scheme the next step is to look at different geologic models.

3.3 WAG Pilot Study on Multiple Realizations

This study presents an approach similar to section 3.2 but with multiple realizations of the model. Each model is precisely known for the purposes of the numerical simulation, but unknown as far as the control scheme is concerned. The reactive control scheme again only requires the flow rates for each well segment at the producers.

This approach will test the robustness of the reactive control scheme. The information will provide insight into when the control works best, with limited success, or even when it may not work.

3.3.1 Scope for Improvement – Smart Well

The ranges for the reservoir parameters and the choice of WAG ratios can be seen in **Table 1**. Twenty-seven simulations, all successful, were run covering every combination of the 3 parameters. This results in a distribution of recovery for the conventional and smart well cases. All production wells are placed on a reactive control mode at this time.

The reservoir simulation model was run for 10 years with the oil recovery at 10 years recorded. The models prior to optimization provided an average recovery of 15.5% with a standard deviation of 1.25% after 10 years. Additionally the range was limited to 13.1% to 17.1% for the conventional well as can be seen in **Figure 7**.

Incorporating the smart wells with a reactive optimization strategy significantly increased the recovery. By optimizing only the production settings the average recovery is raised to 35.5% with a deviation of 2.7%. **Figure 7** shows the assessment of recovery distribution for the conventional well case. **Figure 8** shows the assessment of recovery distribution for the smart well case.

Relative Range	Low	Medium	High
WAG Ratio	1:03	3:03	3:01
Areal Perm. Multiplier	2	4	6
Mobility Oil	0.9	1	1.1

Table 1: Parameter Ranges for the simulations

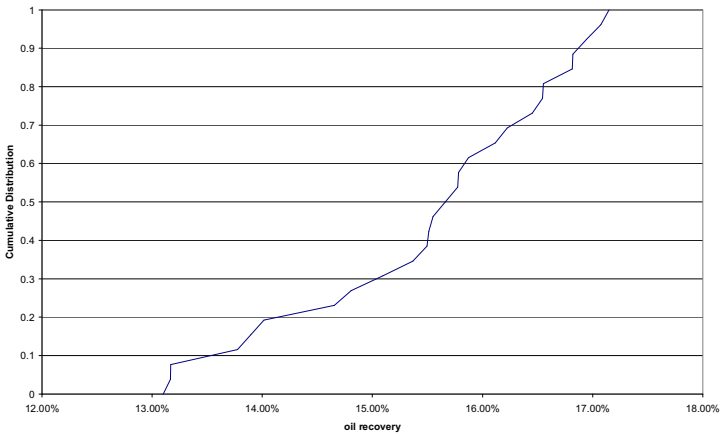

Figure 7: Oil recovery distribution with conventional wells. From 27 simulations.

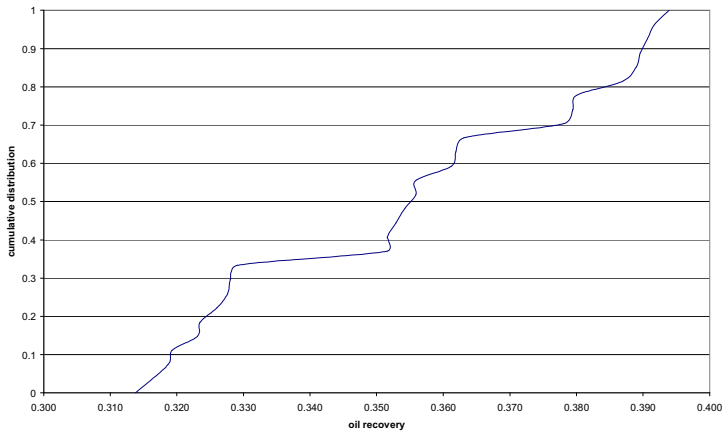

Figure 8: Oil recovery distribution with smart wells. From 27 simulations.

Two primary observations can be made from the increase in recovery and the decrease in standard deviation. First, the improvements seen with the reactive control appear to be robust as they work over the range of models seen here. Second, as the standard deviation is decreased with the smart wells, this shows that the worse the production problems are, the better the improvement is. The reduction in the associated risk is also apparent as the decision maker is able to narrow the range of the possible outcomes.

3.3.2 Scope for Improvement – Smart Well and WAG ratio

In the previous control scheme the reactive control required information only at the production wells. What if the reservoir model is known? The WAG ratio is an operational parameter controlled by the operator. It is therefore possible to optimize the WAG ratio within the reactive smart well control environment. This section further improves the recoveries seen in the previous section.

Figure 9 shows the assessment of the distribution of recovery for the optimized smart well with the optimal WAG setting. Each model is assumed to be perfectly known and therefore the optimization is unique to each realization. This is where this optimization requires more data than for the reactive control seen previously.

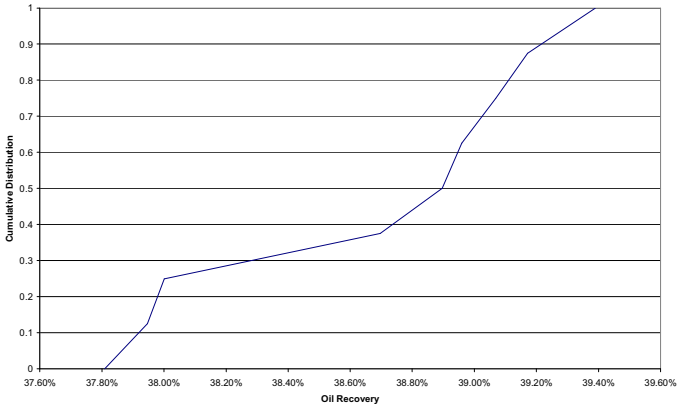

Figure 9: Oil recovery distribution from 27 reservoir realizations with smart wells. The optimal control of the WAG ratio with a reactive control of the valves is shown in this figure.

Incorporating an optimization of the WAG ratio, as done in Chapter 2, the average recovery is raised to 38.6% with a standard deviation of 0.59%. Optimizing the WAG ratio in combination with the reactive control scheme also improves the robustness of the control scheme and reduction in the risk.

3.4 Fractured Reservoir

A reactive control scheme was successfully implemented in the previous section so the control scheme is now tested on a different reservoir. Described in the previous chapter the flow physics in a fractured reservoir is different than in a conventional reservoir.

The producers were divided into two sections each controlled in a reactive manner. The simulation results to within 0.01% recovery were identical with and without the smart wells in place. The reactive control only provides control near the wellbore of the producer. In the previous reservoir the viscous forces in the near wellbore region were influenced by the well control. In the fractured reservoir the only control occurs in the fractures and not in the matrix. The gas immediately moves from the worse offending connection, which is closed, to the nearest connection through the fractures bypassing the matrix.

In the previous section an optimal control of the WAG ratio was implemented to improve the recovery. What is ideally required is an optimal control of the valve operations, on the injectors and producers, which influence the flow patterns in the entire reservoir. The high permeability fracture system precludes this kind of control in naturally fractured reservoirs.

3.5 Waterflood w/OCT

The model used here was developed by Brouwer[3] and represents a dynamic or proactive optimization using optimal control theory. This was tested on a waterflood model because the adjoint was not available at the time for a WAG flood and the CPU time would have been prohibitive. Traditionally operators operate wells using what would be described as a heuristic algorithm, or intuitive approach to optimization. This means that the operator waits to see water breakthrough before choking the well to control water influx. This does not lead to an optimum drainage of the reservoir although it is an improvement over no control. This is the control scheme previously referred to as reactive control.

Optimal control theory implemented in the optimization algorithm used allows for dynamic water flooding control. The optimization objective used was NPV for a given time under rate constraint. The total injection / production of the wells are kept constant and the rates are allocated over the different sections of the well. This is the same NPV model described earlier, but with no gas in the system.

3.5.1 Simulation Model

The reservoir model is 300 by 300 by 10 m, modelled using 30*30 grid blocks. A horizontal water injection well and a horizontal production well are placed at either side of the reservoir section with all sides bounded by no flow boundaries. Each well is divided into 30 segments allowing individual flow allocation to each segment of the well. A high permeability streak is set perpendicular to the well direction connecting the two wells as can be seen in **Figure 10**. The two phases, oil and water, are at unit mobility ratios and the model is of uniform porosity.

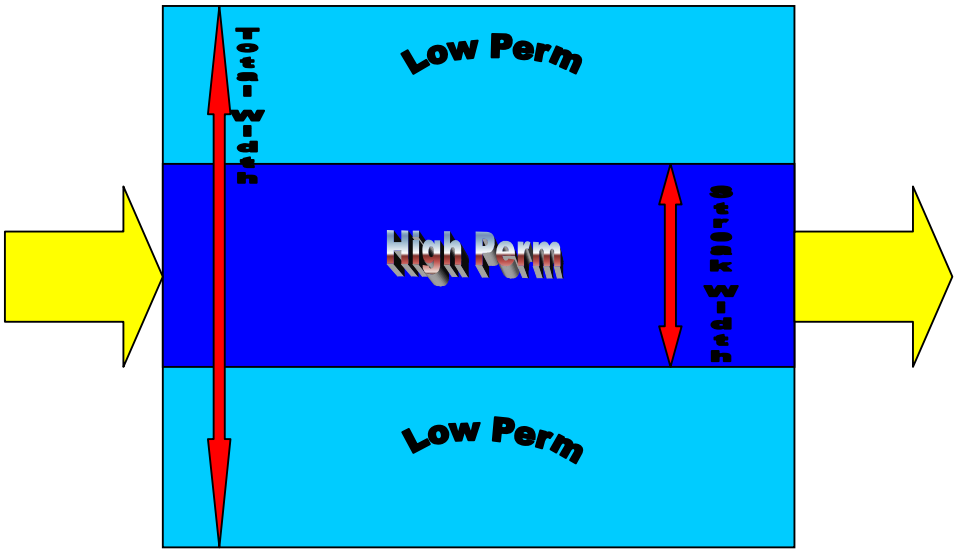

Figure 10 – Waterflooding with horizontal smart injection and production wells.

3.5.2 Scope for Improvement

Figure 11 shows how the flooding pattern is optimized with smart wells. The first picture shows the water shooting through the high permeability streak without sweeping the reservoir very efficiently. The second picture shows intermediate iteration in the water flooding optimization process showing the injection front moving more stable.

The full scope of improvement in the NPV is seen by looking at the definition of NPV. The NPV is a function of the oil and the water production. This means the improvement is a result of mitigating water production in conjunction with the improved sweep efficiency. **Figure 12** shows the production curves for one of this simulation run. All the positives are seen in this figure. This includes delayed water breakthrough, and extended peak oil production as well as larger cumulative oil production and lower cumulative water production.

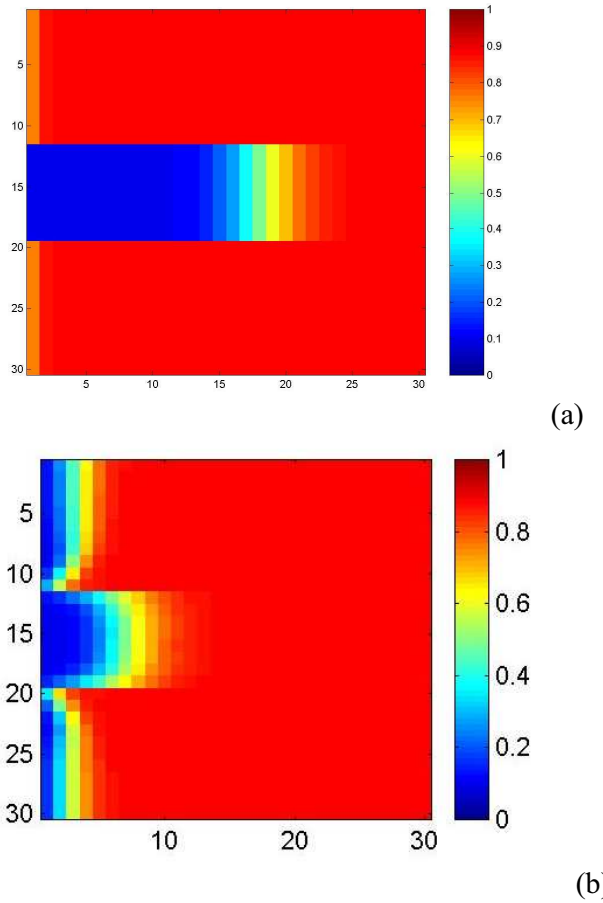

Figure 11 – Injection front for conventional well (a) and smart well (b) showing improving front propagation.

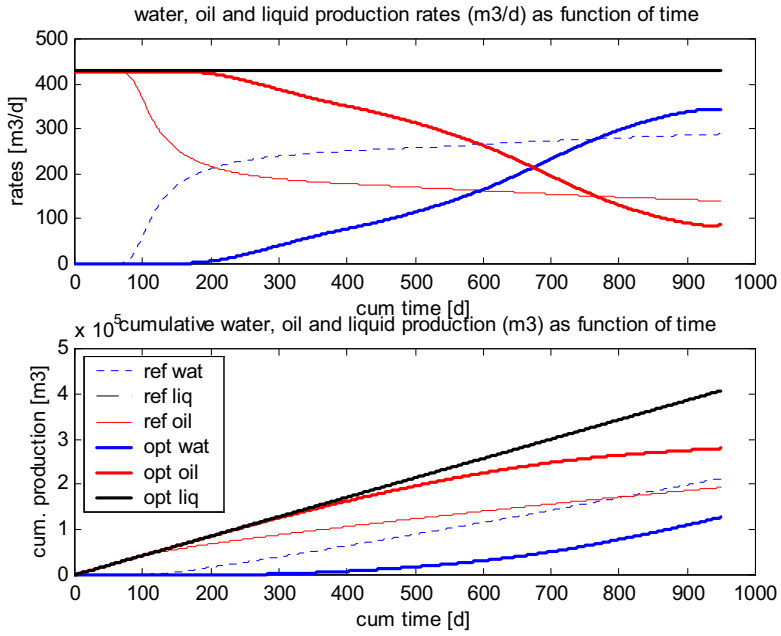

Figure 12 – Comparison of oil and water production with conventional and smart wells (1 example).

The proactive optimization by optimal control theory requires knowledge of the simulation model. The primary benefits include adding control of the injector to the scheme providing influence over a larger area of flow, and using the derivative information to anticipate breakthrough problems and mitigate them rather than waiting for problems to occur and reacting to them.

3.6 Conclusions

The flexibility of smart wells allows improved control of production significantly improving global sweep of the reservoir. The selective shutdown of different portions of the well resulted in an improved recovery of 39% for the WAG model in a giant carbonate reservoir. The performance though can vary widely depending on the properties of the reservoir but has been shown to be fairly robust.

One of the major benefits of smart wells is the ability to react to unforeseen flow events such as early breakthrough. This is done with some influence in the near wellbore flow region. One example of a reactive smart well providing little benefit was in a highly fractured reservoir. As there is a small viscous component and a high permeability fracture conduit between the 2 sections of the wellbore, the fracture short circuits the smart well therefore providing no benefit.

A proactive OCT based optimization requires knowledge of the reservoir, but allows control of the flood fronts for improvements in recovery economics. Though the value of flexibility is high, how sure is one of the single model used. One major issue in all reservoir engineering studies is the treatment of the uncertainties in the reservoir. The next chapter will address these issues through a systematic design approach to relate uncertainties to performance.

References:

1. Minerals Management Service, "New World Water-Depth Drilling Record Set in Over 10,000 Feet of Water," November 18, 2003. (press release)
2. Nurmi, R.: “Horizontal Highlights,” Middle East Well Evaluation Review, Nov. 16, 1995
3. Brouwer, D.R., and Jansen, J.D.: “Dynamic Optimization of Water Flooding using Optimal Control Theory” SPE Journal, December 2004, pgs. 391-402

The grand aim of all science is to cover the greatest number of empirical facts by logical deduction from the smallest number of hypotheses or axioms.
Albert Einstein (1879–1955)

Chapter 4 Uncertainty and Design

4.1 Concept of Uncertainty

Frank H. Knight[1] made a famous distinction between "risk" and "uncertainty". In Knight's interpretation, "*risk*" refers to situations where the decision-maker can assign mathematical probabilities to the randomness. Knight's "*uncertainty*" refers to situations when this randomness "cannot" be expressed in terms of specific mathematical probabilities.
John Maynard Keynes said:

> "By `uncertain' knowledge, let me explain, I do not mean merely to distinguish what is known for certain from what is only probable. The game of roulette is not subject, in this sense, to uncertainty...The sense in which I am using the term is that in which the prospect of a European war is uncertain, or the price of copper and the rate of interest twenty years hence...About these matters there is no scientific basis on which to form any calculable probability whatever. We simply do not know."

Many economists argue this distinction so here a definition will be provided as to how risk and uncertainty are treated in this text.

In the context of these reservoir engineering studies uncertainty is used as the mathematical probability that can be assigned to a factor. This can be for example the ranges of permeability or other rock / fluid parameters as well as the available ranges for valve setting or injection / production parameters. In this study they are treated in 2 different manners.

To perform the studies a number of simulations are run to relate the output of the simulation, i.e. Recovery or NPV, to the parameters in the simulation. In constructing the design described below the parameters are assigned an uncertainty range from high to low. At this stage all parameters are only assigned a range and not any distribution. This is used for the generation of the response surface models (i.e. proxy models). The proxy model is an algebraic expression that relates the input parameters to the output. The model is trained and tested to fit the output from the flow simulations.

The fitted response surface model then acts as a proxy to the flow simulation. This proxy is a function that acts as a substitute to the flow simulator. The posterior analysis of the proxy model implements different mathematical models for the description of the randomness of the factors. These are typically models such as normally distributed porosity or lognormal distribution of permeability.

In the context of this study risk is associated with the resulting outcome or distribution of the objective function. The oil recovery, net present value or other measure does not have an assigned mathematical probability but is a function of the factors that do have an assigned probability. Therefore the risk is associated with a calculated range of expected monetary values, average recovery or another measure.

4.2 Design of Experiments – DOE

Reservoir simulation is too computationally expensive to typically allow a vast number of simulations to be performed. This problem grows quickly when more parameters are added as can be seen in **Table 1**. DOE[2,3] and the associated response surface (proxy) analysis allow for the reduction in the number of simulations as the number of regression parameters for popular choices of response surfaces increases far slower than the number of runs required for a full factorial design. Despite the huge reduction of computational effort, the resulting proxy models in general yield statistically significant results.

Number Parameters	Regression Parameters	3-level full factorial
4	15	81
5	21	243
6	28	729
8	45	6561
10	66	59049

Table 1: Growth in simulation requirements for full factorial design. The number of regression parameters is for a 2nd order polynomial with cross terms. With simulation times for the reservoir simulator ranging from 10 to 60+ minutes per run it becomes clear that a full factorial run is not feasible for more than 5 to 6 parameters.

There are two primary issues to be addressed in Experimental Design. The first is how to design an optimal experiment and the second is how to analyze the results of the experiment. First a set of definitions to better understand the concepts is provided.

Factors – input variables. These are reservoir parameters such as permeability, valve setting, or even WAG ratios.

Levels – The values of the factors scaled to a minimum represented as -1 and a maximum value coded to +1. A value of 0 would be the medium value in a 3 level design.

Design - List of experimental conditions. The matrix as shown in **Table 2** provides a full factorial 2-level, 3-parameter design indicating 8 simulation runs to be performed.

Responses – the system outputs such as the recovery, NPV or some other performance indicator. These are typically observed data or in these studies output from a reservoir simulator.

Response Surface Model (RSM) – function that is fit to the observed data from results of the simulation experiments. The functional form of the RSM is a polynomial equation of the factors specified in the design. The data being fit to the model is the simulation output, or response, obtained at factor values given by the experimental design.

Proxy model – the fitted RSM can be used as a proxy model for the reservoir simulator. The proxy, if done properly, is valid at all values between the minimum and maximum setting for each parameter and can therefore be used as a proxy for the simulator. The proxy is several orders of magnitude faster that the reservoir simulator facilitating Monte Carlo analysis.

Confounding – When factors are arranged such that some effects are indistinguishable from others. In other words higher order terms are lumped together. Terms of interest which are the main effect and first order interaction effects are not confounded.

Design Resolution (R) – certain interaction effects are confounded with other effects. The resulting design is not of full resolution. The resolution is where no *l*-way interactions are confounded with interactions of order <R-*l*.

Main effect – difference between the response, or average response in a multi parameter setting, of the factors at +1 and -1. These are especially important when performing screening studies as will be explained in the Plackett-Burman design below.

Interaction effect – parameters are often not independent of each other. The factors are said to interact when the effect of one factor depends on the effect of another. In other words the response of varying one factor on changes of another factor is set at a different level.

Saturated design – design where all interactions are confounded with "new" main effects. All information in this design is used to estimate the parameters leaving no degrees of freedom to estimate the ANOVA error term.

Full factorial design – design where all the terms are varied to try all combinations of settings. An example is shown in **Table 2** below.

	Scaled Setting		
	A	**B**	**C**
run 1	1	1	1
run 2	1	1	-1
run 3	1	-1	1
run 4	1	-1	-1
run 5	-1	1	1
run 6	-1	1	-1
run 7	-1	-1	1
run 8	-1	-1	-1

Table 2: A sample coded 2 level 3 parameter full factorial screening design.

In general there are 2 types of designs. These are classical and optimal experimental designs. Classical designs can best be explained as full and partial factorial designs.

To evaluate a full 3-level factorial design, 3^K (K: number of factors) experiments are needed. An experiment is defined as the combination of these factors. Obviously, as the number of factors increases, the number of experiments becomes more unmanageable and impossible to implement in a reservoir simulator as seen in **Table 1**. Partial factorial designs are notated as 2^{k-p} and provide a lower resolution model.

The first step to construct a design is to identify those factors that are expected to have a large influence on the response (e.g. cumulative oil production). Afterwards, the factor ranges are usually scaled to lie between "-1" and "1" to represent factor's maximum (1), minimum (-1) and mean (0) values. Factor ranges should be chosen carefully to avoid dominance of numerical error on the response (small ranges) and to decrease the possibility of construction of a complicated response model (large range). Then a design depending on time and computer power can be constructed. The combination of factors derived from DOE is used to feed into a simulator or to implement physical experiments.

Table 2 shows a sample screening design. This 2 level design allows for a faster assessment of the ranking of the parameters compared to a full 3 level design. For further quick screening a Plackett-Burman[4] design is used. This design looks at a partial factorial 2 level design that screens the main effect of a parameter. For the detailed study to be performed a 3 level optimal design is used. The responses from this design are used in creation of the proxy model.

Two designs were used extensively in this research. These are the Plackett-Burman design and d-optimal design. These are briefly described below.

4.2.1 Plackett-Burman[4] screening design

Initially a large number of factors must be screened at each time step. These are the status of each valve for each well as well as the WAG setting at the time step being optimized. To screen a large number of parameters the interaction terms are confounded with the new main effects. These new saturated designs would then have 2^k runs. The saturated design uses all the information in the design to estimate the parameters and therefore has no degrees of freedom to estimate the error.

Plackett and Burman provided a new way to fractionalize the full factorial yielding designs where the numbers of runs are 4*ceil((k+1)/4) rather than 2^k. In this example a choice of 8 runs can be used to cover the parameters rather than 16, 32 or 64 runs (k = 4, 5 and 6 respectively). The design becomes more flexible with larger numbers of parameters.

4.2.2 D-Optimal[3] Design

A D-optimal design attempts to minimize the average size of the variance matrix by minimizing the average eigen-value. A maximization of D-efficiency results in finding a design where the factor effects are maximally independent.

$$\textit{D-efficiency} = 100 * (|X'X|^{1/p}/n) \quad (1)$$

Where X is the regression matrix, p is the number of parameters in the model, and n is the number of observation point or simulations. The design is optimized for the response surface model the data will be fit to.

Optimal designs offer significant advantages over classic experimental designs. A D-optimal design can be modified to allow the number of simulation to be chosen independently. Therefore, the number of simulations runs, or experiments, is not limited to a partial factorial of the full set. Classic designs typically are not as flexible (more granular) in allowing the experimenter to control the parameters. The design can also be augmented to add additional runs if needed. This augmentation can be used to add additional factors to the study at a later time or provide testing runs to validate the model. This can be done while maintaining the optimality given the set of runs already performed therefore maximizing the additional information gained.

The design space is meant to encompass the entire range of the properties and not just at a single point. A cube would spatially represent the design space of 3 parameters with the volume and not just the corner points being of interest.

4.2.3 Response Surface Modeling

Response surface models (RSM) are parametric functions fit to the observed results from the reservoir simulation. The parameters of the RSM are determined by fitting these models to observed data from the results of the detailed reservoir simulations performed at parameter levels defined by the design. Through the design (and their functional form) the response surface models incorporate the effects of the input parameters on the response. These models become the proxy models desired in this study.

The observed data from the simulation, called the response is denoted y. In these simulations the response may be the recovery or NPV for the process being simulated. The true response function generally can be written as:

$$y = f(x^*_1, x^*_2, ..., x^*_k) + \cancel{error} \quad (2)$$

where x* are the input variables. The error term here is assumed to be zero since the true response function is the reservoir simulator. If the same experiment which is one simulation were run again the answer would be the same resulting in a zero error for the true response function. The expected value of y is transformed to E(y) and x* to x when the input variables are coded to the range [-1,1].

This results in:

$$\mathrm{E}(y) = f(x_1, x_2, ..., x_k) \quad (3)$$

where the simple first-order model can be written as:

$$\mathrm{E}(y) = \beta_o + \sum_{j=1}^{k} \beta_j x_j \quad (4)$$

where β_o is an estimate of the mean of y over the domain (design space) and β_j is an estimate of the gradient of y with respect to x_j. The resolution of this model does not typically allow for a statistically significant fit to the estimate y. As this model is too simple a popular RSM used in many modelling studies is the general second-order model.

The second-order model in general form is given as:

$$\mathrm{E}(y) = \beta_o + \sum_{j=1}^{k} \beta_j x_j + \sum_{j=2}^{k} \beta_{jj} x_j^2 + \sum \sum_{i<j} \beta_{ij} x_i x_j \quad (5)$$

that includes a constant, linear effects, single-term quadratic effects, and two-term interactions. The choice of models is subjective as it must be representative of a complex underlying process. When the process is fit to this simplified analytic model it must be validated.

Significance testing[5] of the models is performed in order to validate the results. The purpose of analysis of variance (ANOVA) is to test for significant differences between means. Wikipedia[6] defines ANOVA as:

> *In statistics, analysis of variance (ANOVA) is a collection of statistical models, and their associated procedures, in which the observed variance is partitioned into components due to different explanatory variables, usually called factors in Design of experiments.*

The purpose of analysis of variance is to test differences in means for statistical significance. The test is performed by analyzing the variance by partitioning the total variance into the component due to true random error and the components that are due to differences between means. These due to differences between means are then tested for statistical significance. The procedure that compares means is called analysis of variance due to the fact that in order to test for statistical significance between means, variances are actually being compared. Additionally, test runs at intermediate coded values, are ran to test the predictability of the model across the design space.

4.3 Five spot reservoir WAG

The model used here again represents a giant carbonate reservoir with 4 distinct layers apparent in the model. The correlation lengths were in the order of 2000 ft areally and strongly correlated vertically within each of the 4 layers. The top 40 ft and bottom 30 ft had average permeabilities of 10's of mD and in the order of 100 mD for the middle 80 ft of the reservoir. This reservoir is an ideal candidate for a miscible WAG flood as demonstrated in **Chapter 2**.

Wag floods as with most floods are sensitive to the parameters of the model being used. As the simulation model was derived from a larger model and in general is representative of a large section of the reservoir, determining the sensitivity to these input parameters is important. This section describes an experimental design approach to determining these sensitivities.

4.3.1 Results and Discussion

In this study, 80 different combinations of 6 factors on 3-level variations were constructed using a D-optimal experimental design as seen in **Table 3**. The regression analysis is then applied to fit the field oil production total (FOPT) by a polynomial quadratic function to the factor setting specified by the D-optimal design. Other responses like the total water (FWPT) and gas (FGPT) production also were considered. The correlation coefficient between response surface model and simulator's FOPT, FGPT, FWPT are 0.96, 0.95 and 0.61 respectively. This indicates a satisfactory match for oil and gas total production and a disappointing fit for total water production. The low correlation coefficient and hence the inappropriateness of the chosen RSM approach for FWPT is attributed to discontinuities in the response surface, since there are some sudden changes from low to no water production among the 81 runs. The water cut never went above 0.1% in the runs.

			Level		
Factor	Symbol	Unit	-1	0	1
Gas relative permeability end point	krge [X1]	-	0.8	0.9	1.0
Water relative permeability end point	krwe [X2]	-	0.4	0.5	0.6
Oil relative permeability curvature	kroc [X3]	-	0.5	1.0	1.5
Horizontal permeability correlation length	kcor [X4]	ft	973	1946	2919
Horizontal permeability multiplier	kh [X5]	-	1	4	7
Water viscosity	viscw [X6]	cp	0.3744	0.416	0.4576

Table 3. Factors ranges and scaling

The response surface model is employed to analyze the sensitivity of cumulative oil production to each individual factor and quantify the factor's effect on production. The sensitivity of the response to each factor is defined as the partial derivative of the response with respect to that factor. The Pareto chart **Figure 1** then demonstrates the most significant terms affecting the cumulative oil production in this study. As can be seen from the chart, eight terms that consist of some single terms (e.g. oil rel-perm curvature factor), some quadratic terms (e.g. correlation length squared) and some interactions between factors (e.g. product of '$k_{ro.c}$' and permeability multiplier (k_h)) have the largest effect on cumulative oil production. The interaction term of two factors implies that the effect of the one factor is more considerable when the other factor is moving towards its extreme. For example the cross term of '$k_{ro.c}$&k_h' is found to influence the oil production quite significantly. This means that the sensitivity of oil production to 'kro' is high when the value of horizontal permeability multiplier is high.

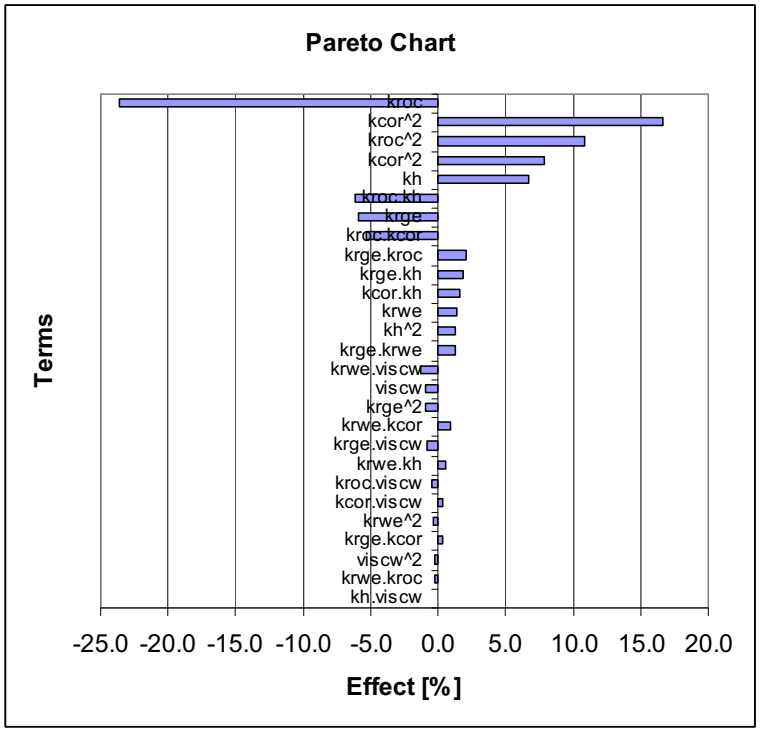

Figure 1. The Pareto chart shows the influence of each term on the cumulative oil production. An negative value leads to a reduction in FOPT.

Figure 1 shows the influence of each individual factor on the total field oil production. According to the graph, the cumulative oil production increases as the end-point of the gas relative permeability decreases. As the gas mobility increases, this leads to a faster gas breakthrough and consequently lower oil production.

Changes in water relative permeability and water viscosity show a negligible effect on the total oil production. The oil production increases as the water mobility increases which appears to be counter intuitive. This appears to be attributed to the fact that the loss of water injectivity is compensated by a more stable vertical front. This results in improved global sweep resulting in contacting more oil in the reservoir.

As the oil relative permeability curvature factor becomes smaller, the FOPT increases sharply. According to the 3-phase relative permeability model used by simulator[7], the smaller curvature factor shifts the oil relative permeability curve upward for both gas-oil and water-oil systems. Both increasing and decreasing the correlation length leads to an increase in cumulative oil production. Apparently there is an optimum within the interval given by the range. In the 5-spot pattern, the permeability field with scaled correlation length of 0 has a relatively higher permeable area near to the production well(s). Thus injected gas flows faster through this area and not only a lot of oil is bypassed but also gas reaches the production well causing well shut-in and consequently less oil is produced. However, this fluctuation leads to construct a permeability field with smaller higher permeable areas. Therefore the injection fluid can sweep the oil that exists in the higher permeable zone as well as the oil around that. Thus the breakthrough time for this model when the other factors are the same is delayed which implies greater production for model with k_{cor}=-1. On the other hand, the model with 'k_{cor}'=1 has been constructed with a correlation length comparable with inter-well spacing. The permeability field in this case shows almost a uniform distribution. As a result, there exists no considerable higher permeable area to cause early breakthrough of injection fluid. This model potentially yields larger oil production.

Two-dimensional slices (of the 6-dimensional design region) through the factor space can visualize the response surface model that is computed by regression analysis using the design matrix and cumulative oil production. Factors that are not plotted in each surface are adjusted to zero. The associated contour map of the interaction term can be used to identify the values of factors that maximize the production.

The response surface model can also be used to assess the risk in production as a function of the uncertainty in the reservoir. Having used the RSM model as a substitute for the cpu-intensive simulator, one can run as many Monte Carlo simulations as needed to analyze a distribution of factors. Of course, direct Monte Carlo simulation using a simulator will generally not be economically feasible , in particular if the number of factors increase which is why the RSM is so valuable.

4.4 WAG in Fractured Reservoirs

The second model discussed in this chapter is that of a WAG flood in a fractured reservoir. The reservoir model is 1,320 by 1,320 by 500 feet, modeled using 10 by 10 grid blocks aerially and 5+5 (matrix + fracture) in the vertical. One injector and one producer are placed in opposite corners and all sides are bounded by no flow boundaries. The

wells are connected to all 5 fracture grid blocks. The purpose here is to investigate the sensitivity of the WAG flood to several parameters as outlined in **Table 4**.

Following the investigation in **section 2.3** of the performance of WAG in naturally fractured reservoirs we now look at sensitivity issues of the WAG process. Several parameters were varied, namely fluid parameters: the density and viscosity of the oil, physical reservoir parameters: matrix and fracture permeability and the shape factor and injection parameters: injection rate and WAG ratio. The ranges that are used in this study are provided in **Table 4**.

Relative Range	Units	Low	Medium	High
Coded Value	[-]	-1	0	1
Oil density	[lb/ft^3]	50	55	60
Oil viscosity	[cP]	20	70	120
Sigma	[1/ft^2]	0.1	1	1.9
Matrix permeability	[mD]	10	50	90
Fracture permeability	[mD]	1000	2000	3000
Injection rate	[bbl/day] [Mcf/day]	5000	6000	7000
WAG ratio	[-]	1:3	3:3	3:1

Table 4: Coded parameters with values used in the water, WAG and gas pattern flood simulations

To understand how all these parameters influence the recovery, two dimensionless numbers are derived and calculated as a function of the reservoir operating conditions. The two numbers represent different physical force ratios in the reservoir. If we can identify flow regions based on these numbers, we can forecast reservoir performance and hence optimize operations. This requires validation of the choice of these two dimensionless numbers. The relative magnitude of these forces is defined by the following two dimensionless numbers based on literature about the scaling of multiphase flow[20]:

$$N_{cv,m} = \frac{Lp_c^* k_m}{H^2 q_m \mu_o} \frac{M}{1+M} \qquad (16)$$

for the capillary over viscous forces ratio, in which L is the reservoir length, p_c^* is the characteristic transverse capillary pressure, k_m is the average matrix permeability, H is the reservoir thickness, q_m is the total Darcy flow velocity in the matrix, μ_o is the oil-viscosity, M is the mobility ratio and:

$$N_{gv,f} = \frac{\Delta\rho g L k_f}{H q_f \mu_o} \frac{M}{1+M} \qquad (17)$$

for the gravity over viscous forces ratio, in which $\Delta\rho$ is the density difference of the injectant and the oil, g is the gravitational constant, k_f is the average fracture permeability and q_f is the total Darcy flow velocity in the fracture.

The total Darcy flow velocity is approximated by the oil inter-block flow in a gridblock in the middle of the reservoir in the matrix or fractures and is averaged over time. This approximation is good in homogenous reservoirs. However in more heterogeneous reservoirs an average over a vertical line of gridblocks is needed to have a proper approximation of the Darcy velocity. The density difference during WAG injection is taken as an average, weighted by the WAG ratio, of the water, gas and oil density.

4.4.1 Results and Discussion

Several simulations have been run to validate the proxy model that can be seen in **Figure 2 and Figure 3**. A top view of a combination of response surfaces is shown in **Figure 2** where the maximum recovery is used to select the response surface at each point. The recovery after four years of gas injection, WAG 1:3, WAG 3:3, WAG 3:1 and water injection as function of the capillary to viscous and gravity to viscous forces can be determined relatively easily. In **Figure 3** the three-dimensional plot of the five response surfaces can be seen. It is clear that in the gravity-dominated area the injection of gas is the most efficient. Towards the more capillary-dominated area the injection of more water becomes very important. However it is very clear that the injection of only water is in every case less favorable.

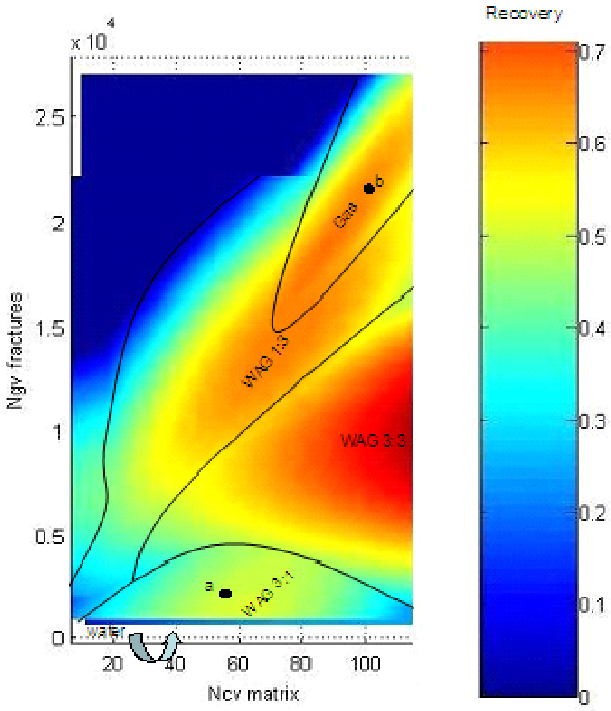

Figure 2: The top view of the overlaying different response surface models of the five injection methods. Recovery is displayed as function of the main physical forces

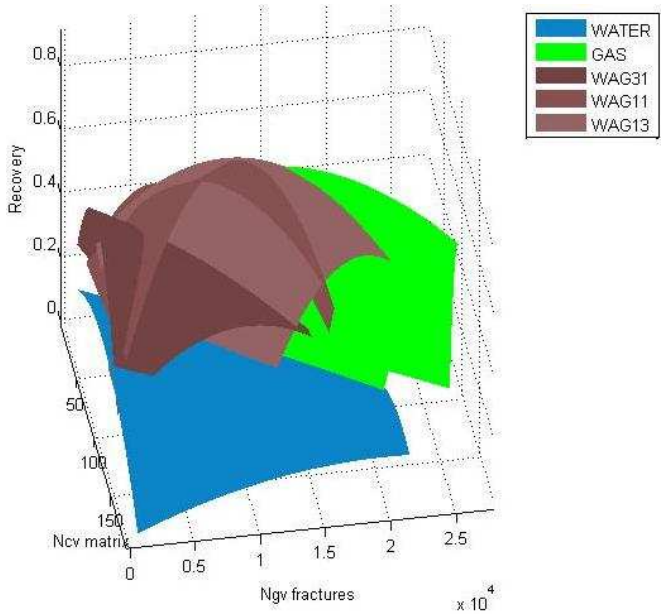

Figure 3: The 3D view of the response surface models

4.4.2 Sensitivity to production

The Pareto chart in **Figure 4** demonstrates graphically the most significant terms (i.e. main effects and the interaction terms) affecting the oil recovery in this study for water-, WAG 3:3- and gas-injection. As can be seen from the chart, the six dominant terms consist of some single terms, some quadratic and some interactions between factors. The interaction term of two factors implies that the effect of one factor is more considerable when the other factor is moving towards its extreme. For example the cross term 'injection rate*matrix permeability' during gas injection has some effect on the recovery. This means that the sensitivity of oil recovery to 'injection rate' is high when the value of 'matrix permeability' is high. This is due to high viscous forces present.

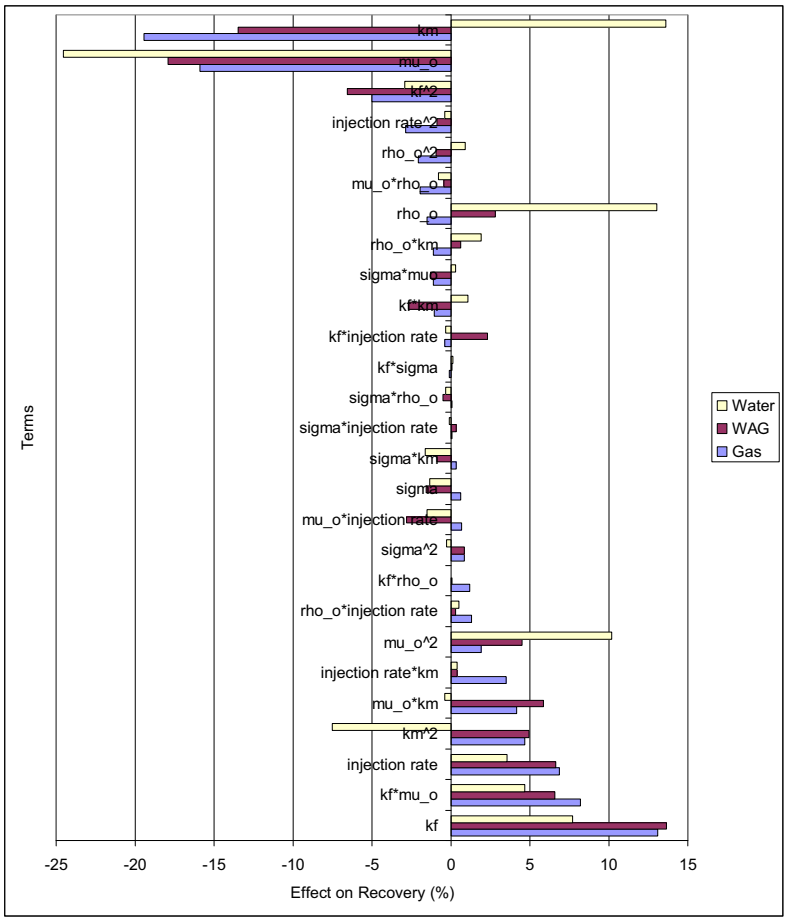

Figure 4: The Pareto chart shows the influence of each term on the recovery.

It can also be seen from the chart that sigma, the shape factor, does not have a lot of influence on the recovery. That is in line with what we expected from actual field data. A small sensitivity study on a bigger range of sigma (0.01 -100) was performed because the range of sigma in the initial screening was small (0.1-1.9). This study did not show any bigger influence of the shape factor on recovery. The type of reservoir investigated in this work is more dependent on matrix properties of the rock or fluid properties of the oil than upon the nature of the fracture network.
Another interesting phenomenon is the matrix permeability. When it is increasing it benefits the recovery of the water injection but it is lowering the efficiency of the WAG- and gas-injection. This may be caused by model limitations as the capillary pressure was not tied to the permeability in the models. If the model were changed to reflect this fact the results are likely to differ. An explanation based on the model used is due to the fact that higher matrix permeability is causing a faster gas breakthrough and is not influencing the water breakthrough time. Higher oil viscosity has also an interesting side effect. As expected a higher viscosity is really decreasing the recovery, but a higher density is increasing recovery during WAG- and water-injection. When the density difference between oil and water decreases, the water does not sweep only the bottom part of the reservoir but has a much better macroscopic efficiency.

4.5 Water Flooding

The model used here is the same basic model introduced in **Section 3.5**. Optimal control theory implemented in the optimization algorithm used allows for dynamic water flooding control. The optimization objective used was NPV for a given time under rate constraint. The total injection / production of the wells are kept constant and the rates are allocated over the different sections of the well. This is the same NPV model described earlier, but with no gas in the system.

Chapter 3 demonstrated the application to a single model. This section will apply this optimization approach to a set of models as described in **Table 5**. This will demonstrate how well or how badly the application of smart wells works across a set of reservoir models.

4.5.1 Simulation Model

The reservoir model is 300 by 300 by 10 m, modelled using 30*30 grid blocks as described in earlier chapters. A horizontal water injection well and a horizontal production well are placed at either side of the reservoir section with all sides bounded by no flow boundaries. Each well is divided into 30 segments allowing individual flow allocation to

each segment of the well. A high permeability streak is set perpendicular to the well direction connecting the two wells as can be seen in **Figure 5**. The two phases, oil and water, are at unit mobility ratios and the model is of uniform porosity. Therefore the total oil in place is constant for all the simulation runs.

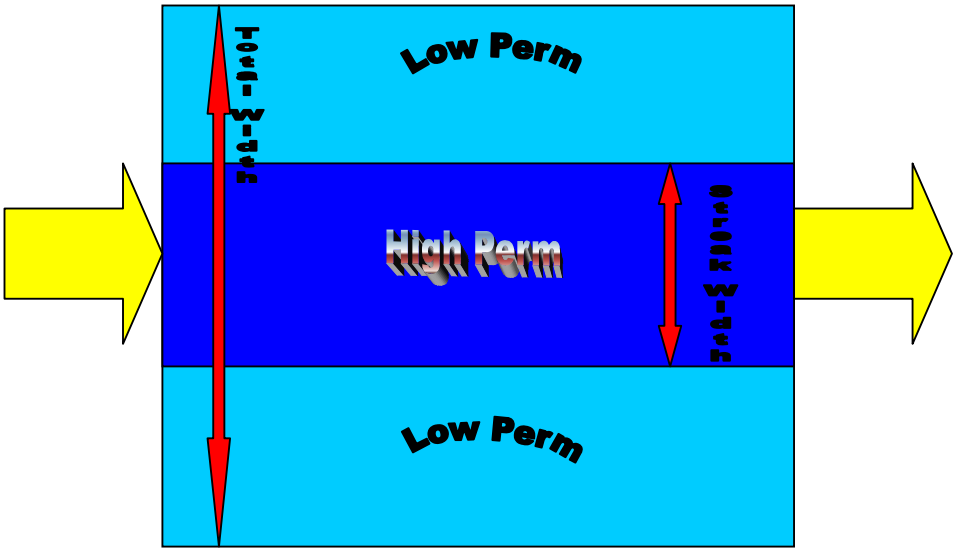

Figure 5: Waterflooding with horizontal smart injection and production wells.

The parameters studied and the level setting for each factor can be seen in **Table 5**.

k = permeability ratio streak / background
p = relative pore volume (or width) of streak
r = revenue of oil per bbl / cost of water per bbl
q = pore volume injected per day

The relative width of the streak varies from 0.20 to 0.33, the revenue of oil produced r_o ranged from to \$40 to \$120 per m^3, and the total cost of water produced r_w was set to \$10 per m^3 which includes all costs associated with water production and injection. The injection rate varied by a factor of two and the permeability ratio varied by an order of magnitude.

	Minimum	Median	Maximum
CODED	-1	0	1
k [-]	10	31.6	100
p [-]	0.2	0.27	0.33
r [$/bbl]	40	80	120
q [-]	0.05	0.07	0.1

Table 5: Coded parameters with values used in the simulations

4.5.2 Methodology

A small set of parameters was chosen for this study as seen in **Table 5** for two reasons. First of all the scope of the project grows significantly with an increased number of parameters. Secondly, to do significance testing and more complete model validation, a full factorial design was performed.

The parameters are coded and scaled such that the low value is coded to -1, the median to 0 and the maximum value to +1. Three d-optimal designs were set up with 20, 40, and 60 runs as well as a full factorial design requiring 81 runs. Additionally 8 test simulations were done at coded parameter setting values corresponding to -0.5 and +0.5. It is important to note that the test runs are within the ranges of the design but not at the same levels as the training observations.

The response surface model has 15 terms to represent the NPV. A model is then made for the base NPV relating to conventional well deployment and a model for smart well optimal NPV. This is done for all four designs and they are compared and tested with the test model.

For further analysis the models derived from the full factorial design will be used. If a larger number of parameters were used and the full factorial design was not possible to run due to computing limitations a decision would have to be made on the model that would be used. Possible pitfalls in model selection will be discussed.

Using the proxy model derived from the D-optimal design Monte Carlo analysis is used to quantify the NPV distribution for different scenarios. This allows a quantification of the mean value increase and the variance reduction for the smart wells relative to conventional wells given an uncertainty in the inputs parameters. This is a yardstick measure of the flexibility/robustness of smart wells deployment.

4.5.3 Data and Results

Scope for Improvement

Without seeing an increase in the expected value of the project due to the smart wells there would be little reason to create a proxy model. **Figure 6** shows the percent improvement of the smart well NPV over the convention well NPV for all 81 runs of the full factorial design. The average scope for improvement for this reservoir model as tested is 44%, which is quite significant. Additionally it can be seen that the scope for improvement varies significantly from a few percent to well over a hundred percent in some runs.

Figure 7 shows a sample of how the flooding pattern is optimized with smart wells. The first picture shows the water shooting through the high permeability streak without sweeping the reservoir very efficiently. The second picture shows intermediate iteration in the water flooding optimization process showing the injection front moving in a more stable manner.

The full scope of improvement in the NPV is seen by looking at the definition of NPV. The NPV is a function of the oil and the water production. This means the improvement is a result of mitigating water production in conjunction with the improved sweep efficiency. **Figure 8** shows the production curves for one of the sample runs. All the positives are seen in this figure. This includes delayed water breakthrough, and extended peak oil production as well as larger cumulative oil production and lower cumulative water production.

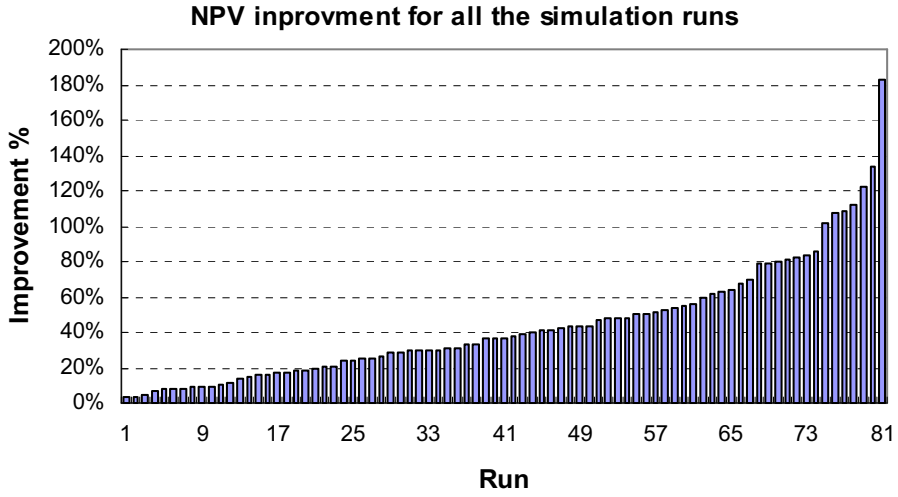

Figure 6: NPV improvement for all 81 simulations performed.

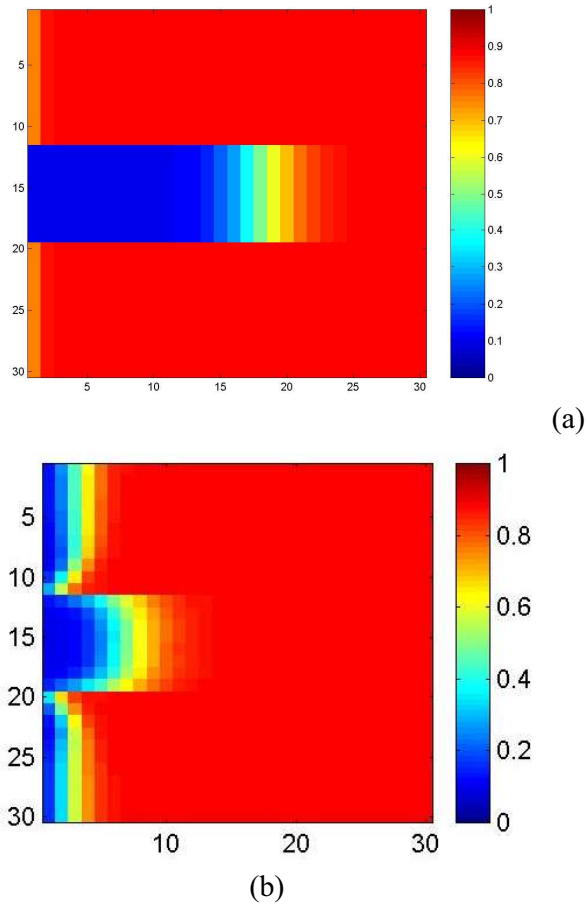

Figure 7: Injection front for conventional well (a) and smart well (b) showing improving front propagation.

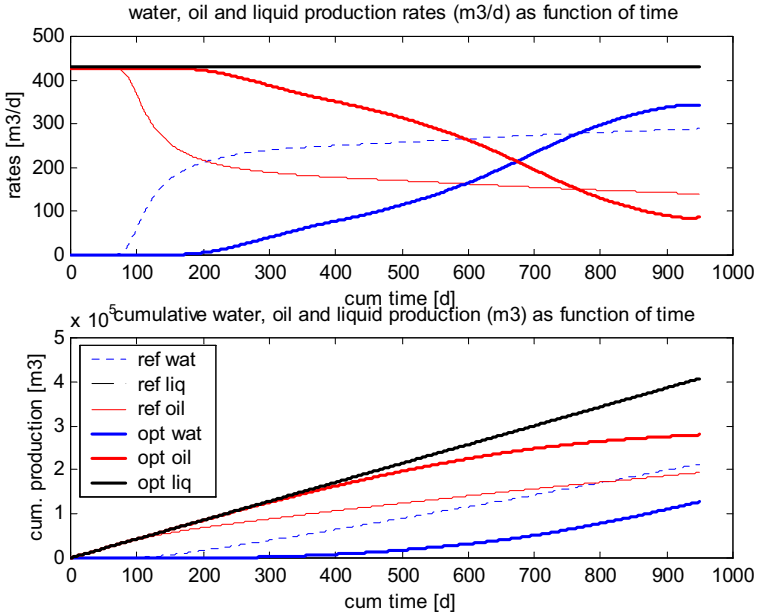

Figure 8: Comparison of oil and water production with conventional and smart wells.

Proxy Model

Regression models were created for 4 different designs conventional and smart well models. These are the D- optimal designs of 20, 40, and 60 runs as well as the full factorial design for the base conventional NPV and the smart well

optimized NPV. The statistical analysis of the 4 conventional well designs is shown in **Table 6**. The statistical analysis of the 4 optimized smart well designs is shown in **Table 7**.

ANOVA (Conventional Well)						
		df	*SS*	*MS*	*F*	*Significance F*
20	**Regression**	14	17.44	1.25	3435	5.49231E-09
	Residual	5	0.00	0.00		
	Total	19	17.44			
40	**Regression**	14	42.93	3.07	1262	7.17244E-31
	Residual	24	0.06	0.00		
	Total	38	42.99			
60	**Regression**	14	59.52	4.25	1309	8.17113E-53
	Residual	44	0.14	0.00		
	Total	58	59.67			
81	**Regression**	14	82.08	5.86	1494	8.58348E-77
	Residual	66	0.26	0.00		
	Total	80	82.34			

Table 6: ANOVA statistical analysis of d-optimal experimental design based regression model for conventional well for 20, 40, 60 and 81 run models.

ANOVA (Smart Well)						
		df	*SS*	*MS*	*F*	*Significance F*
20	**Regression**	14	37.678	2.69	8496	5.71034E-10
	Residual	5	0.002	0.00		
	Total	19	37.679			
40	**Regression**	14	80.453	5.75	11919	1.45071E-42
	Residual	24	0.012	0.00		
	Total	38	80.464			
60	**Regression**	14	125.781	8.98	5406	2.44077E-66
	Residual	44	0.073	0.00		
	Total	58	125.854			
81	**Regression**	14	167.690	11.98	5222	1.08027E-94
	Residual	66	0.151	0.00		
	Total	80	167.841			

Table 7: ANOVA statistical analysis of d-optimal experimental design based regression model for smart well for 20, 40, 60 and 81 run models.

Regression analysis is often limited to observing that R^2 is near one and then concluding that "everything is fine". Although the trend is not evident in the R^2 analysis it is evident in the full statistical analysis that the model improves with additional runs. The analysis shows that the 20 run model is not suitable and that the 40 and 60 run models are suitable to use. This is similar to history matching in reservoir simulation in the sense that it is ultimately the ability to have a model to predict the future that is the goal of history matching and not simply a model that can replicate the past. In this case the history is the training set and the future, or predictive mode, is validated with the test set. **Figure 9** shows the fit of the full factorial model to the 81 data points as well as the fit in prediction mode for the 8 test data points.

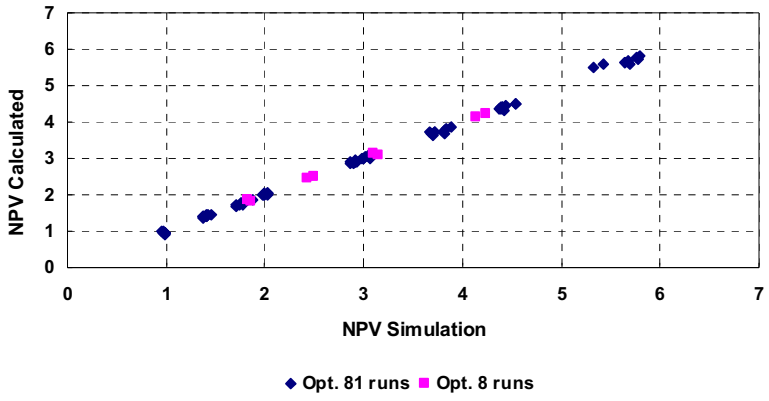

(a)

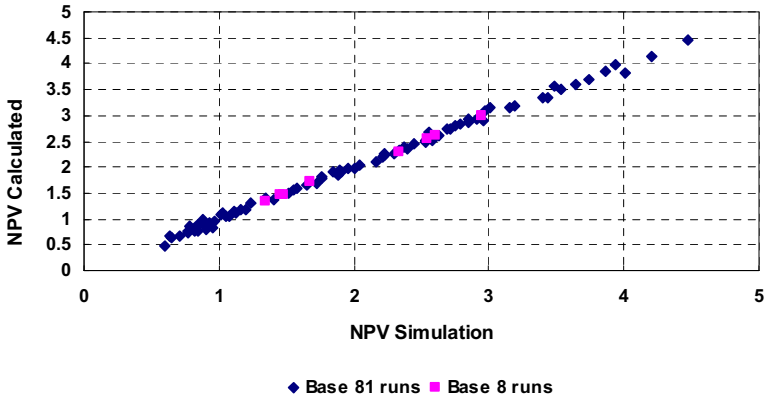

(b)

Figure 9: Validation of NPV fit for (a) optimized smart well and (b) conventional well. Note the clustering in (a) due to the improved control. The 8 runs in pink are validation runs done at -0.5 and +0.5 to further validate the fit.

The results of the full factorial model are expressed as a Pareto chart in **Figure 10** and in tabular format in **Table 8**. These are normalized values to show the fraction contribution of each parameter to the model. The revenue parameters that dominate the NPV have been removed from the Pareto chart to see the other parameters more clearly. This is due to the fact that the per bbl revenue term dominates the NPV of the model.

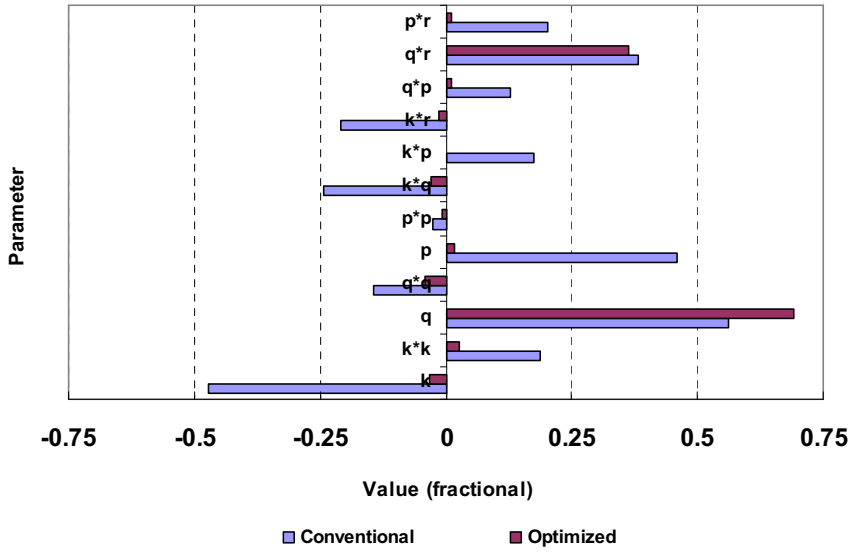

Figure 10 – Pareto chart of the normalized regression parameters for the conventional well (series1) and smart well (series2).

	Normalized Coefficients	
PARAMETER	**CONVENTIONAL**	**SMART WELL**
k	-0.149	-0.015
k*k	0.059	0.012
q	0.178	0.315
q*q	-0.045	-0.019
p	0.145	0.008
p*p	-0.008	-0.003
r	0.683	0.55
r*r	0	-0.007
k*q	-0.077	-0.013
k*p	0.056	0.001
k*r	-0.066	-0.006
q*p	0.04	0.006
q*r	0.121	0.165
p*r	0.064	0.005

Table 8: Normalized regression parameters for the response surface models based on the full factorial design.

Already some conclusions can be drawn from the Pareto chart. This chart shows the influence of:
k = permeability ratio streak / background
p = relative pore volume (or width) of streak
r = revenue of oil per bbl / cost of water per bbl
q = pore volume injected per day

The two most interesting ones are the geologic parameters k and p seen in the chart. As is expected a high permeability contrast is very detrimental to a conventional well. This is seen primarily in its 1st order term but also in its interaction terms. The smart well is able to mitigate the problems caused by the fast water breakthrough due to the streak. This is also seen quantitatively by the fact that the negative effects due to k are much smaller for the smart well.

The next geologic parameter is the relative pore volume of the streak. The wider the streak the better the conventional well works. Another way to put this though is that narrow streaks cause severe problems. The smart well is able to mitigate this problem as well.

The NPV of the smart well is primarily defined by the allowable injection / production rate and the price of the oil. The geologic parameters that caused major problems for the conventional well have a much smaller effect on the smart well. The value gained from this will be investigated below.

Figure 11 shows the sensitivity of each factor, with the other factors at the mean, and the confidence intervals. The sensitivities are for the full factorial design showing the slope of the proxy model constant and the confidence interval, in dashed lines in the results. The confidence interval gives a range of values around the mean where we expect the "true" population mean to lie. This shows that if we repeat the experiment we have a 90% chance that the mean is again within the confidence interval. Note that the terms with small influence as seen in the Pareto chart have a wide interval of confidence.

The optimized smart well appears at first to show problems due to the large confidence intervals seen in **Figure 11**. When this data is analyzed in conjunction with the Pareto chart shown in **Figure 10** it is apparent than the effects of the parameters with wide confidence are actually insignificant since they have little effect on the NPV. The parameters with a good confidence also are most important to the NPV calculation.

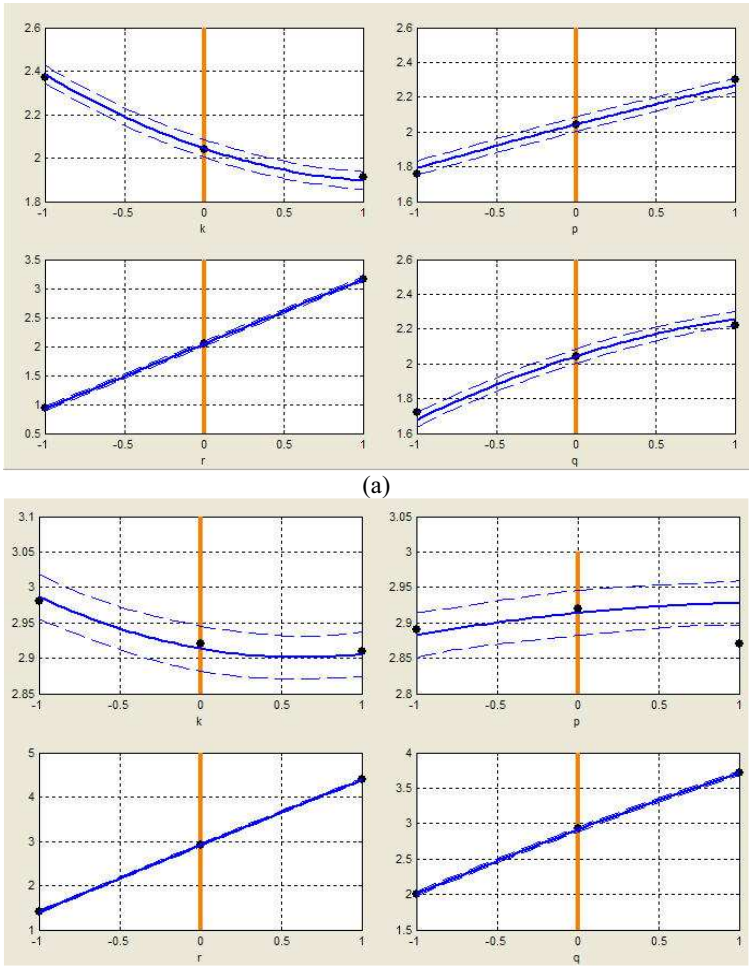

Figure 11: Sensitivity of each factor on NPV for (a) conventional well and (b) optimized smart well. Dashed lines represent the 90% confidence intervals.

Response Surfaces

Contour plots of the RSM are useful as a visualization tool. These surfaces are useful to see the interaction of two parameters but this must be done with caution. The surfaces only show two parameters at a time and can therefore be deceiving when performing a multi-parametric optimization or sensitivity analysis.

For visualization purposes sample contour maps of NPV are provided in **Figure 12**. These are shown for all 4 design models for the conventional and optimized smart well. These contour maps easily show that the smart wells mitigate the problems caused by the geologic parameters that significantly hurt the performance of the conventional well.

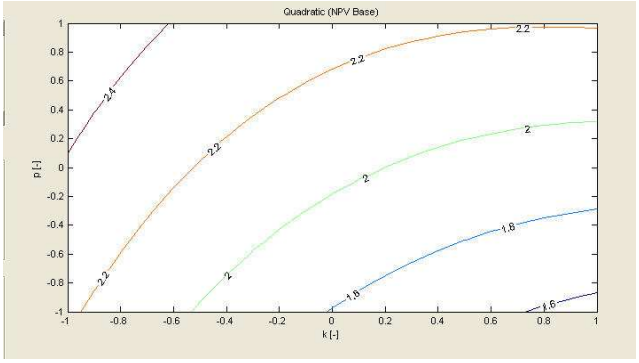

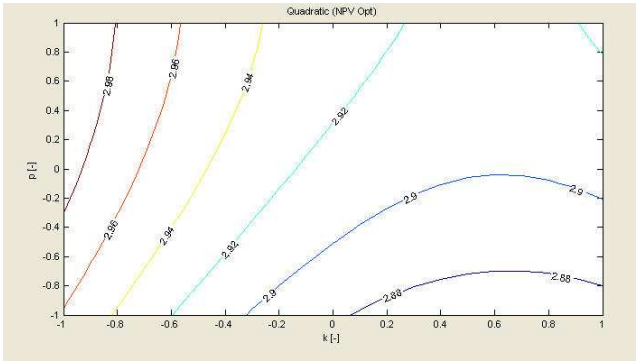
Quadratic (NPV Opt)
p [-]
k [-]

(a)

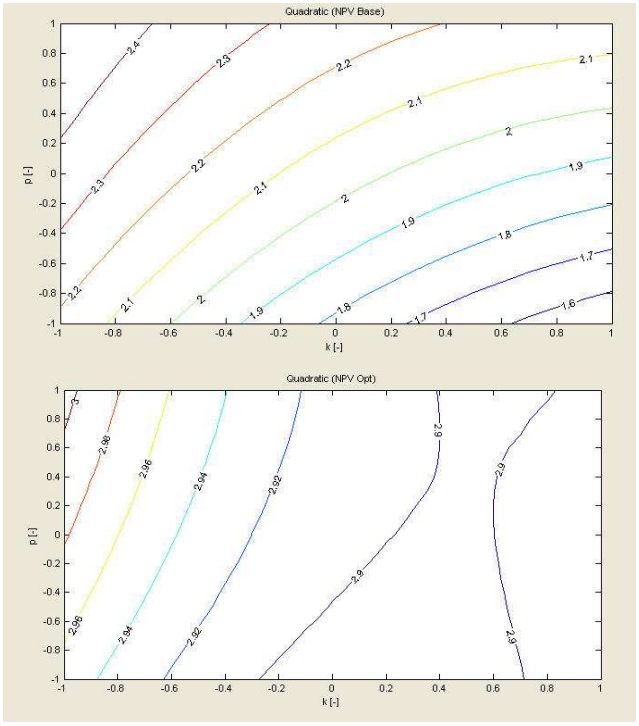
Quadratic (NPV Base)
p [-]
k [-]
Quadratic (NPV Opt)
p [-]
k [-]

(b)

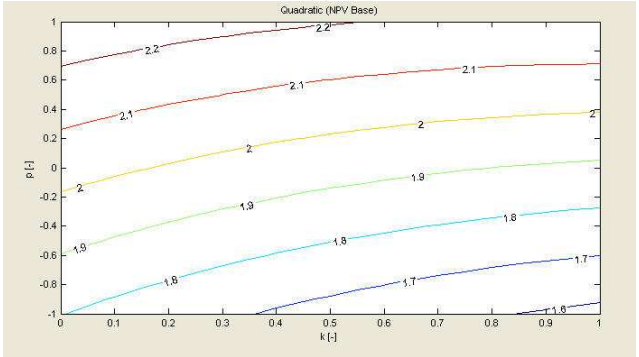
Quadratic (NPV Base)
p [-]
k [-]

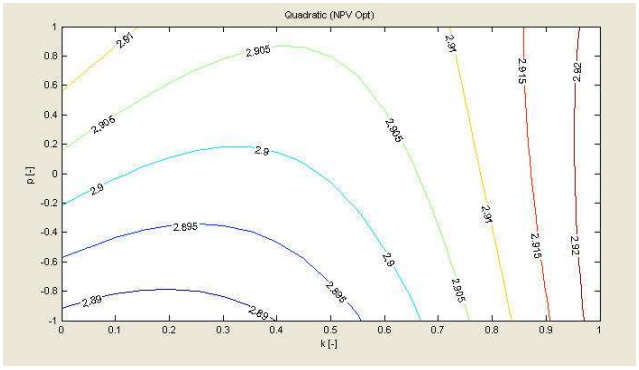

(c)

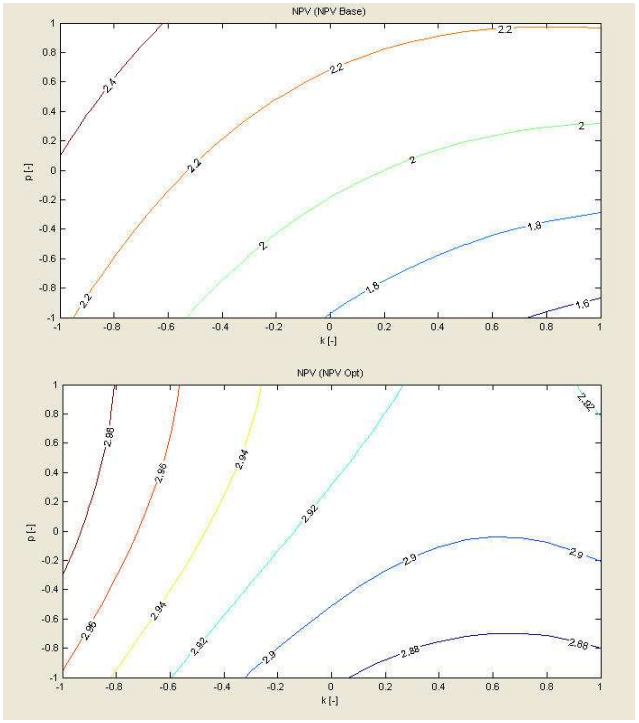

(d)

Figure 12: Contour maps show the effect of k (permeability ratio) and p (relative streak bulk volume) on NPV for the conventional and optimized smart well for (a) 20 run model, (b) 40 run model, (c) 60 run model, (d) 80 run model.

Monte Carlo Analysis

Monte Carlo simulation is used to quantify the variance of the NPV given uncertainty in the input parameters. As value quantification is not the major focus of this study only a few samples have been shown. Note that these analyses are possible due to the accuracy and computational efficiency of the proxy model. These results are presented in **Table 9**.

	NPV Variance	
RUN	**CONVENTIONAL**	**Smart well**
BASE	0.193	0.0846
SEISMIC	0.145	0.0845
OIL FUTURES	0.183	0.0268
CORE ANALYSIS	0.124	0.0783

Table 9: NPV variance for different uncertainties in the input parameters

The base run is an uncertainty analysis around the mean values of all the parameters. There is a gain of 869 k$ as well as a reduction in uncertainty for the optimized smart well. This is an additional value gained that is realized through the NPV distribution and not just the expected monetary value or single point NPV.

What would be the value of information gained by performing a seismic survey to reduce the uncertainty in the reservoir geometry? This assumes that the uncertainty in the width of the high permeability streak is reduced in half. The run named seismic shows a reduction in variance of 0.048 for the conventional well and nearly 0 for the smart well.

This means that where a seismic survey, if less costly than the options gain was justified for the conventional well, it would not be for the smart well. These are examples of the value of information versus the cost of information.

Another example of value of information is the reduction in variance gained by core analysis to reduce the uncertainty in the permeability model. Again this assumes the maximum and minimum values are +0.5 and -0.5. The results are similar to those of the seismic study above.

The oil futures run shows the variance reduction by selling the oil by contract at a fixed price at the mean. This approach further demonstrates how this approach can provide information on cost versus value. This run illustrates the importance of taking into account possible changes in the market conditions in assessing the value of a project.

4.6 Conclusion

The DOE approach allowed a reasonable number of simulations to be run to determine sensitivities under several reservoir models. The fit response surface models acts as a valid proxy model to the recovery and NPV allowing further statistical analysis using the proxy model in a Monte Carlo approach.

The major benefit of a DOE approach as applied in this chapter is two fold. The Pareto analysis of the RSM provides the major sensitivities to the reservoir parameters. Additionally the Monte Carlo analysis of the proxy model provides a value versus cost of information outlook.

As seen in the previous section, the flexibility of smart wells allows improved control of production significantly improving global sweep of the reservoir, even under uncertainty in the reservoir model. This was shown with the water-flooding model under a range of reservoir properties.

The next chapter will extend the DOE approach to incorporate optimization into the workflow.

References

1. Knight, Frank H., “Risk, Uncertainty, and Profit”, Hart, Schaffner & Marx; Houghton Mifflin Company, 1921.
2. Myers, R.H., Montgomery, D.C., “Response Surface Methodology”, John Wiley & Sons, 1995.
3. Box, G.E.P., Hunter, W.G., Hunter, J.S., “Statistics for Experimenters”, John Wiley & Sons, 1978.
4. Plackett, R.L., Burman, J.P., “The Design of Optimum Multifactorial Experiments”, Biometrika, Vol. 33, Issue 4, June 1946.
5. Lindman, H. R., Analysis of variance in complex experimental designs. San Francisco: W. H. Freeman & Co., 1974
6. Wikipedia: The Free Encyclopedia: http://en.wikipedia.org/wiki/Anova, created in 2001; Wikimedia Foundation

The quest for certainty blocks the search for meaning. Uncertainty is the very condition to impel man to unfold his powers.
Erich Fromm (1900–1980), U.S. psychologist

Chapter 5 Decision Analysis under uncertainty

Decision analysis is a discipline in which important decisions are made in a "formal" or systematic fashion. This chapter discusses the optimization process and the choice of objective functions used during the decision analysis. Ronald A. Howard, a professor at Stanford University, coined the term decision analysis in 1964. Several manual or automated approaches can yield varying success in determining an optimum production strategy.

This chapter discusses three approaches to the decision making process. These approaches all incorporate results from the experimental design but in different manners. The first approach is applied to the fractured reservoir described earlier. This approach only optimizes the WAG ratio and is not incorporated in a smart well environment. This approach uses a combination of a systematic design approach and a "human" input.

The second approach is applied to the water-flooding model described earlier. This approach uses the integrated optimal control based optimization on single realizations of the model across a design space. This study demonstrates the difficulty in the decision making process when uncertainty, such as multiple models, is added to the system.

The final approach discussed involves a more fully automated approach to the optimization problem. The WAG pilot model with smart wells is used to incorporate multiple controls into the decision making process. Although human interaction, as in most studies, is required to oversee the process, the approach incorporates a high degree of automation.

5.1 WAG – Fractured Reservoir

5.1.1 Dynamic optimization

The use of optimal control theory as a dynamic optimization algorithm for the valve settings in smart wells has already proven to be useful. The focus was on purely pressure- and rate-constraint optimization for a horizontal injector and producer for the waterflooding of heterogeneous reservoirs.

The use of dynamic optimization in WAG injection in naturally fractured reservoirs could have some advantage. All good performing WAG runs seem to have the same trend. In **Figure 1** the production plot of a good performing WAG run, run **a** from **Figure 8** in chapter 2, can be seen. Clearly three different stages can be distinguished; before water breakthrough, after water breakthrough and after gas breakthrough. For the different stages there are different optimal WAG ratios. Attempting to find the optimal WAG ratio manually is very time consuming and difficult. The difficulty lies in determining when to search for new WAG setting as a brute force monthly search is too time consuming.

The objective function selected results in the optimization of the total field oil production over an 8-year period. The control parameters are the choice of injectant, water or gas, at each time step that the parameter may be varied. To be able to vary the injectant monthly, we have 96 control parameters. A change of optimal WAG ratios is expected to coincide with the three stages of production.

Three time periods explained below and the 3 WAG ratios provide a set of 27 simulation runs to find the brute force solution. A brute force method can be loosely defined as a method that prefers calculation over knowledge. Most combinatorial optimization algorithms are partially brute force algorithms with some sense of smartness included. Below a full brute force approach is compared to a design approach to optimization a WAG flood.

5.1.2 Manual Optimization

Even if we cannot get the optimal WAG ratio for every period yet, we can try to approximate it. The successful WAG simulations all showed similar behavior to that shown in **Figure 1**. The stages are an increase in production followed by a breakthrough of one phase resulting in declining production and then a breakthrough of the second phase. Previous experience has shown that the optimum WAG ratio often remains the same until breakthrough occurs or just prior to breakthrough. This combined information brings us to a division into three time periods. Therefore the water and the gas breakthrough times will divide the three time periods.

A Plackett Burman design utilizing only 4 simulation runs, 4*ceil((k+1)/4) where k is 3, already showed that the late time strongly favored a WAG ratio of 1:3. This is seen in **Figure 2a**, which would also indicate the middle period favoring a WAG ratio of 3:1 and the early period showing little sensitivity. The early time was not very sensitive in this linear Plackett Burman design based model. To validate these results a brute force search is performed.

If we again consider the division in three periods, as seen in **Figure 1**, as a good approach of getting three optimal ratios, we have a rough method of improvement. For every period we varied the WAG ratio from 1:3 to 3:3 and 3:1, so there are 27 combinations. All 27 runs of the full factorial model are run as the design space is relatively small with only 3 parameters. If now a proxy model is fitted, we can again plot a Pareto chart, which is visible in **Figure 2b**. First of all we can see that for this run after gas breakthrough, the late period, a WAG ratio of 1:3 increases recovery. This is the same as is seen in the initial screening above. As mentioned before, and now can be seen in the chart, the importance of this late time is substantial.

Before water breakthrough, the early period, a WAG ratio of 3:1 is more beneficial. It can also be concluded that for this run the importance of what the optimum WAG ratio is between water and gas breakthrough is less important. This is not what would be concluded from the initial screening. This is due to the fact that all the terms in the Plackett Burman design are reduced to the three linear terms in the screening model. Often the results mimic some of the full results such as the optimal WAG ratio for the late period, but can over or underestimate other factors.

Although this optimization is only valid for run *a* it delivers a methodology that can increase recovery. Already the difference in recovery of a preferable WAG ratio of 3:1 for the entire simulation and the preferable WAG ratio of 3:1 followed by 3:3 and 1:3 is 3%. Although the Plackett Burman design results did not identify all the optimal settings it did identify the most critical time period and its optimal setting.

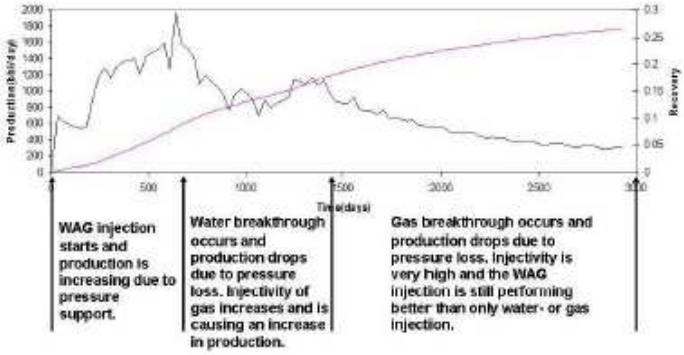

Figure 1: The 3 stages of a successful WAG injection in fractured reservoirs. From run a in Figure 8 chapter 2.

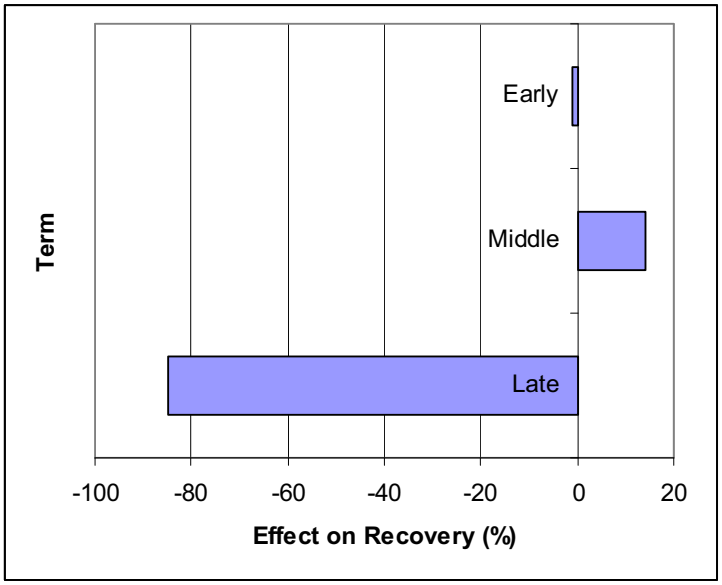

(a)

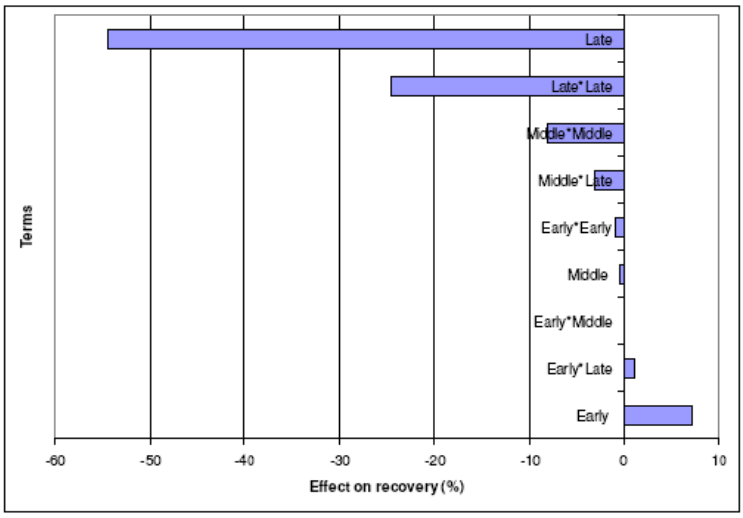

(b)

Figure 2: Pareto chart derived from the (a) Plackett Burman design and (b) 27 simulation runs showing the normalized effect of the WAG ratio during the 3 phases of the production.

The results of the optimization provide additional insight into the mechanisms in play during the 8 years of production. The early time period favors a 3:1 WAG ratio indicating a more important role for the water phase of injection. Capillary imbibition is the dominant and preferred recovery mechanism in the early part of the production cycle. This is understandable as the model was chosen to be a water wet reservoir and there is no free water in the matrix at the start of the production. Spontaneous imbibition of water into the matrix displaces the oil into the fractures. The second phase of the production cycle shows the need to balance the imbibition and gravity drainage drive mechanisms by balancing the slug sizes of water and gas. The late time period favors larger slugs of gas than water after breakthrough of both phases. The late period is gravity drainage dominated and is still very important to the recovery. Gravity drainage is a relatively slow process and there is not a steep decline in production. After 8 years rates are still at 20 percent of peak rate at gas breakthrough.

5.2 Waterflooding

In Chapter 4 Monte Carlo analysis was used to quantify the NPV distribution for different scenarios. This allows a quantification of the variance reduction for the smart wells relative to conventional wells given an uncertainty in the input parameters. This is a yardstick measure of the flexibility of smart wells. The difficulty was that each model was assumed to be precisely known and therefore has a unique optimal solution. In this manner robustness under uncertainty was not addressed.

The first approach to obtaining a robust solution is to consider a brute force approach to the solution. Although an optimal design set adequately represented the recovery the full factorial set of 81 simulations was ran in Chapter 4 as a base line solution. To do a full study under uncertainty 6,400 additional simulations runs were needed beyond the 81 original simulations. The next step in deriving a single injection / production profile to optimize the NPV over the entire design space, meaning all 81 reservoir models, requires a definition of the objective. A comprehensive search applying all 81 injection / production profiles to all 81 runs (80 additional) was performed in a computationally demanding exercise. This approach does not guarantee that the global optimum is among the 81 optimal strategies, but this does test the robustness of the strategies.

Optimal Control Theory based gradient optimization of a single simulation model showed very promising results. Figure 3 shows an average improvement of 44% for all the simulation runs. This average is based on **equation 3** and the implications of the choice of average will be discussed below. This improvement shows that the optimization works well for an *a priori* known model. Having a certain *a priori* known model allows a customized injection / production profile that serves to both increase the NPV and reduce the variance over the 81 models.

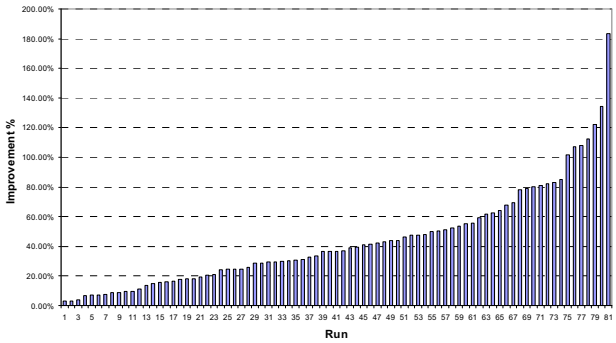

Figure 3: – NPV improvement for all 81 simulations performed using individual injection / production profiles.

The 44% improvement reported was the mean average of the improvements of all 81 models. When taking the set of models as a whole a new definition of improvement is required. This new objective is the improvement in the mean NPV of all 81 models. With the individual optimal solutions the mean NPV, or expected monetary value EMV, increased 40.6% as defined by **equation 4**. The reason for this difference as noted in Chapter 4 is that the worse performing runs had more scope for improvement.

$$\text{Average of Mean} = \frac{\sum_{i=1}^{n} (NPV_{opt} - NPV_{base}) / NPV_{base}}{\#\,\text{models}} \tag{3}$$

$$\text{Mean of Average} = \frac{\sum_{i=1}^{n} NPV_{opt} - \sum_{i=1}^{n} NPV_{base}}{\sum_{i=1}^{n} NPV_{base}} \tag{4}$$

The optimal solution is the solution of the model with the medium value of permeability contrast and streak width, and the larger value of oil price and injection rate. The results are summarized in **Table 1** showing an increase in the EMV of 13.2% and an increase in the average model improvement of 11.8%.

Relative Improvement	Mean of Average	Low	High	Average of Mean
Customized	44.1%	3.06%	183.3%	40.6%
Worst	5.0%	-21.3%	65.4%	-6.5%
Robust	11.8%	1.0%	77.8%	13.2%

Table 1: Relative improvements in NPV for the water flooding optimization.

Introduced above is the importance of defining the objective function in determining the optimal solution. A second consideration would be to improve the low end of the NPV range. This solution is for a very conservative approach that places much more emphasis on the downside than the upside of the project. This would be a possible scenario if we assumed there were some costs to acquiring the rights to produce from this field therefore shifting all the NPV values lower. This would result in an initial solution with the possibility to loose money. This solution rests very close to the worst solution in Table 1. The solution allows a lot of lost revenue on the high NPV models in exchange for large percentage increases in the worst performing models. This result also greatly reduces the standard deviation of the solution. These results are summarized in Table 2.

NPV MM$	Mean	STD
Customized	2.88	1.45
Robust Risk	2.11	0.82
Robust EMV	2.32	1.52

Table 2: NPV for the water flooding optimization with *a priori* known models, highly risk adverse attitude, and an EMV goal.

5.2.1 Computational Concerns

The full brute force approach is not computationally efficient and is often not feasible as only an optimal design set of simulations would normally be run to assess the scope for improvement as discussed in Chapter 4. As the full set was run in this study an analysis of clustering methods to see self similar solutions is available.

Figure 4 plots the NPV of the base case conventional well versus the improvement in the NPV with smart wells. There is a clear pattern of clustering in this figure and therefore further analysis is justified. **Figure 5** shows the

cross plots of each of the 4 parameters versus NPV, optimized NPV and the relative improvement in NPV. The clustering is visible in the NPV of the optimized well **Figure 5b** and not with the other two sets of figures.

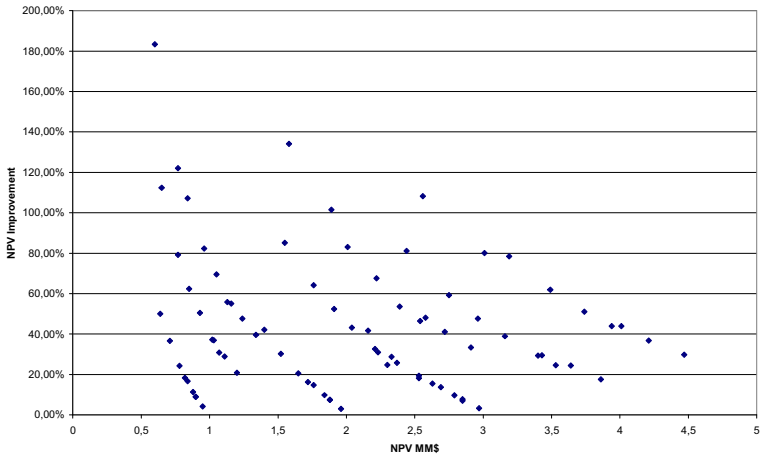

Figure 4: A plot of the NPV for the conventional well versus the improvement in the NPV utilizing an optimized smart well.

Figure 4 indicates there are some trends and clusters in the data. One thing to point out given the trends is that there is increased scope for improvement in general for the worse performing models. This makes it clear why the difference in Equation 3 and 4 is important. To get a further indication of the trends visible in this graph cross plots with the design parameters are presented below.

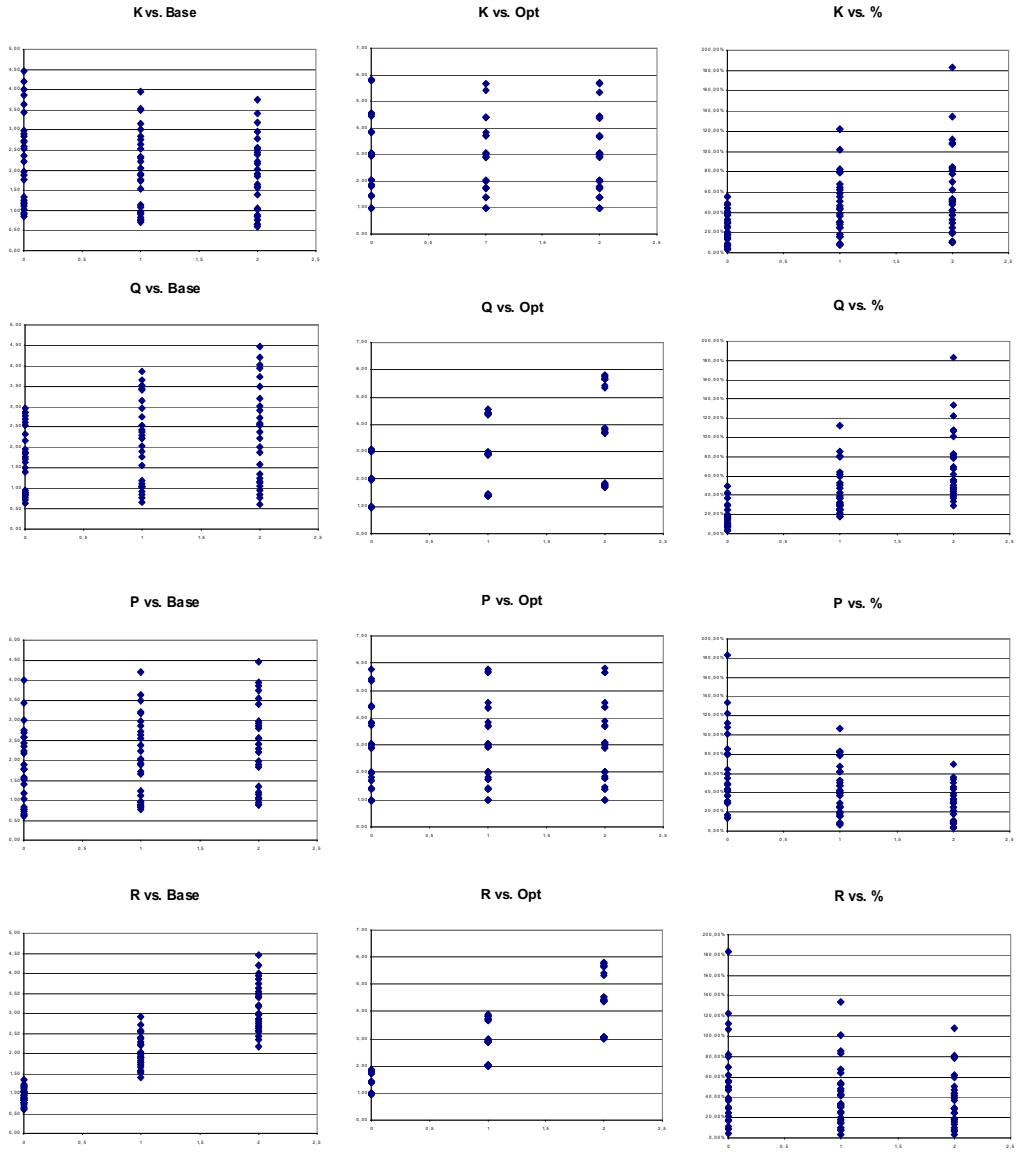

(a) (b) (c)

Figure 5: Cross plots of each parameter at the low, medium and high setting versus the base case NPV, optimized NPV and Improvement in NPV.

Figure 5 shows several single parameter cross plots to get an idea of the clustering visible in the models. These show the results of each parameter at the three settings for the solution to the conventional well, optimized well, and relative improvement. The strongest clustering is for the rate and oil price terms as expected from Table 3. This does not necessarily mean that these solutions cluster in the same manner for the robust solution. Implications of looking at just three solutions will be discussed in the next section.

	Normalized Coefficients	
Parameter	**Conventional**	**Smart well**
k	-0.149	-0.015
k*k	0.059	0.012
q	0.178	0.315
q*q	-0.045	-0.019
p	0.145	0.008
p*p	-0.008	-0.003
r	0.683	0.550
r*r	0.000	-0.007
k*q	-0.077	-0.013
k*p	0.056	0.001
k*r	-0.066	-0.006
q*p	0.040	0.006
q*r	0.121	0.165
p*r	0.064	0.005

Table 3: Normalized regression parameters for the response surface models based on the full factorial design.

The previous section determined the best solution of the 81 strategies. This approach attempts to find sets of solutions that provide similar results. The first attempt is to divide the 81 models into 4 clusters.

Initially 4 sets of solutions were tested as the entire set of runs was already run. This solution looked to see if simply clustering solution by 1 parameter proved to be of any value. These results showed no discernable pattern for solutions based on a clustering by rate or oil price but did show a definite trend in the solutions by relative streak width and permeability contrast. Table 4 shows that the solutions at all three levels, at 27 runs per level, of flow rate show identical solutions within 2 percent. The same holds true for the oil price as the solutions are nearly identical.

In contrast there is a definite trend seen in the solutions for the streak width and permeability. There is a higher EMV for the median setting of both the permeability and streak width. These solutions indicate that the solution is too aggressive for the high permeability and the narrow streak width solution but not aggressive enough for the wide streak and low permeability solutions. The trends visible in the permeability contrast and streak width showed promise but yield to much spread in the EMV. A clustering based on more than a single parameter will now be looked at.

	EMV MM$		
Setting	Low	Medium	High
k	2.12	2.23	2.17
p	2.17	2.26	2.10
r	2.16	2.18	2.17
q	2.18	2.18	2.16

Table 4: Results for clustering by a single parameter.

The next logical clustering is of the combination of the 2 parameters showing promise above, streak width and permeability. This results in 9 clusters of 9 samples each with setting of low, medium and high for each of the 2 parameters. These results show a clear clustering with the best solutions all being in the same cluster as the optimal solution shown in Table 2. The best results come in the solution set with the medium value of permeability (k) and streak width (p) as would be suggested in the results of Table 4. The worse solutions come from the most aggressive floods.

Decent clusters can be seen in a basic 4 cluster solution and strong clustering is seen when using 9 clusters. The results for the oil price can be explained due to the constraints in the reservoir. The absolute NPV of an individual model is very dependant on the oil price, but the solution to the optimal flood is much more related to the geology since the models are total fluid rate constrained. Similarly, the flow rate is in a 2-dimentional model without gravity and therefore there are no gravity forces to balance the viscous component. Therefore the EMV is sensitive to the total flow, but the solutions are not very sensitive to the flow rate.

Setting		EMV
k	p	MM$
-1	-1	2.15
-1	0	2.23
-1	1	1.99
0	-1	2.21
0	0	2.31
0	1	2.18
1	-1	2.15
1	0	2.25
1	1	2.12

Table 5: Results of 9 clusters.

5.2.2 Lessons from Random Sampling

To test the robustness in a random manner three injection profiles were chosen as the P10, P50, and P90 NPV values as ranked by non-optimized NPV and were applied to all 81 models. These 3 profiles were then applied, as a subset of the above results, to all 81 reservoir models of the full factorial design to test their robustness.

This would represent a fraction of the brute force approach but with minimal logic to reduce the computational requirements required. This search proved not to be very robust and resulted in some bad recovery schemes. **Figures 5, 6 and 7** show the recovery improvements using the P10, P50 and P90 injection / production profiles. In some cases the NPV actually decreased. The average improvements are shown in **Table 4**. This indicates that this approach is not robust compared to the solution previously derived.

This approach will also create more problems as the design space number of parameters increases. The sensitivity of NPV to the reservoir, fluid and economic parameters can be determined using an optimal design approach but this would not provide the optimal injection / production profile over the design space. These may have well been three random samples as they were not chosen in a smart manner. Choosing the P10, P50, and P90 profiles in this manner was not the best approach. These may have well been three random samples as they were not chosen in a smart manner.

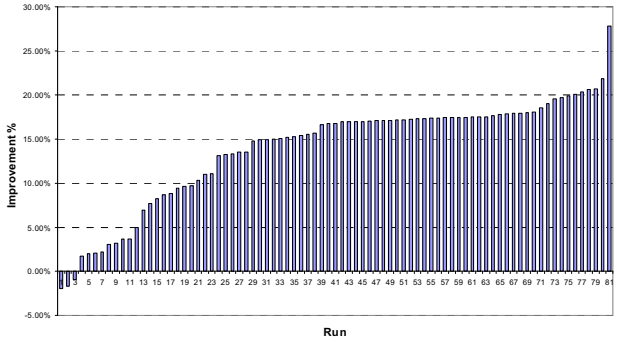

Figure 5: – NPV improvement for all 81 simulations performed using P10 injection / production profiles.

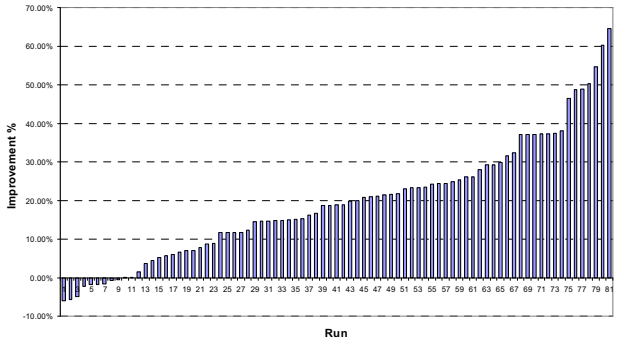

Figure 6: – NPV improvement for all 81 simulations performed using P50 injection / production profiles.

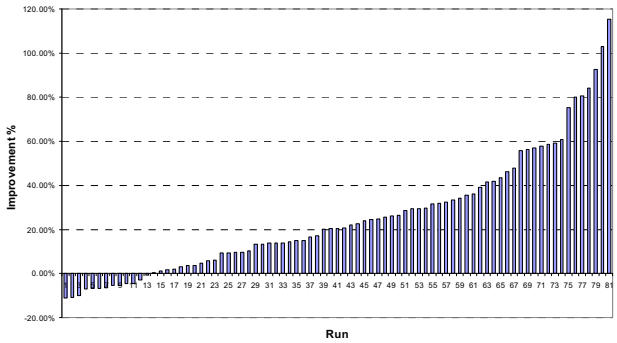

Figure 7: – NPV improvement for all 81 simulations performed using P90 injection / production profiles.

Relative Improvement	Mean of Average	Low	High	Average of Mean
Customized	44.1%	3.06%	183.3%	40.6%
P10 Settings	13.9%	-2.0%	27.8%	10.1%
P50 Settings	19.6%	-6.0%	64.5%	12.2%
P90 Settings	25.6%	-11.0%	115.5%	-0.07%

Table 4: Relative improvements in NPV for the water flooding optimization.

The decision making process in the water flooding optimization has proven to be computationally difficult to perform. This is because the optimization is separated from the uncertainty analysis. Even if the computational requirement were overcome the optimal production / injection settings of the uncertainty range may not be the settings of one of the optimized models. Therefore, even if all setting are applied to all models this would not prove to be a robust approach.

Several considerations beyond the available computing resources are important here. The primary consideration is the choice of objective function as it affects the optimal solution. The next section integrates the decision making process into the design approach in a new manner. Attempts at robust optimization over several geological realizations[4] or several geological and control parameters[5] attempt to provide a robust solution. The approach by van Essen et al. [4] incorporated a gradient based optimization method where the gradients are obtained with an adjoint formulation. The approach by Esmaiel and Heeremans[5] incorporated a gradient based optimization method where the gradients are obtained with an experimental design based approach. The approach by van Essen is more computationally efficient but is limited by the adjoint formulation which at the time of this writing did not include WAG parameters. Below an experimental design based robust optimization approach is discussed.

5.3 Utility Theory and Robust Control

The previous section demonstrates the application of a brute force approach to determining an optimal solution. The scope of the problem was kept small by limiting the optimization to 3 time steps. This was performed on a single reservoir model and does not take into account the risk associated with geologic uncertainty. A robust optimization allows the optimization process to be carried out over a set of models, here being the design space, to actively account for the uncertainty during the optimization. The optimizations presented here do not incorporate history matching or model updating.

When optimizing a single reservoir model the choice of objective function is relatively simple. The choice is often total recovery or the economic measure Net Present Value (NPV). Optimizing over a set of models poses a more difficult question of how to define the objective function. The average or expected NPV, also called Expected Monetary Value (EMV), is popular but does not take into account the risk. A utility approach as described below takes into account risk and reward into the decision making process.

5.3.1 Utility

Risk and reward are ever present in the decision making process. A comparison of an EMV approach to a utility theory approach will be presented in brief.

The history of the incorporation of risk and uncertainty in economics has a relatively brief history. Utility can be loosely defined as a measure of happiness and therefore a utility function has a higher value for preferred choices. The translation of an economic value such as NPV into utility can therefore take into account the risk attitude of the decision maker.

The concept of marginal utility was first introduced by Daniel Bernoulli[1] in his 1738 solution to the St. Petersburg Paradox[2] posed by his cousin Nicholas Bernoulli in 1713. The two concepts arising from this was that people's utility from wealth is not linearly related to wealth and that the associated value of a risky venture is not the EMV but the expected utility.

The formal incorporation of utility theory[3] came in 1944. This formally incorporated choice based on preferences of distributions of outcomes. By Bernoulli's logic, in order to value a risky venture the expected utility is:

$$E(u \mid p, X) = \sum_{x \in X} p(x)u(x) \quad (1)$$

where X is the set of possible outcomes, p(x) is the probability of a particular outcome $x \in X$ and $u: X \rightarrow R$ is a utility function over outcomes. This implies if $u(x) > u(y)$ then x is preferred to y.
The function used in this study is the logarithmic approach such that:

$$U(x) = a\log(x) \quad (2)$$

Where x is the NPV. This function provides for a risk averse attitude to the decision making process. This process reduces the EMV and spread into one additive measure of "value". The approach used to quantify the uncertainty in the NPV calculations is Monte Carlo sampling. NPV can then be directly converted into utility to facilitate the decision making process. The speed and accuracy of the proxy model allows this to be done.

5.4 WAG

The problem being addressed is the optimal recovery of oil under the economic constraints imposed on the wells. The problem of uncertainty in reservoir and fluid parameters is added to the mix to further compound the decision making process. In one case the oil price is varied to show the consequences of taking into account economics and not just recovery.

The first step taken in addressing the issue looks at sensitivity issues of the WAG process. This phase of the study used the initial WAG parameters and well settings without optimization to study the sensitivity to the uncertainty of several reservoir properties. This work was performed on the same model introduced in Section 2.3. Gas breakthrough problems occurred in all the simulation runs and loss of water injectivity occurred in a significant number of the runs. Very few of these scenarios suffered major water production problems due to the water injectivity decline seen in many of the runs. In Chapter 4 several reservoir parameters were studied to examine the sensitivity of the oil recovery.

The first step in the optimization was reducing the scope of the study for the purposes of testing this methodology of optimizing under uncertainty. The problem was reduced to two uncertain parameters, the mobility of the oil phase and the absolute permeability. The ranges used in the study are provided in **Table 7** along with the control setting.

A primary reason for choosing the absolute permeability is so that the range covers different flank sectors of the reservoir that the model was derived from. This has the added benefit of applying the technique to different sectors using different probability distribution functions (PDF) in the Monte Carlo analysis of the results.

The next step is deciding the control parameters available for optimization of the oil recovery. To maintain a reasonable number of simulations to test the process and validate the results the number of control parameters was reduced to five. An initial WAG ratio of 1:1 is used with 3 months per injection phase and two additional options with a ratio of 1:3 with 1 month water and 3 months gas, and 3:1 with 3 months water and 1 month gas are implemented along with the original WAG setting. Additionally the producer and injector have two completion intervals that can each be closed or open to flow.

The initial goal is determining the optimum WAG parameters at the start of the project with only a reactive control scheme. This is done by setting up a design with three parameters that include the permeability, mobility, WAG slug size, and well type. For ease of analysis two separate proxy models were generated, one for the conventional well and one for the smart well. All production wells are placed on a reactive control mode at this time. The optimum WAG parameters determined at this stage remain constant throughout the simulation. To calculate NPV and assess the value of the smart well, a cost of $200,000 is taken for the conventional wells and $500,000 for the smart wells.

The parameters are coded and scaled such that the low value is coded to -1, the median to 0 and the maximum value to +1. The ranges for the WAG parameters and reservoir uncertainty parameters and their corresponding coded values can be seen in **Table 7**. There are then some assumptions made that all runs can be performed at any combination of these settings. If this is not true the design is modified with constraints. In this case closing all connections can be simulated but provides no useful results for the optimization process. These runs would also populate the data set with results that would pollute the proxy model fit.
Oil prices are incorporated in the post processing of the simulation data. A decision is made on the valve setting at the current time step and then the simulation moves forward. This process is repeated till the end of the 10 year simulation.

5.4.1 Results - Monte Carlo Analysis

A flow chart of the overall process in shown in **Figure 9**. After validating the RSM further analysis can be performed using either Monte Carlo analysis or the analytic solution can give the distribution. The continuous uniform distribution on the interval [0,1] has probability density $f(x) = 1$ for $0 \leq x \leq 1$ and $f(x) = 0$ elsewhere. The standard normal distribution has probability density:

$$f(x) = \frac{e^{(-x^2/2)}}{\sqrt{2\pi}} \quad (5)$$

If a random variable X is given and its distribution admits a probability density function f(x), then the expected value of X (if it exists) can be calculated as:

$$E(x) = \int x f(x) dx \quad \text{or} \quad (6)$$

$$NPV = \alpha_1 \frac{e^{(-k^2/2)}}{\sqrt{2\pi}} + \alpha_2 \frac{e^{(-k^2/2)}}{k\sqrt{2\pi}} + \alpha_3 \frac{e^{(-q^2/2)}}{\sqrt{2\pi}} + \alpha_4 \frac{e^{(-q^2/2)}}{q\sqrt{2\pi}} + \alpha_5 \frac{e^{(-p^2/2)}}{\sqrt{2\pi}} + \alpha_6 \frac{e^{(-p^2/2)}}{p\sqrt{2\pi}} +$$
$$\alpha_7 \frac{e^{(-r^2/2)}}{\sqrt{2\pi}} + \alpha_8 \frac{e^{(-r^2/2)}}{r\sqrt{2\pi}} + \alpha_9 \frac{ke^{(-q^2/2)}}{\sqrt{2\pi}} + \alpha_{10} \frac{qe^{(-k^2/2)}}{\sqrt{2\pi}} + \alpha_{11} \frac{ke^{(-p^2/2)}}{\sqrt{2\pi}} + \alpha_{12} \frac{pe^{(-k^2/2)}}{\sqrt{2\pi}} +$$
$$\alpha_{13} \frac{ke^{(-r^2/2)}}{\sqrt{2\pi}} + \alpha_{14} \frac{re^{(-k^2/2)}}{\sqrt{2\pi}} + \alpha_{15} \frac{qe^{(-p^2/2)}}{\sqrt{2\pi}} + \alpha_{16} \frac{pe^{(-q^2/2)}}{\sqrt{2\pi}} + \alpha_{17} \frac{qe^{(-r^2/2)}}{\sqrt{2\pi}} +$$
$$\alpha_{18} \frac{re^{(-q^2/2)}}{\sqrt{2\pi}} + \alpha_{19} \frac{pe^{(-r^2/2)}}{\sqrt{2\pi}} + \alpha_{20} \frac{re^{(-p^2/2)}}{\sqrt{2\pi}}$$

Based on the *a* values in **Table 3**.

The average simulation time was between 10 and 20 minutes while the proxy model to determine the oil recovery takes approximately one second. The multiple order of magnitude increase in speed has facilitated the performing of Monte Carlo simulations to provide a reasonable PDF for the base and optimized oil recovery, the NPV, and the utility of the project under reservoir uncertainty. **Figure 10** shows the assessment of recovery distribution for the conventional well and optimized smart well. **Figure 11** shows the assessment of the NPV distribution for the conventional and optimized smart well. **Figure 12** shows the assessment of the utility distribution for the conventional and optimized smart well.

Ultimately the properly optimized flood is robust enough to increase the ultimate recovery significantly and reduce the uncertainty in the recovery. This stepwise optimization procedure to determine a robust solution is shown in the flowchart below.

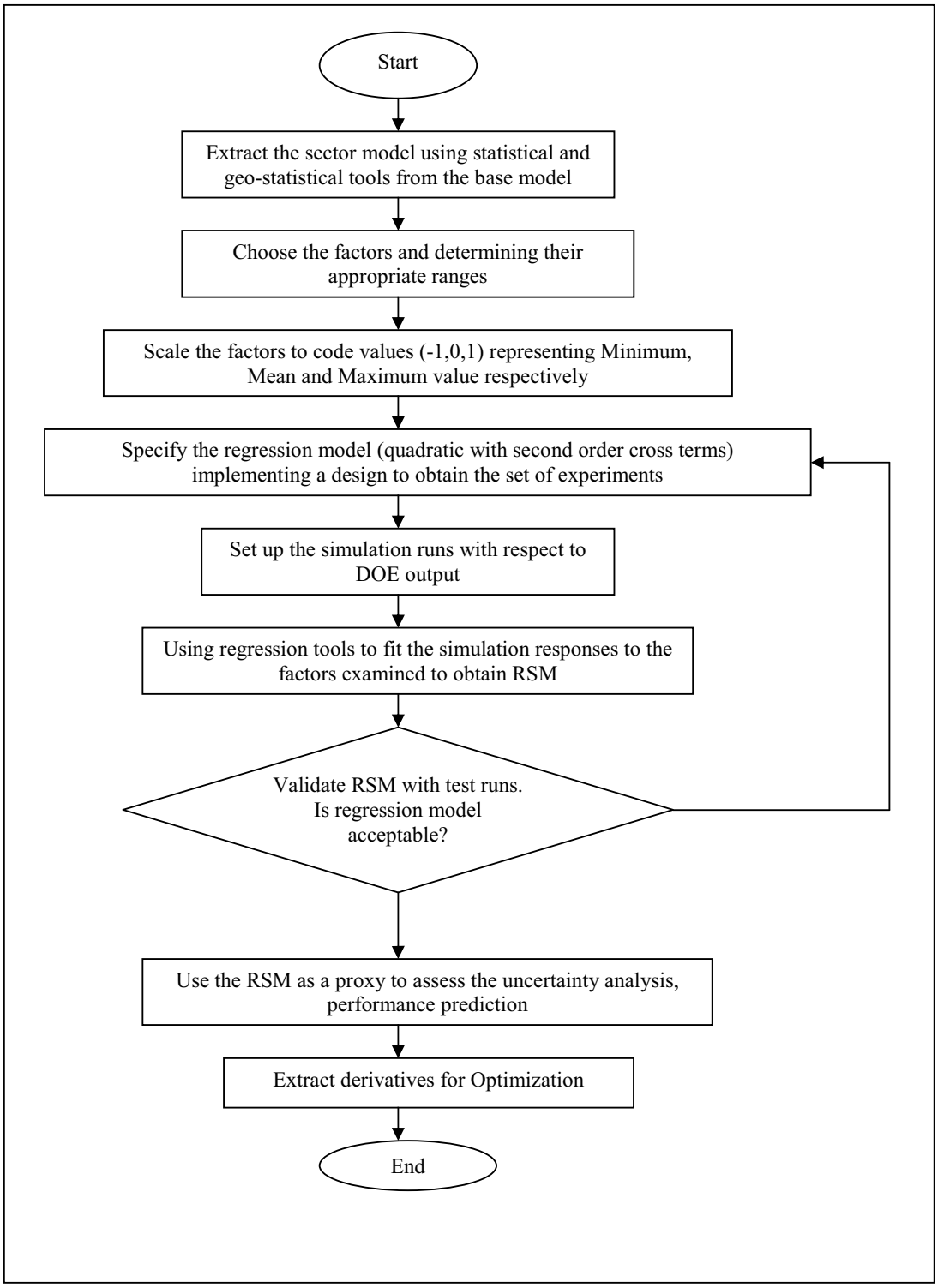

Figure 9: Flow chart of the overall process.

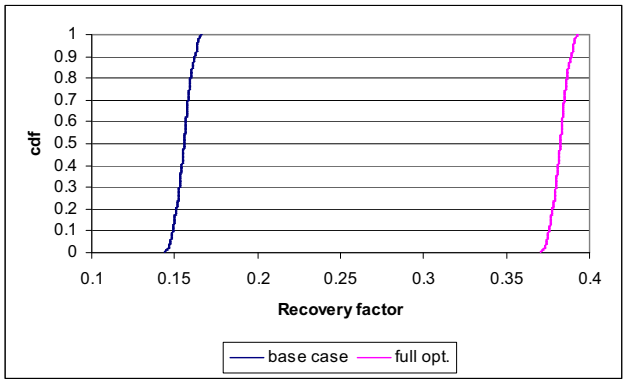

Figure 10: Recovery distribution

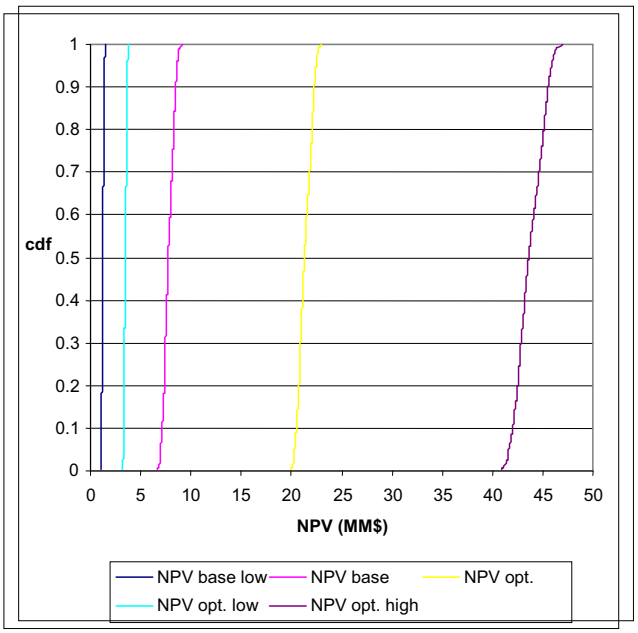

Figure 11: NPV distribution

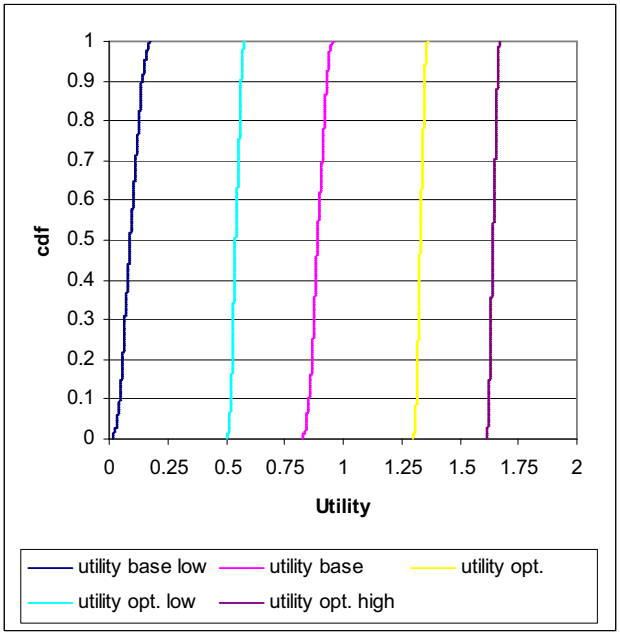

Figure 12: Utility distribution

Relative Range	Low	Medium	High
Coded Value	-1	0	1
WAG Ratio	1:3	3:3	3:1
Arial Perm. Multiplier	2	4	6
Mobility Oil	0.9	1.0	1.1
Well Completion i prod	shut		open
Well Completion i inj	shut		open

Table 7: Coded parameters with values used in the WAG pattern flood simulations.

5.4.2 Discussion

An experimental design and response surface proxy model based approach integrates the optimization with the model sensitivities. This approach treats the well operations as a parameter in the design space rather than a secondary control parameter. Therefore the well status becomes a term in the proxy model. By incorporating the control parameters, well and WAG settings, with the parameters in the design this integrated approach optimizes simultaneously over the entire design space to provide a robust control algorithm. This approach differs from the earlier brute force approach that applied an optimal solution to one model to all other models. This integrated approach makes singular decisions across the entire set of models.

The reservoir simulation model was run for 10 years with the recovery and NPV at 10 years modeled by proxy models. The optimization routine initially was aimed at maximizing the ultimate recovery of the pattern flood. The same approach using proxy models for NPV was applied to optimize the NPV.

In order to visualize the process 2 contour maps are shown in **Figure 13** and **Figure 14**. **Figure 13** comes from the beginning of the conventional well run prior to any optimization. As this is not a smart well there is only one control parameter, the WAG ratio. This figure clearly shows that a WAG ratio of "1" is best and referring to **Table 7** this corresponds to a 3:1 WAG.

Figure 14 comes from a late time in the simulation of the smart well. It clearly indicated the valve should be opened at this time and this is verified with the model. Updates in the valve settings were taken every month and the time steps were chosen at the end of each WAG cycle to update the WAG settings. This figure is plotted with the remaining parameters set at a mid level. The goal of this exercise is to optimize all 5 control parameters under the reservoir uncertainty. All these decisions are made from the proxy model but are somewhat more difficult. All 5 control parameters must be simultaneously optimized.

The results of the analysis at $50/stb are summarized in **Table 8**. The base model provided an average recovery of about 15% after 10 years. The results of the complete optimization of recovery provided much better results. The proxy model provides optimal settings and the estimated increase in recovery. Taking advantage of the derivatives provided by the proxy model optimizing injection and production as well as the WAG, results in an increase in the mean recovery to 39% when applied to the simulation model. This provides an increase in the expected recovery and an increased value in the optimization.

Means	Fully Optimized	Opt. Comp	Opt. WAG	Conv. Well
Recovery	0.39	0.35	0.30	0.15
NPV MM$	21.35	16.78	13.51	7.78
Utility	1.33	1.22	1.12	0.89

Table 8: Results of the optimization based on 3 different goals.

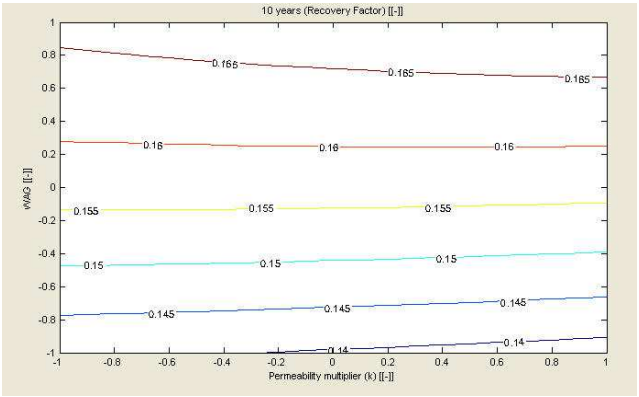

Figure 13: Contour map of recovery for WAG setting and the permeability at an early time step. (only conventional well)

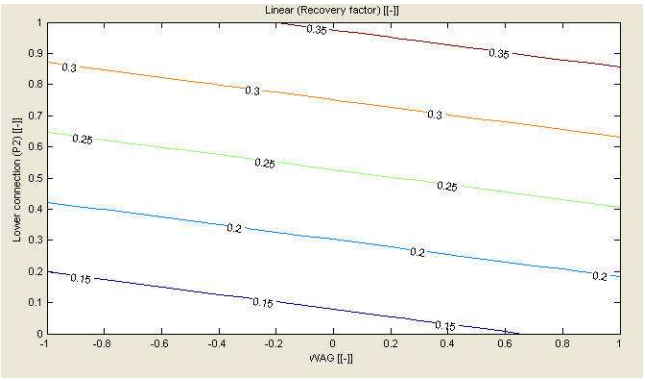

Figure 14: Contour map of recovery for WAG setting and the lower completion interval of the producer at an early time step.

5.5 Oil Prices and Capital Expenditures – An example

The oil recovery uncertainties for the conventional and optimized smart well are shown in **Figure 10**. To represent the recovery over the entire design space the Monte Carlo Simulation drew samples of the reservoir properties distributed over the entire design space. This section will provide an example of the implications of different oil price models and a change in capital expenditures, or purchasing cost.

In the period between World War I and the Gulf War inflation adjusted average annual oil prices in year 2000 dollars ranged from under $9.00 in the Early 1930's to over $60.00 during the height of the Iranian revolution of the early 1980's. These historic oil price variations are seen in **Figure 15**. Even the 1980's showed a range of under $20.00 to over $60.00. The base price of $50.00/stb was used in all previous calculations. To assess the risk of spending extra capital on the project under uncertain economic conditions two different oil price scenarios were used.

> "I don't think it's going to go to 100 US$ but if it does the crash is going to be even more spectacular…It will make the hi-tech bubble look like a picnic … this thing is not going to last." Steve Forbes

Even a respected business man like Steve Forbes believes there is a great uncertainty in oil prices. Many companies and organizations within and outside the oil industry use various price forecasting models with a high spread of future prices. Therefore for this example an optimistic (from the author's point of view) price of $50 and a pessimistic price of $10 are used to compare risk attitudes.

An interesting observation can be made comparing the $10 and $50 results for the 2 simulations. The NPV after subtracting capital costs was positive for all 4 cases with mean NPV values of 1.23 MM$ and 7.78 MM$ for the conventional well and 13.51 MM$ and 21.35 MM$ for the smart well.

Initially these all seem very profitable and good returns on investment of $400,000 and $1,000,000 respectively. The utility approach tells the same story. As seen in **Figure 11** all the values were positive along the entire distribution of NPV. If a higher capital cost or a purchase cost were introduced this could drastically change the decision making. This is due to the risk attitudes normally existing in management decisions. In a risk adverse world a 50% chance of making or losing money may have an expected monetary value of $0 but in truth has a negative utility. This means no one would choose this venture unless of course they are inherently risk prone.

Cost overruns were not a part of the data presented above. To illustrate the point above for one example, the low oil price conventional well, additional costs were added after the fact. The project with $1,000,000 in cost overruns had a negative utility even though the mean NPV remained marginally positive at 0.23 MM$. This is due to the fact that some of the models lost money while other made money. An EMV approach has gives an equal probability of making or losing 1 $ a value of 0. A utility approach with a risk adverse attitude results in a negative utility for the same problem.

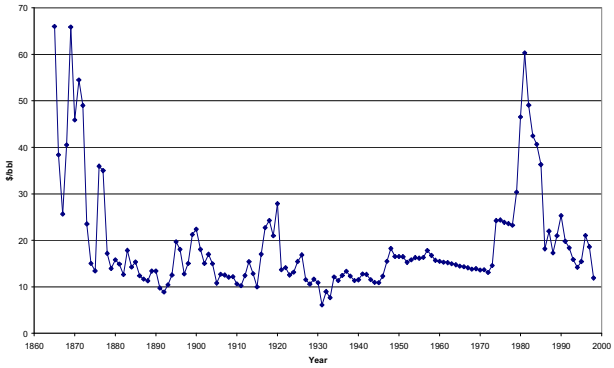

Figure 15: – Historic oil prices adjusted for inflation[6].

5.6 Conclusions

WAG, smart wells, and uncertainty can all be incorporated into the decision making process. Although decision analysis is defined as a systematic approach to making decisions it is often done in an adhoc fashion. This chapter compares three approaches to the optimization of a flood under reservoir uncertainty.

The least complex model only has one parameter to optimize at a time. The fractured reservoir model demonstrates the ability of the experimental design approach to provide a derivative for the WAG setting. This parameter readily optimized for the start of the production period. To further improve the flood the reservoir life is divided into three cycles manually and each cycle is optimized. This process is beneficial but is not strictly systematic and requires a manual division of reservoir lifecycles.

The water flooding model uses a different approach to the optimization. Several models, in this case the full factorial, are run with an OCT optimizer implemented on each model. This provides excellent results on the individual runs but presents a difficulty in the decision making process. Appling any single simulations optimal well setting to the entire design set results in suboptimal results. A brute force approach to testing all results on all models provided a robust solution. It is computationally expensive as n optimization runs, 81 in this case, requires n^2, 6,561simulations, to determine which setting is best. To test for a robust solution all 6,561 simulations were ran and analyzed showing a set of similar robust solutions corresponding co a cluster of 9 similar acting models.

A formal decision making process is presented for the 5-spot WAG model. This approach incorporates the WAG process, smart wells and reservoir uncertainty into a robust optimization. Here the optimization parameters, WAG and well setting, are incorporated with the uncertainty parameters into the design approach. This approach allows the optimal setting with respect to EMV, recovery, or utility to be made in a formal manner.

The design approach with screening and optimal designs reduces the required runs and provides for a formal decision making approach. The approach is flexible being able to incorporate multiple controls and reservoir parameters into the approach.

References

1. Bernoulli, Daniel, "Exposition of a New Theory on the Measurement of Risk", 1738, (translated in 1954, Econometrica 22, 23-36)
2. Eric W. Weisstein. "Saint Petersburg Paradox." From MathWorld--A Wolfram Web Resource. http://mathworld.wolfram.com/SaintPetersburgParadox.html
3. Neumann, John von and Morgenstern, Oskar Theory of Games and Economic Behavior. Princeton, NJ. Princeton University Press. 1944
4. van Essen, G.M., et al., “Robust Waterflooding Optimization of Multiple Geological Scenarios”, SPE 102913 SPE Annual Technical Conference and Exhibition, San Antonio, Texas, USA, 24-27 September 2006.
5. Esmaiel, T.E.H. , Heeremans, J.C., “Optimization of the WAG process under Uncertainty in a Smart Wells Environment: Utility Theory Approach”, SPE 100009 SPE Intelligent Energy Conference and Exhibition, Amsterdam, The Netherlands, 11-13 April 2006
6. US Department of Energy Statistical Database, Annual Oil Market Chronology, EIA, 2006 http://www.doe.gov/

Chapter 6 Conclusions and Recommendations

The primary objective of this study is to develop a systematic approach to finding the optimum injection and production strategy for various reservoir models concentrating on WAG injection. The use of a gradient based optimization algorithm founded on an experimental design approach shows positive results. The value of this approach has been demonstrated on a fractured reservoir model and a 5-spot pattern flood reservoir.

Secondary objectives included investigation of the sensitivity of various reservoir, fluid, and production parameters to the NPV, recovery, and scope for improvement using smart wells. These also used information from the DOE approach featured in this study.

Several streams of value creation have been discussed in this report. The conclusions will highlight some of the important insights gained during these studies

6.1 Value Creation

The primary motivation for this study was to add value to the reservoir engineering studies presented in this report. Three sets of models, water flooding, WAG in a fractured reservoir, and WAG in a pattern flood with smart wells, formed the basis for these studies. Below some of the insights gained from each of the three models will be discussed.

6.1.1 Water Flooding

The early objective of this study was to test the validity of the DOE approach to model the NPV of a water flood with and without smart wells. The proxy model was able to adequately represent the NPV calculations computed with the flow simulator and water flood optimizer for the standard and smart wells. The proxy model allowed the study of the full distribution of NPV rather than just its expected value. This allowed better judgments in assessing the value of the smart well versus the conventional well setup in this study.

The information obtained in the Pareto chart analysis of the output provided further insight into to value chain. This provided not just the amount of NPV gain expected, but which factors determined this gain. This information would prove to be invaluable when determining the major uncertainties in the reservoir and their relative effect on the NPV spread.

Smart well technology offers various benefits over conventional wells. Primarily smart completions allow the control to respond to the non-optimal conditions caused by reservoir heterogeneities as well as market influences. The average improvement in NPV for the simulations run to train the model was 44%, but this does not tell the entire story. The flexibility of the wells results in risk reduction as well as reduced data needs. The value of information, although difficult to quantify analytically, is often important. Cost reduction on the operation phases of the project due to reduced down time not modelled in this study would provide additional gains.

The polynomial model used for NPV modelling worked well but this does not guarantee success using the same type model on other data. Cumulative oil production would be a viable candidate but data such as water cut with abrupt changes would need to be treated differently.

Determining a robust control strategy proves to be a computationally expensive but valuable exercise. Performing an exhaustive global search provided the data to analyse various clusters of the design parameters. A robust control could then be determined from the 81 individual solutions previously established.

Some of the main points of this phase of the study include:

- Quick screening of the most important parameters with a Plackett-Burmann design proved useful for an early set of large parameters.
- Optimization was performed with OCT but the potential improvement relative to the reservoir properties was obtained with the DOE approach.
- VOI analysis was possible through Monte Carlo analysis of the proxy model. This provides additional information on what further studies, i.e. seismic / core analysis / etc., would be most beneficial.
- This approach provides a risk based assessment of the NPV / EMV and not just a single NPV value.
- Cluster analysis provided for a set of robust controls over the entire design space.

6.1.2 Pattern flood near-Miscible WAG

The base case WAG study was on a single model representing a pilot study area of a larger reservoir. Several production scenarios were compared in this study to show the general benefits of WAG, both optimized and not. WAG outperformed both water flooding and gas flooding in this pattern flood.

The study provided a systematic approach to both evaluate the potential of the WAG flood as well as determine the sensitivity to various reservoir properties. The reservoir model used in this study showed that the value

gained by reducing the uncertainty in the fluid characterization would prove more valuable than reducing uncertainty in the permeability field's description.

A DOE approach to this model allowed the production parameters to be treated as design parameters. This approach, although not revolutionary, allowed the theory to advance to incorporate non-reservoir parameters into the design process. This second main finding to be seen in this study is that the proactive optimization of the WAG process showed significant gains over the reactive WAG case.

The reservoir model underwent a grid block size sensitivity test to determine an adequate gridding size to limit numerical dispersion. The response surface model was also used to perform a sensitivity analysis of the grid size prior to DOE analysis to validate the model. The model has rate and pressure constraints that are reasonable field values as it is based on a real oil field. This also means the analysis of the results do not force themselves to the limiting conditions of rate controlled or pressure controlled.

Some of the main points of this phase of the study include:

- Fast tool to determine initial optimal WAG settings.
- Multiple WAG setting can be addressed simultaneously with the design approach including PVI, and WAG ratio.
- Easily implemented in a commercial reservoir simulation package allowing for gravity, compositional and other effects to be taken into consideration.
- The major issues addressed from a field perspective were maintaining reservoir pressure and limiting breakthrough. Pressure maintenance is much more important when gas is involved as the loss of miscibility is detrimental to the recovery.

6.1.3 Fractured Reservoir and WAG

This study provided two major points of interest. WAG is generally considered a nonviable option in fractured reservoirs. The initial phase of this study was to screen candidates where WAG was able to outperform water and gas floods. This was found to work in lightly fractured reservoirs.

The second objective having found viable candidates was to determine under what conditions WAG was successful. The design set was reduced to two dimensionless numbers representing the ratios of viscous, capillary and gravity force in the reservoir. It was the viscous gravity forces in the fractures and the capillary viscous forces in the matrix that determined the flow performance.

The initial WAG settings were optimized with a DOE approach but these setting were kept for the entire simulation time. In optimizing the flood over time a visual breakdown of the production regimes allowed the WAG setting to be optimized only 2 additional times during the life of the reservoir. This limit was needed due to computational constraints during the study.

Some of the main points of this phase of the study include:

- WAG can be viable in a fractured reservoir providing the flow regimes fall into certain ranges.
- The DOE approach helped identify the critical forces playing a role in the WAG flood.
- The viability of WAG floods in these types of fractured reservoirs can be analyzed with two parameters, the viscous gravity force in the fracture and the capillary viscous forces in the matrix.

6.1.4 Smart Wells and WAG

Smart wells were shown in the water flooding to be of great economic benefit to the lifecycle optimization of the reservoir. Intuitively additional control parameters, although more difficult to optimize, should result in better control and therefore further improvements during a WAG flood. The static and dynamic optimization of a single reservoir model showed vast improvements over base case models in a conventional reservoir. In this single reservoir model improvement of more than 100% were possible. Smart wells were shown to be much less successful in fractured reservoirs.

Some of the main points of this phase of the study include:

- These results are still limited to a single model. This issue will be addressed below.
- The combination of further control parameters allows for improved front control and results in further improvement in recovery.
- The DOE approach allowed the number of simulation to be low enough to perform these studies in a reasonable time frame.
- Although WAG was successful in fractured reservoirs, smart wells proved to be less useful in a fractured reservoir.

6.1.5 Uncertainty Scenarios

Uncertainty and the associated risk are issues that cannot be avoided. It has been generally accepted for some time that this is important but the limits of computing power and proper analysis tools have resulted in few studies that properly address these issues.

The design framework presented here uses the same set of tools to screen over the uncertainty range, determine the sensitivities of recovery or economics measures to input factors that include reservoir parameters as well as smartness and economic parameters.

The design framework also allows different measures of risk and therefore different objective functions to be optimized. Risk attitudes can be incorporated into the decision making process by converting NPV into utility and optimizing for the expected utility. This approach proved that a viable and robust optimal production strategy could be determined while incorporating uncertainty into the decision making process.

Furthermore, this approach provided a methodology to quantify the value of flexibility for the smart well, and the value of information associated with the parameter uncertainties and their influence on the objective function.

Some of the main points of this phase of the study include:

- Utility functions provide a good measurement of risk-averse value for non normal distributed responses. This is designed for a variety of risk attitudes to be implemented.
- Under many cases the optimal strategy was shown to change depending on the risk attitude applied.
- Beyond the increase in recovery, NPV, or utility seen there is added value in the information seen in the sensitivities.

6.2 Constraints and Limitations

Three major issues are faced in these studies that must be addressed.

6.2.1 Number of Simulations

The first issue is to the number of simulation runs that can result in a useful analysis of the results. A full factorial design will usually provide enough responses but may not be a feasible option computationally. The water flooding study was done by performing the full factorial set of simulations to start the analysis. The majority of the computation time lies in the reservoir simulation as the regression analysis to create the response surface model is relatively fast.

A prior estimate of the number of simulations required can be seen in 2 ways. First, a measure of the d-optimal efficiency provides a good measure. Second, a comparison to the number of regression parameters for the response surface must be done. In general though a rule of thumb of around 1.5-2.0 times the number of regression parameters work well for these small sets.

6.2.2 Validity of the Surface Response

The second issue to address is the validity of the model. Several test simulations are required to validate the model as a high regression coefficient on the fit to the design runs does not guarantee a valid model. The validity also applied to the type of model used for the response surface. In these examples a second order polynomial with cross terms allowed enough resolution to properly model the responses. This may not hold true when many more parameters are used and larger parameter ranges are implemented.

Unreported here were studies that attempted to use a neural network approach to fit and choose the elements of the proxy. This proved to hold little value in small sets where the proxy worked very well but may prove useful in larger design sets where a pre-screening of parameters left many significant parameters in the design study.

6.2.3 Parameter Ranges

This issue of parameter ranges was brought up earlier in discussion of the coding of the parameter levels. This ties in strongly with validating the proxy model. The ranges should not be too small, not be too large, and still represent the uncertainty in the actual reservoir. When this issue is present there are approaches that can be quite useful.

One possible approach is adding star points or centre points to the design. These do add a larger number of runs to the full factorial design and the optimal design but act a built in test runs and help validate the shape of the response function. Ultimately, the narrowing of some ranges or the use of multiple design sets may be required when the response surface cannot be fit otherwise.

6.3 The Future

The scope for future work in this study is significant. This approach can be tested on a full field or sector model with more than 5 wells to see if the approach scales up nicely. In theory the saving in percentage terms versus the full factorial model increases as the number of parameters increase. Here the difficulty lies more on the validity of the RSM than in the computational savings.

Further investigation into the posterior analysis of the proxy model can provide valuable insight into the value of information related to uncertainty reduction. A quantification of value of flexibility associated with the smart wells can also aid in determining the value of the technology.

Future work may be extended to but not limited to:

- Testing the procedure on a larger model with many more wells.
- Model the derivatives calculated within a commercial simulator to determine a robust production strategy. Integration of an optimal control approach across a design space in one joint procedure would be optimal.

Acknowledgements

Those who know me well know I am often a man of few words. Before anything else is said I have to thank my promoter and mentor Cor van Kruijsdijk. Through the ups and the downs of research and life you have pushed, pulled and dragged me to the end of my studies here in Delft. The faith you put in me to supervise students, teach practical assignments, and even cover a few lectures when you forgot you were leaving town I have always appreciated the faith you have had in me. Faith and a bit of pain and sorrow is the best way to describe our working relationship since you moved to Canada but it somehow worked.

Jan Dirk Jansen, it seems you had to continuously adopt me when Cor would disappear and be my connection to Shell and later the ISAPP team. Your insight into smart wells and smart fields and well as the insight provided by people you introduced me to have made the research flow with much more ease.

I have worked with many people along the way whom I will not attempt to name each by person, but one I must. Dr. Dirk Roelof Brouwer, I knew you before you were a Dr. but you were my mini-mentor across the walls from 202 to 203. When professors do not have time it is the fellow PhD candidates that help and mentor each other and you were there from day one.

To the faculty, staff and students here in Delft and to colleagues at Shell it has been a pleasure to work with you all. As I return to Kuwait to work I leave Delft with not only an education but many fond memories of not just my social life but also my work life. I have had the privilege to work with and supervise several students during my time in Delft. Saeed, Ali Reza, Ali, Ahmad and Joost. We shall forever be linked as I have had the pleasure to write papers with all of you.

A special thanks to my committee who is taking the time to give me my graduation day. Rector Magnificus, Prof. ir. C.P.J.W. van Kruijsdijk, Prof. dr. ir. J.D. Jansen, Prof. dr. J. Bruining, Prof. A. El-Sharkawy, Dr. M. Salman, Prof. dr. P. Zitha, Dr. Carlos Glandt.

KISR, It has nearly been a decade since I started in 1997. WOW! Dr. Mohammad Salman and Dr. Mohammad "Steve" Ali Juma. You two have put up with me for 10 years now and have continued to be the rope that keeps me connected while I have been out of the country for 6 years. I am looking forward to seeing all of you in Ahmadi on a regular basis now.

On a social note since I came to Delft in 2003 everyone has made me feel very welcome. To the Mijnbouwkundige Vereeniging, the Society of Petroleum Engineers, Het Mijnbouwkundig Sigarenrookgezelschap "Die Elefanten", Tuesday Night Poker Club, NOCO, WAGgers, the infamous 202 Crew and many more Thank You. I will not attempt to name you all but for a flavor of our years together turn the page and have a smile.

Foremost I would like to express my thanks and gratitude to those closest to my heart – my family. To my parents Ebraheem and Jerry Esmaiel and my brother Dawood…this would never have came to fruition without you. To my immediate and extended family and friends.

I Love You All


UDelft Aula Congrescentr
MIJNBOUW

About the Author

Talal Ebraheem Hamzah Esmaiel was born to Jerry Lee and Ebraheem Hamzah Esmaiel on the 14th of April 1973 in Kuwait. Following graduation from Natrona County High School in Casper, Wyoming, USA in 1991 Talal attended the University of Wyoming in Laramie, Wyoming. After being awarded a BS in Chemical Engineering in May 1996 and a BS in Petroleum Engineering in May 1997 he returned to Kuwait to work for the Kuwait Institute for Scientific Research with whom he is still employed. Talal returned to the USA to attend Stanford University in Stanford, California and was conferred with an MS in Petroleum Engineering in January 2003. In 2003 he commenced his doctoral studies at Delft University of Technology's faculty of Civil Engineering & Geosciences, Department of Geotechnology, specifically in Section of Petroleum Engineering under the supervision of Professor Cor van Kruijsdijk.

Talal Esmaiel has been a member of the Society of Petroleum Engineers (SPE) since 1993 where he has served three terms as vice-president of the student chapters at the University of Wyoming and Stanford University. Talal is a member of the Society Petroleum Engineering's honour society, Pi Epsilon Tau, and served three terms as president of the University of Wyoming chapter. Talal also served one year as the American Institute of Chemical Engineers (AIChE) vice-president at the University of Wyoming. Recently he was elected a Buitengewoon Lid (Extraordinary Member) of the Mijnbouwkundige Vereeniging (MV) at Delft University of Technology.

During his years in Delft Talal has been active in the Society of Petroleum Engineers and the Mijnbouwkundige Vereeniging. Talal has had the privilege of serving a term as president of Die Elefanten, a guild within the Mijnbouwkundige Vereeniging dedicated to cigar appreciation. On an academic level he has had the pleasure of teaching a few classes and assisting in practical exercises in the Petroleum Engineering section. Talal has attended several conferences to present research papers that have been written with students and faculty at the department and has had the pleasure of co-supervising several students during their Masters Degree thesis work.

Talal Esmaiel has held the positions of Associate Researcher and Research Associate at the Kuwait Institute for Scientific Research (KISR). Talal Esmaiel has worked for KISR since 1997 and will return to the company upon graduation with a research position at the Petroleum Research and Studies Center at KISR.